DESIGN AND SIMULATION OF DC MICROGRID FOR ELECTRIC VEHICLE CHARGING STATION (A CASE STUDY HAWASSA CITY)

A THESIS SUBMITTED

IN PARTIAL FULFILLMENT OF THE REQUIREMENTS FOR THE DEGREE OF

MASTER OF SCIENCE

In

POWER SYSTEM AND ENERGY ENGINEERING

BY

MATHEWOS HADERO GUTENA

DEPARTMENT OF ELECTRICAL AND COMPUTER ENGINEERING

HAWASSA UNIVERSITY INSTITUTE OF TECHNOLOGY

HAWASSA (ETHIOPIA)

Dec. 2020

EXAMINERS' APPROVAL SHEET

As members of the board of examiners of the final master's degree open defense. we certify that we have lead evaluated the thesis prepared by Mathewos Hadero Gutena under the title Modeling and simulation of DC Microgrid for EV Charging Station A case study of Hawassa city and recommend that it be accepted as fulfilling the thesis requirement for the degree of M.Sc. in power system and energy engineering.

---------- ---------- ----------
Name of chairperson Signature Date

---------- ---------- ----------
Name of internal examiner Signature Date

---------- ---------- ----------
Name of external examiner Signature Date

---------- ---------- ----------
Name of principal advisorSignature Date

---------- ---------- ----------
Name of Co-advisor Signature Date

Final approval and acceptance of the contingent upon the submission of the final copy of the thesis to the SG and DGC/SGC of the candidate department.

Thesis approved by

---------- ---------- ----------
SGS Signature Date

CANDIDATE'S DECLARATION

I hereby declare that the thesis "**Designing and simulation of DC Microgrid for EV Charging Station A case study of Hawassa city"**is my own work conducted under the guidance of **Baseem Khan (PhD)**, and **Tefera Tadesse (MSc.)** Department of Electrical and computer Engineering, Hawassa University Institute of Technology, HAWASSA (SNNPRS), Ethiopia.

I further declare that to the best of my knowledge the thesis does not contain any part of work that has been submitted for the award of any degree either in this university or any other university without proper citation.

(Mathewos Hadero)

ID No: PGeng 017/09

This is to certify that the statement made above by the candidate is true to the best of my knowledge.

Date:

Dr. Khan Baseem (Advisor)	
Mr. Tefera Tadesse(Co-Advisor)	
Department of Electrical Engineering **Hawassa University** **Hawassa, SNNPRS, 05**	

CERTIFICATE

This is to certify that the work entitled "**Designing and simulation of DC Microgrid for EV Charging Station A case study of Hawassa city** "submitted by **Mathewos Hadero (ID No: PGeng 017/09.)** Department of Electrical and Computer Engineering, Hawassa University Institute of Technology, Hawassa, Ethiopia is a record of a bonafide research carried out by him under my supervision and guidance. The thesis work in my opinion, has reached the requisite fulfilling the requirement of Master of Science Degree. The results contained in the thesis have not been submitted in part or full to any other University or Institute for the award of any degree.

Date:

Place: Hawassa, Ethiopia

Khan Baseem **(PhD)** **Department of Electrical Engineering** **Hawassa University** **Hawassa, SNNPRS, 05**	

ACKNOWLEDGEMENTS

The highest thanks to almighty God because with His mercy and help I have completed my work.

On the completion of this work, it is my proud privilege to express my sincere gratitude and admiration to my supervisor Dr. Baseem Khan and co-supervisor Mr. Tefera for their excellent guidance, unfailing support and continuous encouragement not only during this dissertation work but also over entire phase of my association with them. I offer them my deep sense of respect and profound indebtedness for their thoughtful concerns both my academics and personal welfare.

I would like to extend my thanks to Hawassa metrological agency and one of the staff Mr. Samuel for giving the required three year data for my research work.

I do not forgetto thank my wife Mrs. Marta Abera and my daughter Grace Mathewos for giving their golden time and different encouragements, ideas and motivation which inspire me throughout the work and for the successful completion.

Finally I would like to say thanks all my families and friends who give me different ideas and encouragements throughout the thesis work.

ABSTRACT

Development of electric vehicle has been established as an effective way to ensure energy security and realize emission reduction. However, the public electric vehicles charging station which is important element of using electric vehicles is not installed in Ethiopia. Therefore design of DC microgrid for charging station is proposed in this paper. In Ethiopia the electric energy infrastructure is not modernized enough and it is really difficult to fully depend on the energy obtained from grids. Thus, it is important to integrate the renewable energy (solar), grids and energy storage. However, the reliability of integration of renewable energy is dependent on the ability of the system to accommodate expected and unexpected changes (in production and consumption) and disturbances, while maintaining quality and continuity of service to the customers. Thus to improve real-time control performance and reduce possible seasonal variation forecasting is proposed for the solar energy used in the system. Thus in this study the author used the metrological data from Hawassa station and used machine learning algorithm for train the model with collected data and python used as programming language to develop forecasting model score system. Python is one of a well-known high level programming language in data science.In this thesis, Jupiter notebook is used to write Python codes to develop a solar energy forecasting system.The designed forecasting system can predict the next day irradiance with accuracy of 97.56%. Next MATLAB simulation tool is used to integrate system. The proposed maximum operating voltage of this DC microgrid charging station is 500 Vdc. Power flow management using fuzzy logic controller keeps voltage within expected range with standard voltage deviation 2.2 and improved the response time 1.645 ms. More over the author also investigated the operating costs per year for this design. The operating costs for energy is $43,651per year if you use grid only for charging of EVs. On the other hand if 400 kW of PV and 680 kWh of battery capacity is integrated to the grid it reduce the operating costs to$6,344 /yearwith annualized saving of $37,306.This implies as the hybrid system has investment payback of 3.06 years and an IRR of 32.7%.Thus, clearly the result obtain in this thesis have great potential in future charging station design.

KEY WORDS: DC Micro-Grid, Electric Vehicle, Charging station, Fuzzy logic controller,

CONTENTS

1 LIST OF TABLES

2 LIST OF FIGURES

NOMENCLATURE

AC	Alternative Current
BES	Battery Energy Storage
BEV	Battery Electric Vehicle
DC	Direct Current
EV	Electric Vehicle
EVSE	Electric Vehicle Supply Equipment
G2V	Grid to Vehicle
HEV	Hybrid Electric Vehicle
Km	kilo meter
kW	kilo watt
kWh	kilo watt hour
NOCT	Nominal Operating Cell Temperature
SOC	State of Charge
PHEV	Plugged-In Hybrid Electric Vehicle
PV	Photo-Voltaic
V2G	Vehicle to Grid
PCF	Photovoltaic Charging Facility
IRR	Internal rate of return
NPC	Net Present Cost

CHAPTER ONE

1 BACKGROUND OF THE STUDY

1.1 Introduction

According to the report in 2012 almost 27% of total energy consumption and 33.7% of greenhouse gas emissions in the world were related to the transportation sector [1]. Unlike vehicles with combustion engines, electric vehicles do not produce exhaust gases during operation. This alone makes electric vehicles more environmentally friendly than vehicles with conventional technology. Thus, with the increasing interest in green technologies in transportation, Electric Vehicles (EV) have proven to be the best solution to minimize greenhouse gas emissions. Hence, development of high efficiency, clean and safe transportation has increased rapidly over the past few years. An important milestone was reached in 2012 with more than 100,000 hybrid and all electric vehicles sold globally, and sales figures are approximately doubling each year [2]. .

Currently there are different types of EV in market, namely, Plug-in electric vehicles (PEVs), plug-in hybrid electric vehicles (PHEVs) and fuel cell vehicles. They all are potentially not only environmental friendly and quiet but also cost-effective in terms of energy prices and operating costs compared to conventional vehicles [3]. Furthermore, electrified vehicles are controllable loads which can be utilized as distributed power storage and generation units to support the grid's energy in vehicle to grid (V2G) or vehicle to building (V2B) applications [4–6] and can also be used as spinning reserves in certain conditions [7]. However, the lack of adequate charging infrastructure is a major barrier.

For practical operation of EVs one of the key important and fundamental elements is charging infrastructure. An electric vehicle charging station, also called EV charging station, electric recharging point, charging point, charge point, electronic charging station (ECS), and electric vehicle supply equipment (EVSE), is an infrastructure that supplies electric energy for the recharging of plug-in electric vehicles—including electric cars, neighborhood electric vehicles and plug-in hybrids.

The charging system can be classified as either a slow charger or a fast charger depending on the charging time and charging method. The slow charger usually supplies approximately 3–4 kW of power to the EV and its charging time requires approximately 6–7 h. For this reason, the slow charger is appropriate for night-time charging using a household AC utility. However, the fast charger supplies approximately 50 kW of power to the EV through the charging station, and the charging time requires less than 0.5 h [8-11].

Most electric vehicles (EVs) have an on-board charger that uses a rectifier circuit to transform alternating current from the electrical grid (mains AC) to direct current (DC) suitable for recharging the EV's battery pack. Cost and thermal issues limit how much power the rectifier can handle, so beyond 240 V AC and 75 A it is better for an external charging station to deliver DC to the battery.

For faster charging, dedicated chargers can be built in permanent locations and provided with high-current connections to the grid. In this style of connection, the charger's DC output has no effective limit, theoretical or practical. Such high voltage and high-current charging is called a DC fast charge (DCFC) or DC quick charging (DCQC) [12]. The development of the fast charger has been conducted in many developed countries. However, as the charging station becomes larger, it has been showing negative influences on the power quality in the electricity distribution system. These negative influences often appear as voltage distortions and current harmonics; poor power quality including a low power factor has already been a problem in many countries [13-14].

In the next few years, the numbers of EVs market is expected to increase exponentially, due to the depletion in oil resource and the environmental impact associated with its use. For that reason, different counters have been encouraging investment in development and use of EVs. Ethiopia is one of the countries who started to show its interest in EVs investment to overcome the rise in oil price and also environmental pollutions. However, for countries like Ethiopia whose energy infrastructure is not matured like developed countries one of the most important problem in EV development is the shortage of charging infrastructure which can withstand the countries energy fluctuation issues and which can withstand high power demand and its impact on the grid. To solve these challenges Integration of hybrid renewable energy systems into EVs and the electricity grid is clearly a

promising technique. Integration of grid and renewable energy sources for EVs charging station can avoid uncertainties caused by the discontinuous nature of renewable energies and also could degrade the stress on the grid caused by simultaneous charging of numerous vehicles. Thus in this thesis the author is interested to design a charging station which can be used in Ethiopian for charging EVs. The work mainly focus on DC-micro grid simulation for charging station.

To maximize the use of renewable energy generated from solar energy and also decrease the stress it bring on charging infrastructures it is important to automatically predict the amount of solar energy generated. Thus, in this thesis the author interested to examine a big data driven from historical weather data of one of Ethiopian metrological center named Hawassa metrological center. Then, the big data analysis is used to design sophisticated algorithms and models and try to transform weather data in predicting solar energy. Machine learning is one of the recent technologies that integrated to renewable energy to predict energy generated to early overcome the fluctuation beaver or over storing of energy in storage device. Machine learning helps to forecasts solar energy generated based on the relationships between weather characteristics recorded in the data base. The historical data is articulated as sets of rules in a mathematical model that can forecast solar energy expected in the coming day. This design can transform the DC – grid integration to data-driven decision-making.

To meet the objective of design of DC-micro grid, the author conducted the following key activities. The first is to design size of charging station, the second is design a machine learning predicting algorism for solar energy, the third is integration of solar energy, grid and battery using fuzzy logic; the last is estimating the cost of the charging stations.

The main contributions of this study are summarized as follows

The author used the historical data of Hawassa weather and developed a model which can predict the solar energy for the next day with accuracy of 97.56%. The result illustrates as the developed automatic solar energy predicting system for Hawassa charging station can work if the data are well managed.

1. Design of a smart model which can automatically forecast solar energy generated for EV charging station based on Hawassa weather condition.
2. Integration smart PV system, grid and energy storage using fuzzy logic

algorithm for scheduling the power system either to use solar, grid or battery as source of energy for charging station

3. The developed charging station operating cost estimation analysis is also conducted. Thus, the proposed system can deal with any pricing policies available in the energy market and ensures that the most economic cost reduction is achieved using the integration of renewable energy, grids and battery storage.
4. Design of the DC microgrid for EV charging station design for Ethiopia market which suitable with the weather conditions of Ethiopia

1.2 Statement of the problem

Vehicles are key transportation facilities in Ethiopia for both long distance and in cities. However, Ethiopia has no proven oil reserves and dependence on imported oil. Therefore for Ethiopia the need to shift from combustion engine cars to EVs is an ideal choose. Currently few numbers of EVs have been started giving service in Ethiopia. However, there is no attention given to charging stations yet. Especially, in near future as the number of EVs getting increasing the question to charging station will be clearer. So, this thesis is design and simulation of DC-micro grid for charging station for Ethiopian in particular for Hawassa city. As it is clearly known the Ethiopian electricity grid infrastructure is not yet matured and modernized to support the stress generated on grid system in near future from EVs. Thus, since the country is naturally gifted with abundant renewable energy sources of electricity the author is interested to integrate the renewable energy sources (solar energy) with the grid and battery. Integration of grid and renewable energy sources for EVs charging station can avoid uncertainties caused by the discontinuous nature of renewable energies and also could degrade the stress on the grid caused by simultaneous charging of numerous vehicles. Especially integration of grid-renewable energy source (solar energy) based on the countries perspective is highly essential.

1.3 Objectives

1.3.1 General objective

The research objective is to design and simulate DC micro-grid for EV charging

station and at the same time reducing the impact of electric vehicle on the distribution grid by using solar PV system and battery storage.

1.3.2 Specific objective

- Design of DC microgrid for solar-assisted EV charging stations
- Forecast solar energy of next day using machine learning
- Design solar PV system and battery storage system
- Power flow management using fuzzy logic controller
- Analysis of operational cost of the system

1.4 Scope of the Study

The scope of this study limited to design of DC-micro grid and simulation for charging station. The DC micro-grid integrates solar energy, grid and battery. The solar energy in this thesis is designed to be early forecasted one day in advance; this forecasting model is developed by using machine learning from historical weather data taken from Hawassa metrological station. For integration of grid, solar energy and battery the author used fuzzy logic controller from MTh lab Simulink and effectively simulated the DC micro grid for charging station. The limitation of the study is the author did only simulation and no practical verification/experiment is done.

1.5 Significance of the research

Electric Vehicles (EVs) are a promising technology for reducing the Green House Gas (GHG) emissions and other environmental impacts of road transport. Marathon Motor Engineering assembled the first Hyundai Ioniq electric cars in Ethiopia which can travel up to a 300 kilometerrange of emissions-free driving per a charge [15]. But the public charging infrastructure is not designed in Ethiopia. The research is mainly focused to use solar PV system energy as first option by this we can reduce dependence on fossil fuels, lower greenhouse gas (GHG) emissions and reduce impact of electric vehicles on the grid. Therefore this research is very significant as electric vehicle has limited battery storage.

1.6 Organization of the study

This research paper contains six sections. Section one provides information on background of the study, problem statement/motivation of the study, general and

specific objective, significance, and scope of the study. Section two reviews literatures related to EVs, DC- grids, architecture of DC-grids for charging stations, design consideration of solar energy and overview of machine learning for solar energy forecasting, overview of battery for energy storage applications and overview of fuzzy logic controller. At the end of section two framework of the research was presented. Section three deals research methodology namely data collection and data analysis mechanism. In section four the details of the proposed System Architectures of DC micro-grid for charging station will be presented. In section five performance analyses using matlab simulation is conducted and the result is presented. In the final section of this study conclusion and recommendation of the study is given.

CHAPTER TWO

2 LITERATURE REVIEW

With the large-scale, worldwide promotion of renewable energy and EVs, the joint development of the power and transportation sectors is a relatively new and promising research area. This section reviews existing literature on the electric vehicle development and construction of renewable energy charging facilities according to two aspects, namely, research purpose and methods. Research on the topic of combining renewable energy system and EV charging system from the aspect of technology, economy and actual application is rare. Goldin et al. [16] argued that solar-powered charging stations may significantly weaken the influence of EV charging on the local grid.

2.1 Introduction about electric vehicles

An electric vehicle (EV) is a vehicle that uses one or more electric motors or traction motors for propulsion. An electric vehicle may be powered through a collector system by electricity from off-vehicle sources, or may be self-contained with a battery, solar panels, fuel cells or an electric generator to convert fuel to electricity [17]. EVs include, but are not limited to, road and rail vehicles, surface and underwater vessels, electric aircraft and electric spacecraft.

Electric vehicles (EVs) are a “hot item” in the auto world, with many auto manufacturers offering at least one model. But electric powered autos are not a new technology. Although EVs may seem like the latest and greatest invention, in reality the technology has been around for more than a century. In the 1890s, electric cars were more popular than gas-powered autos because of their simplicity, reliability, and low cost of operation. In fact, Henry Ford’s wife drove an EV [18].

The first mass-produced electric vehicles appeared in America in the early 1900s. In 1902, "Studebaker Automobile Company" entered the automotive business with electric vehicles, though it also entered the gasoline vehicles market in 1904. However, with the advent of cheap assembly line cars by Ford, electric cars fell to the way side [19].

Due to the limitations of storage batteries at that time, electric cars did not gain much popularity, however electric trains gained immense popularity due to their economies and fast speeds achievable.For a variety of reasons, EV technology languished with the rise of gas-powered engines, but today, EVs – once again—are charging to the auto transportation forefront. This resurgence is fueled by significant advancements in power electronics and energy storage technologies.

In the 21st century, EVs have seen a resurgence due to technological developments, and an increased focus on renewable energy. A great deal of demand for electric vehicles developed and a small core of do-it-yourself (DIY) engineers began sharing technical details for doing electric vehicle conversions. Government incentives to increase adoptions were introduced, including in the United States and the European Union [20-21].

The high popularity of electric vehicles (EVs), especially plug-in electric (PEVs) and plug-in hybrid electric (PHEVs) vehicles, of recent years is a result of the heightened concern for climate change and the advancements in battery technology. This trend is expected to continue world-wide as battery technology drives EV prices down and consumer comfort up, increasing the attractiveness of electric driving. For instance, the highly anticipated Tesla Model 3, due fall 2017 was reserved almost 400,000 times within 2 weeks world-wide [22].

2.2 Over view of electric vehicles chagrining stations

An electric vehicle charging station, as explained in section one also called EV charging station, electric recharging point, charging point, charge point, electronic charging station (ECS), and electric vehicle supply equipment (EVSE), is an element in an infrastructure that supplies electric energy for the recharging of plug-in electric vehicles—including electric cars, neighborhood electric vehicles and plug-in hybrids.

Besides the increased use of EVs another trend that is linked to the energy transition is the increase in decentralized power generation. EVs and green, decentralized energy generation can become important keys to unlocking future sustainable energy systems. According to [23] the increase of distributed generation (DG) can lead to situations where the market price no longer follows the market

demand.

Many papers including [23]; tells that between home, work and public charging, drivers most often charge at home. This charging peak time coincides to a large extent with the already occurring residential load peak. Seeing the load of PEVs imposes a significant increase to a normal house load the uncontrolled charging of a large PEV fleet can lead to for instance frequency fluctuations and grid failure for (de)central power systems.

Charging stations fall into four basic contexts [24]:

1. Residential Charging Stations: The EV users plug in when they return home, and their car recharges overnight. A home charging station usually has no user authentication, no metering, and may require wiring a dedicated circuit. Some portable chargers can be wall mounted as a charging station.

2. Charging While Park: A commercial venture, offered in partnership with the owners of the parking lot. This charging may be slow or higher speed, and encourages EV users to recharge their car while they take advantage of nearby facilities. It can include parking stations, parking at malls and small centers.

3. Charging at Public Charging Stations: These chargers may be at rest stops to allow for longer distance trips. They may also be used regularly by commuters in metropolitan areas, and for charging while parked for short or longer periods.

4. Battery Swaps or Charging in Less than 15 Minutes: It is achievable with EV battery swaps and Hydrogen Fuel Cell vehicles. It intends to match the refueling expectations of regular drivers. This had been possible due to the reasons that battery capacity and the capability of handling faster charging are both increasing.

From those charging station types depending on type of EVs and considering the energy challenge the public charging stations was chosen. To use public charging station as explained in section one it is reasonable to design DC microgrid for DC fast charging station.

2.3 Overview of DC Micro-Grids

In the Micro-Grid context, direct current (DC) Micro-Grids are seen as a major advantage, since renewables (PV, Wind, fuel cells), electronic loads, electric vehicles, and storage (batteries, supercapacitors) have DC nature. If they are connected through a DC grid, they would need a smaller number of converters, and

those converters would be simpler than if they are connected through an AC grid. The result would be less expensive materials, and better efficiency (fewer losses). DC micro-grid has the ability of conversion losses reduction on the demand side [25].

Also, direct current can be more efficient due to its simpler topology; the absence of reactive power and frequency to be controlled; the harmonic distortion is not a problem anymore; and there is no need of synchronization with the network. The consequence is a simpler control structure based on the interaction of currents between the converters, being the DC bus voltage the main control priority, that is, the voltage is a natural indicator of power balance conditions. At the same time, the DC Micro-Grid is a challenge because the structure of the current power grid, power supplies, transformers, cables, and protection is designed in alternating current. For this reason, hybrid AC/DC Micro-Grid is seen as a compromise between AC and DC to allow for better integration of these new devices and the classical electric grid [26-28].

2.4 Solar PV system as renewable energy source for charging station

The current grid infrastructure is not capable of supporting the desired high charging rates of level-III. Thus, achieving fast charging rates while solely relying on the electrical grid does not only require the improvement of the charging system, but also the improvement of the electrical grid capacity. Additionally, drawing large amounts of current from the electrical grid will increase the utility charges especially at the peak hours and consequently will increase the system cost. Several factors are driving the steady rising use of RES as follows:

- The global concerns about climate change and the need to reduce greenhouse gas emissions.
- The national dependence on the imported oil associated with higher penetration of renewable energy sources.
- The rising retail tariffs accompanied with the global rise of the oil prices

Solar energy is a preferable DG source in EV charging applications for three reasons:

1. The PV panels are more effective than other renewables (e.g. wind energy) in populated and residential areas due to their noise free operation and low maintenance requirements.
2. PV panels generate most of their energy during the highly priced grid tariff hours of the electrical grid. Thus, the EV charging stations can offset the high costing electricity with solar energy during the peak hours.
3. The PV array will be used as canopy for battery storage or electric vehicles.

2.4.1 Solar Photovoltaic Cell Technology

Solar cells are devices (modules) which convert solar energy directly into electricity either directly via Photovoltaic (PV) effect or indirectly by first converting to heat or chemical energy then to electricity. The most common and focus of this research work is the PV effect solar energy. The physics of the PV cell is very similar to that of the classical diode with a p-n junction in which radiation of photons (light) is falling onto the junction of two dissimilar layers of semiconductor device to produces a potential difference between the layers. This developed voltage is capable of driving a current through an external circuit. The current squared times the resistance of the circuit is the power converted into electricity. The remaining power of the photon elevates the temperature of the cell and dissipates into the surroundings [29].

Figure 2.1 shows the basic cell construction in which metallic contacts are provided on both sides of the junction to collect the electrical current induced by the impinging photons. A thin mesh of silver fiber on the top (illuminated) surface collects the current and lets the light pass through. The spacing of the conducting silver fibers in the mesh is a matter of compromise between maximizing the electrical conductance and minimizing the blockage of the light. The front face of the cell has an antireflective coating to reduce reflection and to absorb as much light as possible at the metallic silicon surface. The mechanical protection is provided by a cover glass applied with a transparent adhesive.

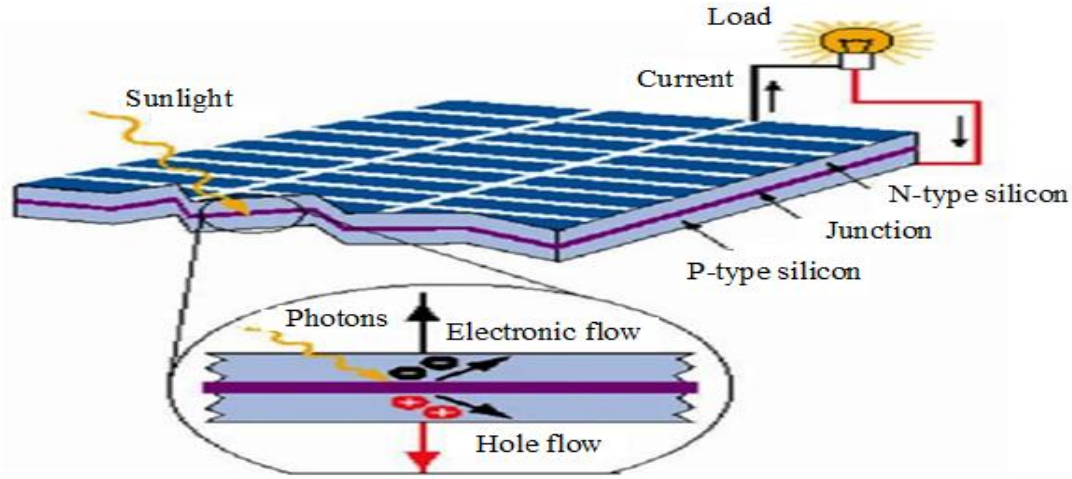

Figure 2. 1 Basic Construction of PV Cell with Performance Enhancing Features [30].

To understand the operation of a Photovoltaic cell both the nature of the material and the nature of sunlight need to be considered carefully. The determining factors for the amount of power generated from a PV device include: type and area of the material, intensity of the sunlight (insolation) and wavelength of the sunlight. The ratio of electrical energy produced by a solar cell to the incident solar irradiance is known as the PV cell efficiency [30].

2.4.2 PV system architecture

The solar cell described above is the basic building block of the PV power system. To generate required amount of power (current and voltage quantities), numerous such cells have to be connected in series and parallel circuits on a panel (module) with an area of several square meters. A single cell only generates a voltage in the range of 0.5 - 0.8 V which is not enough to power the load. PV power system offers the highest versatility among renewable energy technologies. Being the PV systems are modular, the electrical power output can be engineered for virtually any application.

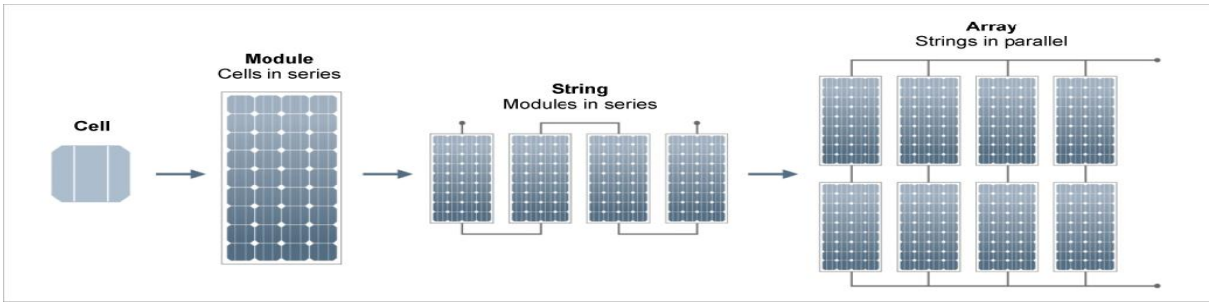

Figure 2. 2 PV system structure from cell to array

The electrical characteristic of the PV cell is generally represented by the I-V curve, Figure 2.3. In the figure, the top left of the I-V curve at zero voltage is called the short-circuit current. The bottom right of the curve at zero current is called open-circuit voltage. In the left of broken line region, the PV cell works as constant current source which is generating a voltage to match with the load resistance. In the right of broken line region, the current drop rapidly with a small rise in the voltage and the cell works like a constant voltage source with an internal resistance. Somewhere between the two regions, the curve has a knee point.

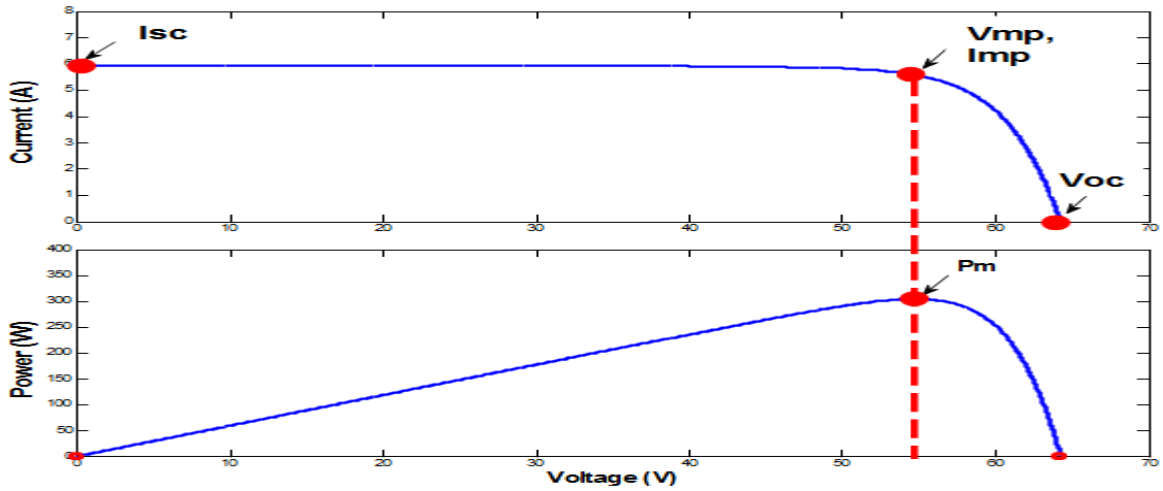

Figure 2. 3 I-V and P-V Characteristics of the PV module In Sunlight

The power output of the panel is the product of the voltage and current outputs and the power is plotted against the voltage in figure 2.3 together with I-V curve. The graph shows, the PV cell doesn't produce power at zero voltage or zero current and generates the maximum power at the voltage corresponding to the knee point of the I-V curve. This is why the PV power circuit is always designed to operate close to the knee point with slight slant to the left side, current source. The PV circuit is modeled approximately as a constant current source in the electrical system analysis. The power output of a PV system is determined by the type and area of the PV material and the incident solar radiation [31].

Mathematically, it can be expressed by equation:

$$P_{PV} = \eta_{mp}\eta_{pc}A_{PV}G_T \quad 2.1$$

Where: P_{PV} = power output of PV array (W)

A_{PV} = the area of the PV (m^2)

η_{mp}= the maximum power point efficiency of the PV module(≈14%-20%)

η_{pc}= the efficiency of power conditioning equipment(≈90%)

G_T = the incident solar radiation on the array (W/m2)

As it is represented in equation (2.1) above the output power of solar PV system variation mainly depends on the incident solar radiation (G_T) and G_T itself depends on related weather conditions of the area. Therefore for effective use of solar energy and system reliability solar radiation forecasting needed.

2.4.3 Solar radiation forecasting for PV system

Currently PV is becoming an important renewable energy source, and large numbers of relatively small photovoltaic systems are thriving around the world. Integration of large amounts of PV into the electricity grid poses technical challenges due to the fluctuating characteristics of available solar energy sources. PV output is not easily predictable in advance and varies based on both weather conditions and site specific conditions. Such variability of solar energy resources at ground level thus raises concerns regarding how to manage and integrate output from the PV to the power grid. Irradiance is a measurement of solar power and usually measures the power per unit area. Today it is widely acknowledged by power producers, utility companies and independent system operators that it is only through advanced forecasting, communications and control that these distributed resources can collectively provide a firm, dispatchable generation capacity to the electricity market. One of the challenges of realizing such a goal is the precise forecasting of the output of individual photovoltaic systems, which is affected by a lot of factors. Machine learning is one of the recent technologies that integrated to renewable energy operation which can be applied to forecasting of renewable energy since they are seasonal. Automatic solar energy forecasting forecasts the relationships between weather conditions and irradiance characteristics according to the data recorded in the data base of metrological stations. These techniques can roughly be categorized into two types:(1) indirect forecasting methods: For the indirect methods, solar irradiance is predicted based on historical solar irradiance and weather data, and then is converted to PV power output. (2) Direct forecasting methods:The direct methods predict PV power output according to their historical data and associated weather information [32].

Most researches consider the solar irradiance forecasting at a site, which is

essentially the same problem as forecasting solar power. The ability to forecast solar irradiation will enable power grid operators to be able to ensure the quality and control of solar electricity supplies in an environment of greater solar panel usage, allow them to better accommodate highly variable electricity generation in their scheduling, dispatching, and regulation of power.

In particular, the possibility to forecast solar irradiance can became fundamental in making power dispatch plans, and also a useful reference for improving the control algorithms of battery charge controllers. Ultimately, the development of more accurate methods for modeling and forecasting solar irradiance remains a key requirement of our future energy system.

Different solar irradiance forecast methodologies have been proposed for various time horizons. Some of them forecast up to 5-30 min, hourly, 24 h, for every 3 h of the next day, next day or even more [31-33]. For this research forecasting is for next day's irradiance. The reason for selection of next day is to use or leave stored battery energy depending on forecasted irradiance level of next day this we can decide the using of battery. If the next day irradiance will be high we will use stored energy today if not will leave it for next day.Accurately forecasting direct normal irradiance or global horizontal irradiance in the time-frame ultimately enables finely-tuned dynamic operational schedules that can reduce fuel costs, increase network stability or maximize system lifetimes.

Machine learning methods have been used to solve complicated practical problems in various areas [34] and are becoming more and more popular nowadays. Several machine learning based methodologies, such as logistic regression, linear regression, decision tree, have been proposed and applied for modeling and forecasting

Even though the application of machine learning based forecasted is become common in developed countries the application of machine leaning for forecasting renewable energy resource in many papers related to this paper is not used and in Ethiopia also it is still not exploited. Since Ethiopia is a country which has its own weather conditions it is very important to develop a machine learning algorithm which can forecast energy generated from solar energy. In this research since the author gets the daily based weather data from Hawassa metrological station and interested to develop a model which canforecast next day solar irradiance using

linear regression based techniques based on meteorological variables such as temperature, wind speed, humidity and solar.

2.5 Battery Energy storage system

2.5.1 Introduction

Battery is made of numerous electro-chemical cells connected in series-parallel combination to provide the desired battery voltage and current levels. The battery stores energy in an electrochemical form. It is the most widely used and important device to avoid components over-sizing in hybrid systems by storing in the time of excess generation and supplying power in shortage times. The rechargeable battery which is commonly called secondary battery converts electric energy to chemical energy in charge mode and converts chemical energy to electrical energy in discharge mode.

The battery rating is usually stated in terms of the nominal voltage during discharge time and the nominal ampere-hour (Ah) capacity it can deliver before the voltage drops below the specified limit (minimum state of charge). The main comparison parameters between different batteries are maximum throughput capacity (Ah) and minimum state of charge (in %). The maximum throughput capacity (Ah) is a life time delivery of ampere-hour (Ah) of a battery and minimum state of charge is the lowest percentage level of a battery will be discharged without losing its performance, it shows how depth it will be discharged.

Energy storage is a critical component in a micro-grid that is based on renewable energy [33]. Energy storage will help to maintain voltage stability and smooth out the fluctuations of renewable energy generation. Batteries which make use of a reversible chemical reaction to store energy and convert chemical energy into electrical energy will be used as the energy storage element in this DC microgrid [36].Rechargeable battery plays important role in future technology since it is potentially to be applied as energy storage element in green technology applications, such as electric vehicle (EV) and photovoltaic (PV) system.

In the aspect of technology, the rechargeable battery is improved from lead acid battery to nickel-based battery and from nickel-based battery to lithium-ion (Li-ion) battery.

Table 2.1 compares the characteristics of the six most commonly used rechargeable battery systems in terms of energy density, cycle life, exercise requirements and cost.

Table 2. 1 Characteristics of commonly used rechargeable batterie

	NiCd	**NiMH**	**Lead Acid**	**Li-ion**	**Li-ion polymer**	**Reusable Alkaline**
Gravimetric Energy Density(Wh/kg)	45-80	60-120	30-50	110-160	100-130	80 (initial)
Internal Resistance (includes peripheral circuits) in mΩ	100 to 2001 6V pack	200 to 3001 6V pack	<1001 12V pack	150 to 2501 7.2V pack	200 to 3001 7.2V pack	200 to 20001 6V pack
Cycle Life (to 80% of initial capacity)	15002	300 to 5002,3	200 to 3002	500 to 10003	300 to 500	503 (to 50%)
Fast Charge Time	1h typical	2-4h	8-16h	2-4h	2-4h	2-3h
Overcharge Tolerance	moderate	low	high	very low	low	moderate
Self-discharge / Month (room temperature)	20%4	30%4	5%	10%5	~10%5	0.3%
Cell Voltage(nominal)	1.25V6	1.25V6	2V	3.6V	3.6V	1.5V
Load Current - peak - best result	20C 1C	5C 0.5C or lower	5C7 0.2C	>2C 1C or lower	>2C 1C or lower	0.5C 0.2C or lower
Operating Temperature(discharge only)	-40 to 60°C	-20 to 60°C	-20 to 60°C	-20 to 60°C	0 to 60°C	0 to 65°C
Maintenance Requirement	30 to 60 days	60 to 90 days	3 to 6 months9	not req.	not req.	not req.
Typical Battery Cost (US$, reference only)	$50 (7.2V)	$60 (7.2V)	$25 (6V)	$100 (7.2V)	$100 (7.2V)	$5 (9V)
Cost per Cycle(US$)11	$0.04	$0.12	$0.10	$0.14	$0.29	$0.10-0.50
Commercial use since	1950	1990	1970	1991	1999	1992

Lithium-ion battery is potentially to be adopted as energy storage system for green technology applications due to its high power density, high energy density and fast charging/discharging capability.

Charging lithium-ion batteries is simpler than nickel-based systems. The charge circuit is straight forward; voltage and current limitations are easier to accommodate than analyzing complex voltage signatures, which change as the battery ages. The charge process can be intermittent, and Li-ion does not need saturation as is the case with lead acid. This offers a major advantage for renewable energy storage such as a solar panel and wind turbine, which cannot always fully charge the battery. The absence of trickle charge further simplifies the charger. Equalizing charger, as is required with lead acid, is not necessary with Li-ion.

Batteries are not faster at responding than super capacitors but they have the ability to store more energy which is a critical design consideration in microgrids [37]. The response time is quicker with super capacitors because the electrical energy can be stored directly without a chemical process [38]. The response time is not as critical in a DC microgrid because we don't have to worry about frequency regulation. Batteries can be damaged due to deep discharge therefore the state of charge should be limited to a reasonable region [39].

If fast charging and high load requirements are prerequisites, lithium-ion battery is best among types of batteries. Table 2.2 summarizes the charge characteristics of lead, nickel and lithium-based batteries.

Table 2. 2 Charger characteristics. Each chemistry uses a unique charge termination.

Type	Chemistry	C rate	Time	Temperatures	Charge termination
Slow charger	NiCd Lead acid	0.1C	14h	0ºC to 45ºC (32ºF to 113ºF)	Continuous low charge or fixed timer. Subject to overcharge. Remove battery when charged.
Rapid charger	NiCd, NiMH, Li-ion	0.3-0.5C	3-6h	10ºC to 45ºC (50ºF to 113ºF)	Senses battery by voltage, current, temperature and time-out timer.
Fast charger	NiCd, NiMH, Li-ion	1C	1h+	10ºC to 45ºC (50ºF to 113ºF)	Same as a rapid charger with faster service.
Ultra-fast charger	Li-ion, NiCd, NiMH	1-10C	10-60 minutes	10ºC to 45ºC (50ºF to 113ºF)	Applies ultra-fast charge to 70% SoC; limited to specialty batteries.

A battery can be modelled as a non-linear voltage source where the output voltage depends on the current and also the battery state of charge (SOC). The SOC is a non-linear function of the current and time [39]. The internal resistance and voltage depend on the battery SOC. The SOC can be defined as the ratio of the ampere-hour remaining in the battery to the total ampere-hour of the battery [40]. The internal resistance of a battery is nearly constant until the SOC reaches 80% then it increases exponentially. A diffusion capacitance builds up within a battery due to concentration difference between chemical species. The two diffusion layers have opposite charges with the electrolytes behaving as a dielectric which produces a capacitance effect called the diffusion capacitance. When a battery is charged faster than the chemical energy conversion process can handle side reactions take place. This causes the battery to be heated and hydrogen and oxygen gasses are produced in a process known as gassing [41].

2.6 Overview of charging station energy management

Numerous methods have been described in literature that aim at peak shifting, i.e. moving the PEV peak load away from the residential peak load. According to [42] there are three ways to optimize the exploitation of the positive effects of PEVs for the power grid (1) using pricing mechanisms (2) introducing demand response algorithms (3) and deploying and using vehicle-to-grid (V2G) technology. But this all methods did not bring solution for the charging station and did not satisfy the customers need. Therefore in this paper the authorused DC micro-grid which comprise PV, grid and battery to reduce impact EV load on the grid and used solar energy forecasting method using machine learning for effective use of energy sources with systemmanagement using fuzzy logic controller.

2.6.1 Fuzzy logic controller for power flow management

Fuzzy logic controller (FLC) is a method to figure out the behavior of the system.

Why fuzzy logic controller chosen? : Traditional optimization techniques and methods have been successfully applied for years to solve problems with a well-defined structure/configuration, sometimes known as hard systems. Such optimization problems are usually well formulated by crisply specific objective functions and specific system of constraints, and solved by precise mathematics. Unfortunately, real world situations are often not deterministic. There exists various types of uncertainties in engineering, social, industrial and economic systems, such as randomness of occurrence of events, imprecision and ambiguity of system data and linguistic vagueness, etc. which come from many ways[43], including errors of measurement, deficiency in history and statistical data, insu□cient theory, incomplete knowledge expression, and the subjectivity and preference of human judgment, etc.

As pointed out by Zimmermann [44], various kinds of uncertainties can be categorized as stochastic uncertainty and fuzziness. Stochastic uncertainty relates to the uncertainty of occurrences of phenomena or events. Its characteristics lie in that descriptions of information are crisp and well defined, however, they vary in their frequency of occurrence. Systems with this type of uncertainty are the so-called stochastic systems, which can be solved by stochastic optimization techniques using probability theory.

In some other situations, the decision-maker (DM) does not think the commonly-used probability distribution is always appropriate, especially when the information is vague, relating to human language and behavior, imprecise/ambiguous system data, or when the information could not be described and defined well due to limited knowledge and deficiency in its understanding. Such types of uncertainty are categorized as fuzziness which can be further classified into ambiguity or vagueness. Vagueness here is associated with the difficulty of making sharp or precise distinctions, i.e. it deals with the situation where the information cannot be valued sharply or cannot be described clearly in linguistic term, such as preference related information. This type of fuzziness is usually represented by membership function which reflects the decision-maker's subjectivity and preference on the objects. Ambiguity is associated with the situation in which the choice between two or more alternatives is left unspecified, and the occurrence of each alternative is unknown owing to deficiency in knowledge and tools. A system with vague and ambiguous information is so-called a soft one in which the structure is ill-defined and it reflects human subjectivity and ambiguity/imprecision. It cannot be formulated and solved e□ectively by traditional mathematics-based optimization techniques or probability based stochastic optimization approaches.

However, fuzzy set theory [45, 46] which was developed by Zadeh in 1960's and fuzzy optimization techniques [43] provide a useful and e□cient tool for modelling and optimizing such systems. Modelling and optimization under a fuzzy environment is called fuzzy modelling and fuzzy optimization.

Fuzziness occurs when the boundary of piece of information is not clear-cut. Fuzzy set theory exhibits immense potential for effective solving of the uncertainty in the problem. Fuzzy set theory is an excellent mathematical tool to handle the uncertainty arising due to vagueness. Making decision in this system fuzzy logic controller is simple and very effective. Typically PEVs arrive at the charging facility with different State-of-Charge (SOC). Furthermore, the PV source is stochastic in nature, its power characteristic is nonlinear and the PEV batteries to be charged should be within certain voltage and current limits.

This process necessitates intelligent control of the power conditioning unit to manage the direction of power flow.

The research objective is to design DC micro-grid for EV charging station and at the same time reducing the impact of electric vehicle on the distribution grid. Using PV and storage battery is wise-ness to reduce the grid impact. But the nature of solar system is uncertain and the availability of vehicle is uncertain that means we cannot determine both of them. To manage power flow in this system fuzzy logic controller is the first and most important one. Because it makes human like decision depending on the inputs and rules given.

CHAPTER THREE

3 RESEARCH METHODOLOGY

3.1 Study Area

The study area is located in the Ethiopia; South Nation Nationalities and People Region, (SNNPR) capital city Hawassa. The Hawassa city is one of big cities in Ethiopia. It is located 273 km south of Addis Ababa via Bishoftu, 130 km east of Sodo, and 75 km north of Dilla. This city is home to Hawassa University (which includes an Agricultural College, a Main Campus and a Health Sciences College), Hawassa Adventist College, and a major market. Important local attractions include the St. Gabriel Church and the Hawassa Kenema Stadium. Fishing is a major local industry. The City lays on the Trans –African High Way which is an international road that stretched from Cairo (Egypt) to Cape Town (South Africa), [47]

Temperature/weather condition: It varies in the range of 5^0C in winter and 34^0C in summer. The city experiences a sub humid type of climate which is called 'WoynaDega' in Amharic language having an average annual temperature of about 20.3^0C and Mean Annual precipitation of 933.4 mm with rainfall of twice in a year (During Belg and kiremit)

Site inspection and data collection: "13 Months of Sunshine" is the slogan of the Ethiopian. Tourist Commission to imply the country's yearlong sunny weather and the 13 months that the Ethiopian calendar has.

Solar potential of study area: In the first step, the data taken from the National Metrological Service Agency. The sunshine duration, temperature, wind speed and humidity data is taken from the National meteorological agency of Ethiopia Hawassa branch. In order to determine the solar radiation from the measured sunshine hour, among different model describing solar radiation and sunshine hour. To access solar irradiation data from nasa site the latitude and longitude of Hawassa city used.

Table 3. 1 Geographical parameters

Station	Latitude	Longitude	Elevation
Hawassa	7°3′N	38°28′E	1708 meters

Table 3.2 Monthly averaged insolation incident of Hawassa (from NASA)

Month	Clearness Index	Daily Radiation (kWh/m^2/d)
January	0.658	6.02
February	0.657	6.410
March	0.616	6.350
April	0.576	6.040
May	0.575	5.920
June	0.537	5.420
July	0.476	4.830
August	0.485	5.010
September	0.547	5.640
October	0.612	6.040
November	0.676	6.250
December	0.685	6.100
Scaled annual average (kWh/m^2/day)		5.83

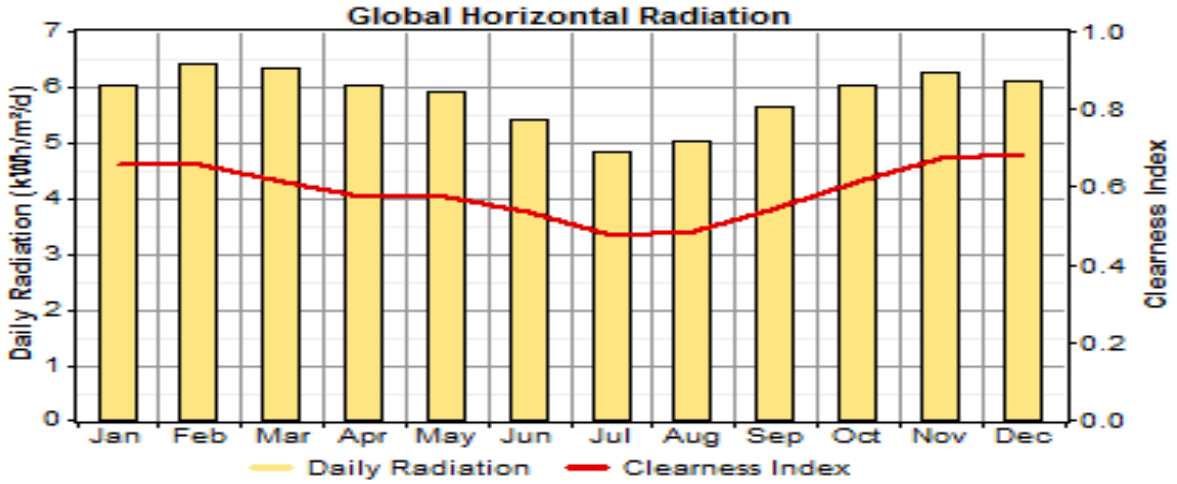

Figure 3. 1 Graph of global horizontal radiation of Hawassa

3.2 Sources and Types of Data

The study is conducted in Hawassa city. The study used secondary data obtained from Hawassa metrology station for design of PV solar forecasting. The study used the historical data of Hawassa metrology center from year 2017 - 2019. For background discussion and theoretical enlightenment a variety of books, reports, and articles were reviewed to make the study successful. The data contains about meteorological variables such as temperature, wind speed, humidity and sun shine and radiation. Additional weather data is also is incorporated from NASA report about solar irradiance for Hawassa.

3.3 Method of data analysis

As indicated in section 1, the main objective of this thesis is simulation of DC micro-grid for charging station. In detail the study is to design a micro grids-renewable energy hybrid system for charging station. Thus this section explains the method of design and analysis used to achieve the objectives.

3.3.1 Method for automatically forecasting of solar energy

As the authoris tried to introduce in section 2 big data driven technologies are becoming key to develop a model which can forecast solar energy. In this study the author developed a forecasting model which can forecast solar energy one day earlier. Machine learning is recognized as an efficient technique for forecasting as it offers a steady analysis based on the contributing features received from metrological stations. A forecasting system is a statistical model developed based on historical data of previous similar weather conditions and irradiance characteristics.

In this study theauthorused the weather data features (parameters) to develop a model which can predicts how likely the irradiation will be in the next day to predict the PV power. Such models are key for prediction of power that can be generated in the coming days and can serve as a means of keeping real time power balance.

In this study the author used machine learning algorithm (python as programming language) to develop forecasting model score system. Python is one of a well-known high level programming language in data science. In detail the author used Jupiter notebook to write Python codes. Jupiter notebook has very interesting libraries like numpy, pandas, MatPlotLib and Sci-Kit learn to make the programming easier. The key steps used in machine learning to develop forecasting model is shown in Fig 3.2.

The highlight of works done at each step is presented in the following section.

1. Importing data: Importing data is the process of bringing data to the jupyter notebook working area. Thus the historical data collected from Hawassa metrological station is imported to Jupiter notebook environment. Then, the data imported to Jupiter notebook working environment was further processed according to the nature of the imported data.
2. Cleaning Data: Since the data which is imported contains a lot of unimportant features for model development, it is necessary to clean the data. This step mainly deals with missing data, duplicated data, data types, correlation among features and extracting features which are important for forecasting process. Since Model cannot handle missing data removing features that have high percent of missing data is the key work in machine learning. The data received from Hawassa metrological station are not complete and the author removed those data which have missing data with certain limit of percentage. In machine learning it is advisable to drop those features which have high percent of missing data or substitute with meaning full data by preprocessing the original available data. Dealing with correlation:To avoid over estimation of the result multicollinearity test of the explanatory variable was studied
3. Train-test splitting of data: In machine learning some portion of the data collected is used for training the model while the remaining part is for testing the developed model. According to previous research findings different sample sizes of train test ratio were used by different authors to build different models. Thus, there are different possibilities to select the ratio of training/testing samples. Among these the 50% vs. 50% is the most commonly used in the literature. Based on these previous works the sampling selection used in this study is 50:50 distributions. That means 50% of the data is used to develop the model while the remaining 50% is used to test the model
4. Model selection: In machine learning based model development selecting appropriate model to train the data is key step. There are different methods such as discriminate analysis, linear regression, logistic regression, neural networks, vector machine, decision tree, decision forest etc.
5. Training the model:So once the model is selected the next step is to train the data using the selected model.
6. Prediction:Once the model is trained it is important to study the performance of the model by testing its prediction performance by using the test data. Thus, we predict the out puts using the test feature data at this step.

7. Evaluating the performance of model: This is the last stage of machine learning process where the performance of the model developed is tested. In machine learning environment there are a variety of approaches to measure predictive accuracy. One of the common methods to assess performance of accuracy.

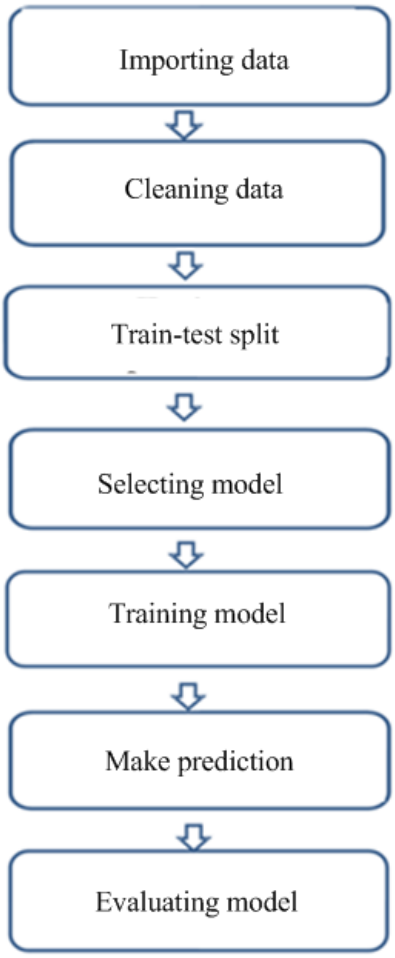

Figure 3. 2 Schematic illustration of machine learning steps

3.3.2 DC-micro grid integration and simulation

The proposed DC-micro grid contains renewable energy part (solar PV), grid, and battery. The integration of the system is simulated using matlab Simulink. The algorism theauthorused is fuzzy logic

Fuzzy logic control algorithm has led to the advancement of the existing smart grid technologies where it requires powerful control algorithm in an uncertain environment due to high penetration of the Renewable Energy Sources (RES). Due to the adaptive and human-like control decisions taken by Fuzzy Inference System (FIS), this would be much suitable to tolerate the uncertainties caused in multi-scenario operation of Micro Grid (MG). Fuzzy logic

controller provides possible solution on selection of distributed generators on the basis of voltage profile of the bus.

Fuzzy logic controllers have mainly three operations. First is fuzzification, which converts the input data in suitable linguistic values. Second is decision making, which makes the decision on the basis of defined rules. Third is defuzzification, which converts the outcomes into the system understandable data. Mamdani based fuzzy logic controller is used to control the complex and non-linear systems which is having the advantage that if changes happen in between the process, it is not required to change in the whole system from the initial condition [48].

Designing the fuzzy system requires that the different inputs are represented by fuzzy sets. The fuzzy sets are in turn represented by a membership function. The membership function used in this paper is the triangular membership function. The triangular membership function was chosen mainly because of its simplicity and appropriateness. Under normal conditions, the load of the electric vehicle and the power that is generated by the solar photovoltaic system are both uncertain and fuzzy due to the uncertainty and time-varying nature of sun and car availability. The input variable is fuzzified, and then the fuzzy rules and logic functions are used for calculation. After anti-fuzzy conversion, the actual reference output load condition of the DC Bus can be obtained.

CHAPTER FOUR

4 PROPOSED SYSTEM ARECHITECTURE DESIGN

4.1 Design of integrated system micro-grid for charging station

AC system is being used since years for power distribution and there are well developed infrastructure-standards and technologies. DC system on the other hand has many advantages, starting with the fact that overall efficiency of the system could be higher and it facilitates the integration of renewable energy sources with fewer power converters. Since PV arrays generate dc power, a charging facility featuring PV power facilitates the charging of PEVs from a dc bus which is more effective, economical and efficient since it does not involve more power conversion stages unlike AC charging. Various methods are there for integrating PEV chargers within a photovoltaic system. Several power electronic topologies for photovoltaic charging facilities (PCFs) are there based on the type and the number of converters from more some are classified as Centralized architecture while others are Distributed architecture.

Centralized architecture:Battery switch station powered by PV is a good candidate for adopting centralized architecture. But this kind of configuration does not support fast charging since installation of a very high power DC/DC converter is very expensive and it is vulnerable to single fault shutdown.

Distributed architecture:Presence of DC/DC converters with high power ratings is an important criterion for fast charging of PEVs. This can be achieved economically through distributed architecture. The system has a dedicated PV panel to support the charging of PEV and DC/DC converter and shares a common dc bus, which connected to an AC utility grid through AC/DC converter. For this research the author preferred to design inverter in another side of DC bus to send excess power from DC micro-grid to near customers or to distribution network back. This is because if one fault or damage occurs in bidirectional inverter the system cannot take power from grid or send to grid. The bidirectional DC/DC battery chargers are connected to the dc bus. It is more reliable since the PEVs can be charged from the grid during the periods of low insolation or cloudy weather. Also, it is important to note that the extra energy generated by PV can be injected into grid, which can be used to balance the PV costs. A PCF requires constant power from the PV or the grid to meet the high demand of PEVs. The reliability of a PCF can be improved by including an energy storage unit like a battery bank. Therefore the proposed architecture of this research is distributed architecture.

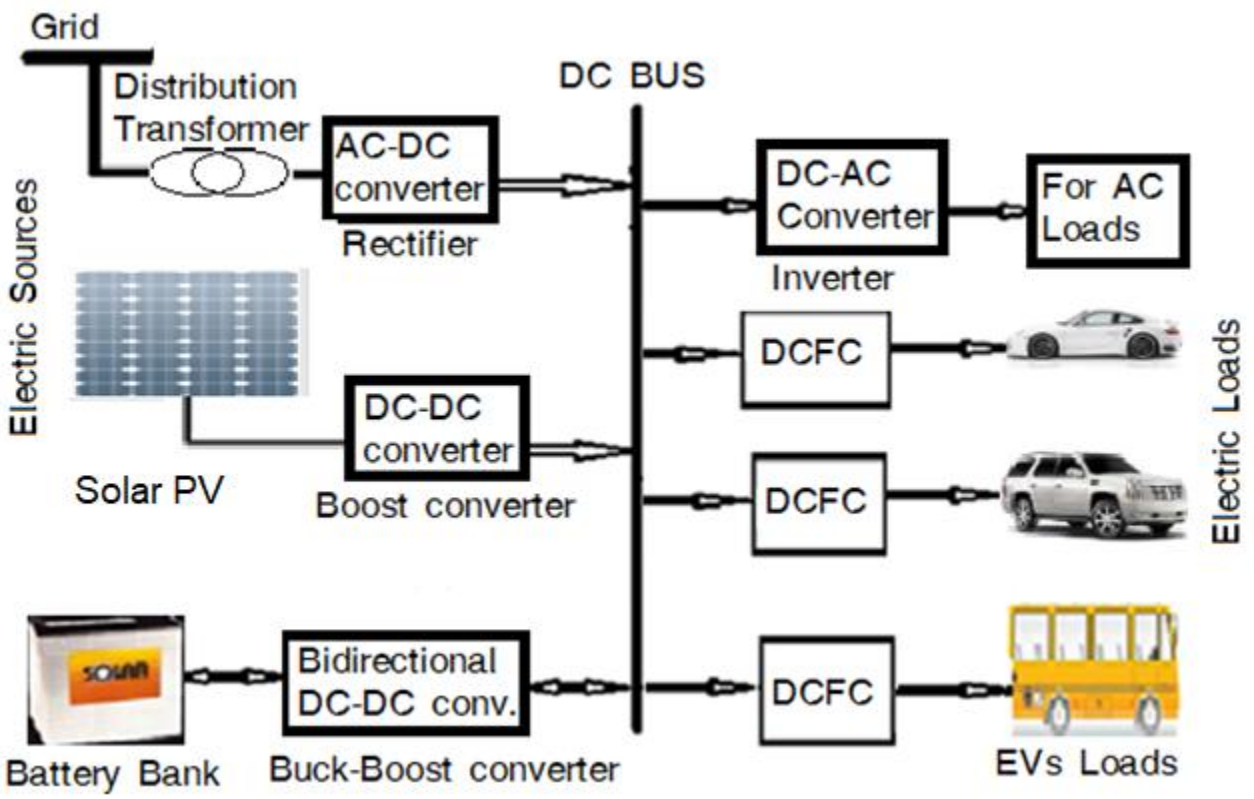

Figure 4. 1 Concept diagram of DC micro-grid for EV charging system

4.2 The Power Grid

The grid is an interconnected web of production and consumption centers and its basic function is to move power from where it is generated to where it is utilized. We can use the grid for dc loads by rectifying (through AC –DC converter) and we can send power from dc sources to grid by inverting it (through DC –AC converter).

4.3 Modeling and Design of Solar PV System part

The photovoltaic system is one of the way that can generate direct current electricity without environmental impact when is exposed to sunlight. This part focus on modeling of the PV system using matlab/Simulink. This detail matlab/Simulink model of PV has been shown how the PV system works using solar energy. The output characteristic of PV module depends on the cell temperature, solar irradiation, and output voltage of the module. The equation below shows the equivalent circuit of a PV array with a load. Usually the equivalent circuit of a general PV model consists of a photo-current, a diode, a shunt resistor $R_{sh,}$ which expresses a leakage current, and a series resistor (Rs), which describes an internal resistance to the current flow. The voltage current characteristic equation of a solar cell is given as,

$$I = N_p\ I_{ph}\ - N_P I_o \left[exp\left(\frac{q(V_{pv}+I_{pv\,Rs})}{N_S\,AKT}\right) - 1\right] - \frac{V+IR_s}{R_{sh}} \quad 3.1$$

The photocurrent mainly depends on the cell's working temperature and solar irradiation, which is explained as,

$$I_{ph=}[I_{sc} + K_i\,(T - T_{ref})]\left(\frac{G}{1000}\right) \quad 3.2$$

The saturation current of the cell varies with the cell temperature, which is represented as,

$$I_S\ =\ I_{rs}\,(\frac{T}{Tref})^3\left[exp\left(\frac{qE_g\ (\frac{1}{T_{ref}}-\frac{1}{T})}{KA}\right)\right] \quad 3.3$$

The shunt resistance $R_{sh}$of the cell is inversely related with shunt leakage current to the ground. Usually efficiency of PV array is insensitive to variation in R_{sh} and the shunt-leakage resistance can be assumed to approach infinity without leakage current to ground.

The open-circuit voltage, V_{oc} and short-circuit current, I_{sc} are the two most important parameters used which describes the cell electrical performance. The above mentioned equations are implicit and nonlinear; hence, it is not easy to arrive at an analytical solution for the specific temperature and irradiance. Normally $I_{ph} \gg I_S$, so by neglecting the small diode and ground-leakage currents under zero-terminal voltage, the short-circuit current is approximately equal to the photo current, i.e. $I_{ph}\ =\ I_{sc}$

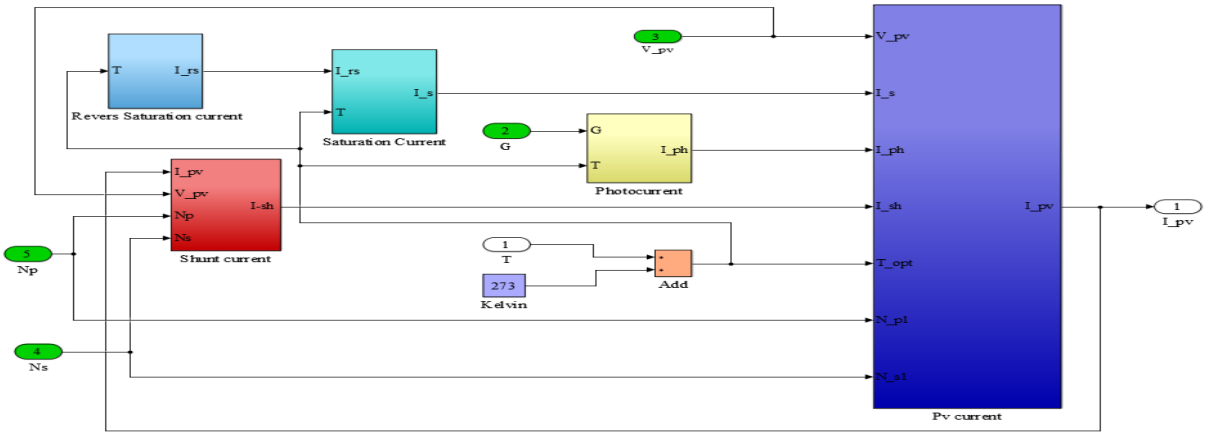

Figure 4. 2 Expanded view of the array subsystem

The open-circuit voltage parameter is obtained by assuming the zero output current. With the given open-circuit voltage at reference temperature and ignoring the shunt-leakage current, the reverse saturation current can be acquired as,

$$I_{rs}\ =\ \frac{I_{SC}}{[\exp\left(\frac{qV_{OC}}{N_S KAT}\right)-1]} \quad 3.4$$

$$I_{pv} = I_{ph} - I_s[\exp\left(\frac{q(V_{PV} + I_{PV} R_S)}{KTA}\right) - 1] \quad 3.5$$

There is no series loss and no leakage to ground for an ideal PV cell, So equation can be rewritten as:

$$I_{pv} = I_{ph} - I_s[\exp\left(\frac{q(V_{PV})}{KTA}\right) - 1] \quad 3.6$$

Therefore, the Matlab mathematical modeling of the equation described above are the following.

The detail of the array subsystem model in the Simulink is given in the Figure 4.3. A PV array is a group of several PV modules which are electrically connected in series and parallel circuits to generate the required current and voltage.

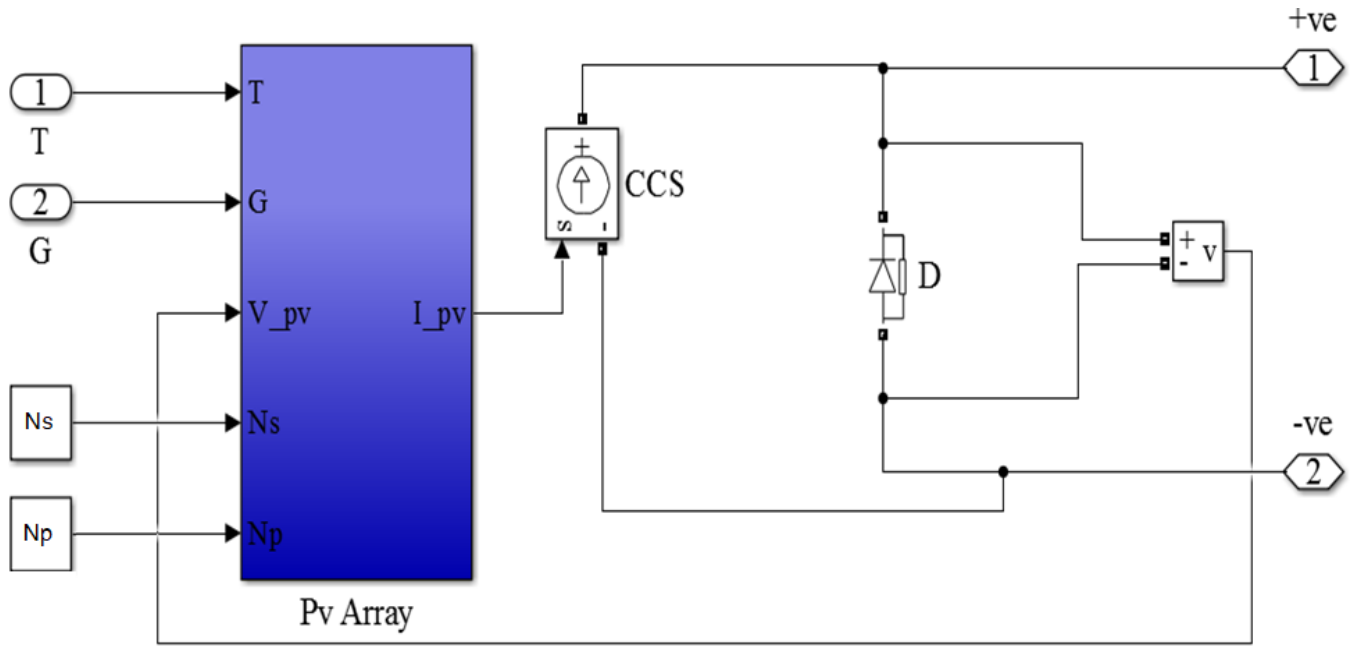

Figure 4. 3 Expanded view of photovoltaic model

Table 4. 1 The parameters used for the modeling of photovoltaic panel specification

Symbols	Value	Symbol Descriptions
K_i	0.0032	Temperature coefficient short circuit current
q	1.602e-19C	Electron charge
K	1.380e-23K	Boltzmann constant
K_v	0.123	Temperature coefficient of short circuit voltage
A	0.77	Ideality factor
Rs	1.302	Series resistance
Rsh	189.269	Shunt resistance
Tref	298	Reference temperature
G	1000	Module illumination (when G is constant)
Eg	1.1	Band gap of silicon
Voc	37.6	Short circuit voltage
Imp	8.20	Current at maximum power point
Vmp	30.5	Voltage at maximum power point
Ncell	54	Cells per module
Np	1	Number of parallel cells

4.3.1 PV Panel Selection and Array Sizing

1) Module Selection:

Module selection is made based on the specifications provided by the manufacturer. The panel's electrical performance is normally described by its characteristics delivered under maximum sunlight i.e. its peak power, voltage at peak power, current at peak power, short circuit current, and open circuit voltage. The module efficiency and the cost are the basic criteria used for this selection.

Number of Modules: Modules in a PV system are usually connected in series and parallel strings in order to achieve the design current and voltage. The chosen PV panel characteristics are presented in Table 4.2

Table 4. 2 Selected PV panel characteristics

Module :Samsung solar panel	Model : LPC250S
Performance at standard test condition(STC):at Irradiance 1000W/m^2, A.M 1.5, Cell Temp 25^{o}C	
Maximum Power (Pmax)**W**	250 W
Maximum Power Voltage (Vpm)**V**	30.5 V
Maximum Power Current (Ipm)**A**	8.20 A
Open Circuit Voltage (Voc)**V**	37.6 V
Short Circuit Current (Isc)**A**	8.66 A
Module Efficiency (%)	15.62%
NOCT	46° C

A solar PV system design can be done in load estimation and estimation of number of PV panels. The loads for this study are the components in the electric vehicles which takes electric energy for work done. The main components are electric motors, storage batteries and converters under the vehicle. The average energy consumption of electric vehicleis set to 0.2 kWh/km [49].

From published reports Table 4.3 illustrates common EVs and their battery capacity.

Table 4. 3Electric vehicles with battery type, range and charge time.

Model	Battery	Charge Times
ToyotaPrius PHEV	4.4kWh Li-ion, 18km (11 miles) all-electric range	3h at 115VAC 15A; 1.5h at 230VAC 15A
ChevyVolt PHEV	16kWh, Li-manganese/NMC, liquid cooled, 181kg (400 lb), all electric range 64km (40 miles)	10h at 115VAC, 15A; 4h at 230VAC, 15A
Mitsubishi iMiEV	16kWh; 88 cells, 4-cell modules; Li-ion; 109Wh/kg; 330V, range 128km (80 miles)	13h at 115VAC 15A; 7h at 230VAC 15A
Smart Fortwo ED	16.5kWh; 18650 Li-ion, driving range 136km (85 miles)	8h at 115VAC, 15A; 3.5h at 230VAC,15A
BMWi3 Curb1,365kg (3,000 lb)	Since 2019: 42kWh, LMO/NMC, large 60A prismatic cells, battery weighs ~270kg (595 lb) driving range: EPA 246 (154 mi); NEDC 345km (215 mi); WLTP 285 (178 mi)	11kW on-board AC charger;~4h charge; 50kW DC charge; 30 min charge.
Nissan Leaf	30kWh; Li-manganese, 192 cells; air cooled; 272kg (600 lb), driving range up to 250km (156 miles)	8h at 230VAC, 15A; 4h at 230VAC, 30A
TeslaS Curb 2,100kg (4,630 lb)	70kWh and 90kWh, 18650 NCA cells of 3.4Ah; liquid cooled; 90kWh pack has 7,616 cells; battery weighs 540kg (1,200 lb); S 85 has up to 424km range (265 mi)	9h with 10kW charger; 120kW Supercharger, 80% charge in 30 min
Tesla3 Curb 1,872 kg (4072 lb)	Since 2018, 75kWh battery, driving range 496km (310 mi); 346hp engine, energy consumption 15kWh /100km (24kWh/mi)	11.5kW on-board AC charger; DC charge 30 min
ChevyBolt Curb 1,616kg; battery 440kg	60kWh; 288 cells in 96s3p format, EPA driving rate 383km (238 miles); liquid cooled; 200hp electric motor (150kW)	40h at 115VAC, 15A; 10h at 230VAC, 30A 1h with 50kWh

To design the system that the batteries of the cars are topped up according to the average energy needs. For this research considering the different types of vehicles arriving charging station the author divided the vehicles ideallyreferring the table 4.3 with their battery capacity as 10kWh, 20kWh, 30kWh, 40kWh, 50kWh and 60kWh. For this research workputting as the charging station will serve three vehicles at once which will fully charge one vehicle with 30 minutes. To reduce grid impact system designed to cover all load from the photovoltaic power source. Based on the resource availability and capacity of energy extracted from solar PV sources storage battery and grid included as support. The energy requirement of system will vary from 0 to 180 kWh that means 0 to 360kW load requirement. Therefore study put 400 kW as peak load.

Time taken to fully charge a vehicle is:

$$t_{charging} = \frac{E_{needed}}{power}$$

Amount of power needed to charge vehicle is energy needed per time taken to fully charge avehicle.

$$power = \frac{E_{needed}}{t_{charging}}$$

2) Determination of System Voltage

System voltages are generally 12, 24, 48 or 120 Volts and the actual voltage is determined by the requirements of the system. As a general rule, the recommended system voltage increases, as the total load increases. For this system the loads going to be larger therefore 260 V is utilized.

The selected system having,

System Voltage (Vdc) = 260 V,

Average solar Radiation for the site (Ra) = 5.83 kWh/m2/day

Daily Average Demand (Ed) from PV subsystem is Ed =1800 kWh/day

Battery Efficiency selected as (ηb) = 0.85

converter Efficiency selected as (ηi) = 0.95

Charge Controller Efficiency selected as (ηc) = 0.90

For sizing, first the daily energy demand required (Erd) is required. Therefore,

$$\text{Erd} = \frac{Ed}{\acute{\eta} i} = 1800/.95 = 1895 \text{ kWh/day} \quad (3.7)$$

$$\text{Required PV av Ah/day} = \frac{Erd}{Vsystem} = 1895/260 = 7.3 \text{ kAh} \quad (3.8)$$

Then, PV array peak amp = $\frac{AV\ Ah/day}{ήc*ήb*ήa} = \frac{7.3}{0.9*0.85*5.83} = 1.64k$A 3.9

The number of parallel module strings (Npm) is calculated by dividing the total DC current of the system by the rated current of one module (Im);

Npm = $\frac{PV\ array\ peak\ amp}{Im} = \frac{1640}{8.2} = 2003.10$

The number of modules in series (Nsm) is obtained by dividing the system DC voltage by the rated voltage of each module (Vm);

Nsm = $\frac{Vdc\ system}{Vm} = \frac{260}{30.5} = 8.523 \approx 93.11$

Then, total number of modules (Ntm),

Ntm=Nsm*Npm=9*200 =1800 3.12

3) Controller Selection and Sizing

Charge controllers are sized according to the voltages and currents expected during operation of the PV system. Thus, the required charge controller current (Ircc) is:

Ircc=Isc*Npm*Fsafe = 8.66*200*1.25 = 2165A ≈ 2.5kA 3.13

4.3.2 Battery Bank selection and sizing

Sizing of the battery begins by determining the estimated energy storage (Eest), which is calculated as follows: The selected battery for the system is deep cycle lithium-ion battery. The nominal voltage (Vb) and rated capacity (Cb) of the selected battery are 100V and 500Ah, respectively. Further, maximum allowable Depth of Discharge (DOD) is 90% and hours of autonomy (Haut) are 8. Then, estimated energy storage,

Eest=Ed*Daut= Eest=1800*0.34= 612 kWh 3.14

A safe energy storage (Esafe) is then computed by dividing the obtained estimated energy storage by maximum allowable depth of discharge (Dod);

Esafe = $\frac{Eest}{Dod} = \frac{612}{0.9} = 680\ kWh$ 3.15

The total capacity of the battery bank in ampere-hours (C_{tb}) is determined by dividing the safe energy storage by the rated DC voltage of one battery (Vb),

$C_{tb} = \frac{Esafe}{Vb} = \frac{680}{100} = 6.8kAh$ 3.16

The total number of batteries (Ntb) is;

Ntb = $\frac{Ctb}{Cb} = \frac{6.8kAh}{500Ah} \approx 14$ 3.17

Number of battery in series (Nsb) is;

Nsb = $\frac{Vdc}{Vb}$ = 500/100 = 5 3.18

Number of battery in parallel (Npb) is;

Npb = $\frac{Ntb}{Nsb} = \frac{14}{5} \approx 3$ 3.19

4.4 Interfacing Energy Source with Charging Station

4.4.1 Modeling and Simulation of the Boost Converterfor solar PV

DC/DC choppers are electronic power components which convert DC voltage level to another DC voltage level. DC/DC converters are basic components for renewable energy system because of the fact that they are employed to adjust DC voltage of energy sources for voltage of loads. Particularly, DC/DC choppers were commonly used for voltage stability and improvement of controllability in smart grid applications. There are two basic chopper types: buck and boost for DC/DC conversion [50].

A boost converter has been made utilizing a capacitor, an inductor, a diode, and a switch that appears in Figure 4.4. The main component of the boost converter is the switching transistor. It turns some portion of a circuit on and off rapidly. Normally the speed of the switching can be more than 1000 times each second.This part will be dedicated to the DC-DC converter modelling with Simulink.

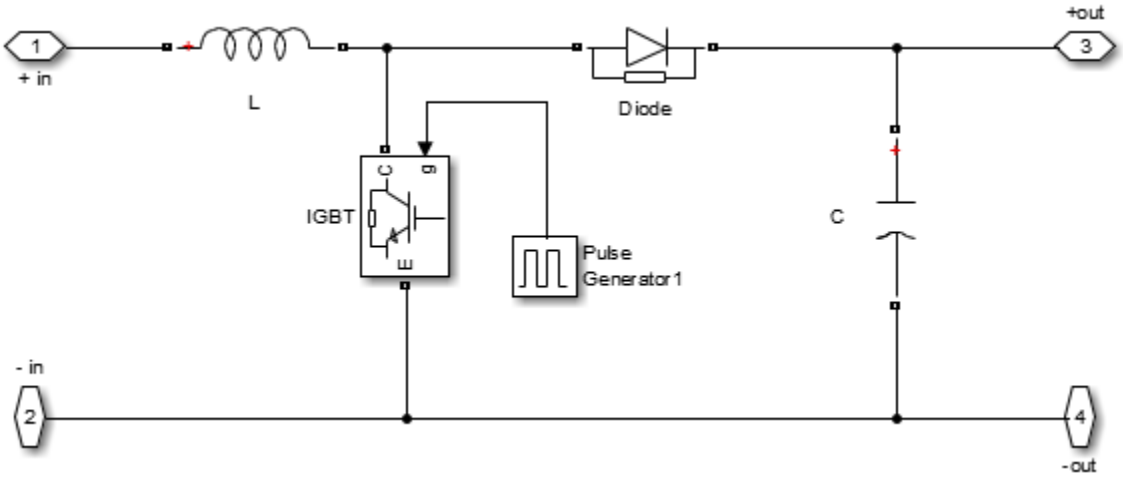

Figure 4. 4 DC-DC boost converter for solar PV in MATLAB Simulink

Switched mode power supply technique is commonly used to control the output voltage of DC/DC choppers. The input generator is a DC voltage source and the output generator is also a DC voltage source. The output voltage is always smoothed by a capacitor. PV array is connected to a DC/DC boost converter. The outputs of the boost converters are connected to a common DC bus of 500 V.

4.4.2 Modeling AC-DC converter

The AC/DC converters can be designed by using controllable (IGBT, Mosfet, Thyristor, etc) and uncontrollable (diode) semi-conductor switches according to required output voltage

[51]. The AC/DC converters are used in drivers, secondary power supply, chemical electrolysis and renewable energy systems. The AC/DC conversion contains three basic steps: Firstly; AC waveform is converted to only positive or negative cycle, secondly; filtering the cycle for reducing voltage ripple and finally; using an appropriate control method to prevent the harmonic distortions and increase the efficiency of the device**.** The rectifying process of the AC/DC converter was performed by the rectifier model of Simulink/Toolbox. The AC/DC converter model, which is designed in Matlab/Simulink environment, is shown in Figure 4.5. The rectifier block of Simulink/Toolbox is used for rectification of AC voltage and the LC pi filter is utilized to filter the ripple and improve the voltage stability for the load. The filter component and switching frequency can be changed according to the power rate.

Carrier-based Pulse Width Modulation Techniques: **T**he objective of a modulation technique is to generate a desired reference waveform with minimum distortion in the low-order harmonics moving the unavoidable distortion to the high-order harmonics making easier the filtering process. PWM is a simple and effective way to produce a switched voltage waveform whose time average is equal to a desired reference. This basic concept is the foundation that all other variations of classic PWM have in common. In PWM, the phase voltage is generated by comparing the reference voltage with a higher frequency carrier. The fundamental-frequency component in the output voltage can be adjusted by changing the amplitude of the modulation index *m*. The frequency modulation index *mf* is defined as the ratio between the frequencies of the carrier *fcr*and modulating wave's *fm*[50].

If *mf* is an integer, the carrier wave is synchronized with the modulating waveform and the modulation scheme is known as synchronous PWM; otherwise, it is called asynchronous PWM, in which *fcr*is usually fixed and is independent of *fm*. However, when *mf* is a small number (i.e. less than 21) its output spectrum contains low frequency harmonics (sub-harmonics) causing high currents in transformers and inductors. Note that in case of mf being a large number, the amplitudes of the sub-harmonics are much reduced and do not pose critical problems with the currents by inductors and transformers [50]. This fact is extremely important in power conversion applications because the necessary output filters can be minimized or even avoided at the expense of increasing the switching losses if *fcr*is too large.A direct method to increase the maximum amplitude of the output fundamental voltage is to raise m to be greater than unity, entering the nonlinear over-modulation region.

The over-modulation generates low-order harmonics and thus is rarely used in practice. Therefore, to increase dc voltage utilization, modified modulation schemes based on injecting zero-sequence signals into the modulating waveforms can be employed provided that the

neutral of the load is floating.

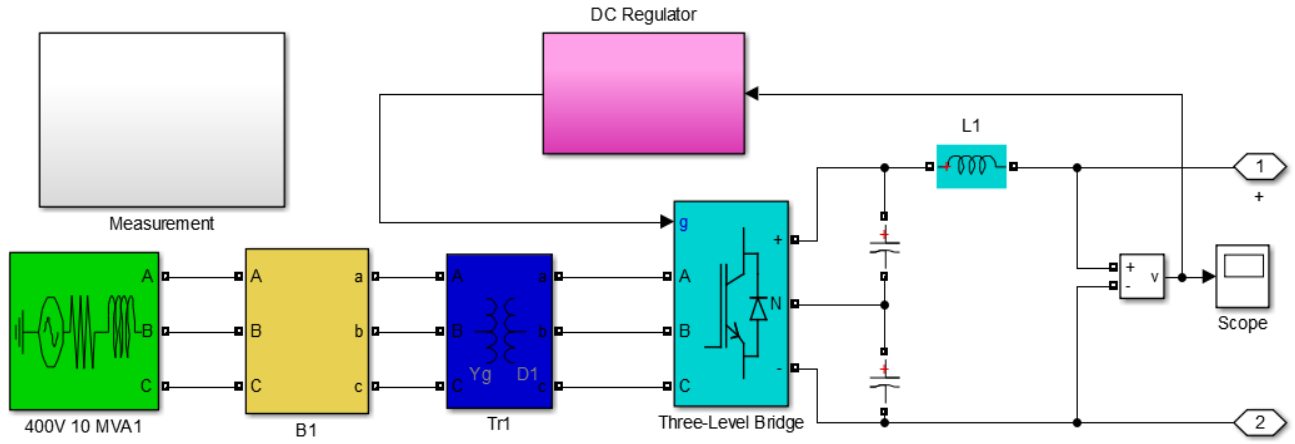

Figure 4. 5 MATLAB Simulink AC-DC converter

Start the simulation. After a transient period of approximately 50 ms, the system reaches a steady state. The 400V, 50 Hz voltage obtained at secondary of the Wye/Delta transformer is first rectified by a six pulse three-level bridge. The DC voltage obtained from rectifier is filtered using LC filter and given to DC bus of 500 Vdc. The harmonics generated by the inverter around multiples of 2 kHz carrier frequency are filtered by the LC filter.

4.4.3 Modeling DC-AC converter

An inverter can be identified as electronic power equipment which converts the DC voltage to one or three phase AC voltage. Inverters can be run in grid-connected and standalone modes according to electric source and load voltages. Therefore, system voltage control has a key role to protect the power quality. Voltage controlled inverters have significant advantages such as cost, compact design and higher efficiency. These inverters are used in power supplies, power quality controllers, marine, renewable energy systems, and military implementations

The filtered DC voltage is applied to an IGBT two-level inverter generating 50 Hz. The IGBT inverter uses Pulse Width Modulation (PWM) at a 2 kHz carrier frequency.

The load voltage is regulated at 1 pu (380 V rms) by a PI voltage regulator using abc_to_dq and dq_to_abc transformations. The first output of the voltage regulator is a vector containing the three modulating signals used by the PWM Generator to generate the 6 IGBT pulses. The second output returns the modulation index. The Multimeter block is used to observe diode and IGBT currents.

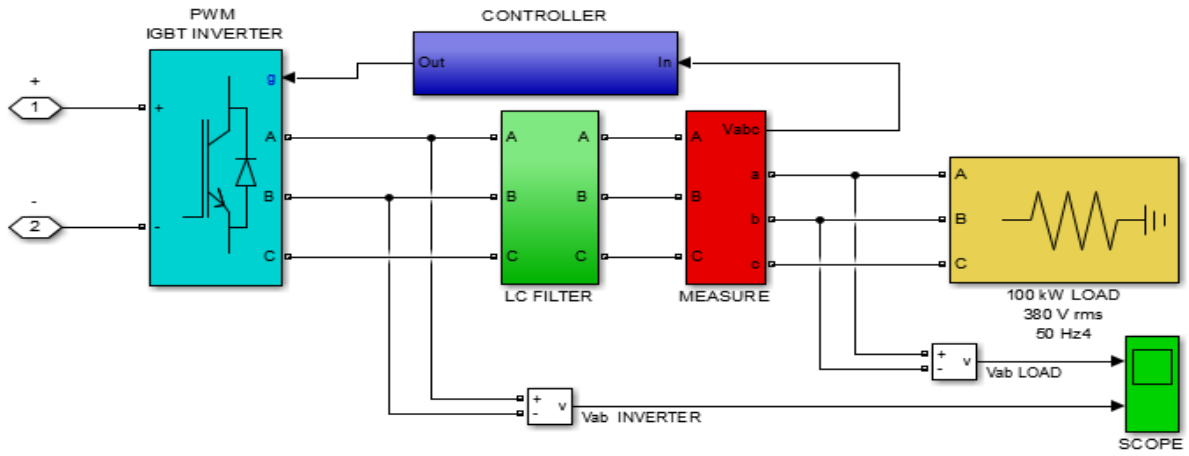

Figure 4. 6Matlab Simulink of DC-AC converter

Harmonic distortion due to inverter:Harmonics filters very effective to protect costly electrical equipment from distorted power outputs due to harmonics. Harmonics are created by non-linear devices connected to the power system. Power system harmonics are multiples of the fundamental power system frequency and these harmonic frequencies can create distorted voltages and currents. Distortion of voltages and currents can affect the power system adversely causing power quality problems. Therefore, estimation of harmonics is of high importance for efficiency of the power system network. Non-linear devices such as power electronics converters can inject harmonics alternating currents (AC) in the electrical power system. The number of sensitive loads that require ideal sinusoidal supply voltage for their proper operation has been increasing. To maintain the quality limits proposed by standards to protect the sensitive loads, it is necessary to include some form of filtering device to the power system. There are different types of harmonics filters available in the electrical and electronics market depending on the rated power, applied voltage, single phase or three phases and other load-dependent parameters.

However, there are two main types of harmonics filters available which are Passive Harmonic Filters and Active Harmonic Filter. The main difference between these two types of harmonic filters is the components used for the filter design. Passive harmonic filters use simple passive components mainly resistors, inductors, and capacitors. Whereas active harmonic filters use active components such as different types of BJTs, IGBTs, MOSFETs and integrated circuits. To achieve an acceptable distortion, increase the power quality and to reduce the harmonics hence three phase passive harmonic filters are used and connected in parallel. Passive harmonic filters are the most common and the easily available harmonic filter. It is affordable filter to suppress the harmonic disturbance in the power line.

As discussed before, passive harmonic filters use standard passive components such as resistors inductors and capacitors. Those passive components are used to form a tank circuit. The tank circuit is designed in a special way so that it can be operated at the same resonance frequency in respect to the unwanted harmonics. The passive harmonic filters block the unwanted harmonics to pass. The passive harmonic filter converts the harmonic current into the heat and protects the end device or load. The filter can be tuned to a certain frequency that needs to be eliminated as harmonics. Passive LC filters are conventionally used to suppress the harmonic distortion in power system.

Passive filters are series resonating or parallel resonating electrical circuit, which offer very high or very low impedance at tuning frequency. The filters are resistive at tuning frequency, capacitive below tuning frequency and inductive beyond tuning frequency.

Filters have two important characteristics: impedance and bandwidth. Low impedance is required to ensure that harmonic voltages have a low magnitude and certain bandwidth is needed to limit the consequences of filter detuning. Types of passive filters are: Single tuned filter, High pass filters, double tuned filters, and double tuned high pass filters, Triple tuned filters, continuously tuned filters. For this design the author selected Single tuned filter.

Single tuned filter

Single tuned filters as name suggests, are tuned to only one frequency and are simplest of all filters. The tuned frequency is depends on the designed value of inductor and capacitor for which it provides low impedance path. The advantages are: (1) Simple configuration with only two components, capacitor and reactor; (2) Quality factor of the filter is high which provides maximum attenuation of one; (3) Negligible losses as there are no resistor for damping etc. and (4) Low maintenance requirements because of fewer components.

On the other hand its disadvantage is high quality factor of the filter gives low bandwidth, which makes filter sensitive to variations in the fundamental frequency as well as the component values.

Formula for component value calculation:

$$C = \frac{Q}{V^2 * 2\pi f} \quad 3.20$$

$$L = \frac{1}{[(2\pi f_r)^2 * C]} \quad 3.21$$

Where

Q = Reactive power to be generated by the filter at fundamental frequency (Assumed)

V = voltage level at which filters are to be installed

f = Fundamental frequency

f_r = Tuning frequency (assumed)

The odd harmonics generated due to the inverter around multiples of 2 kHz carrier frequency before filtering was 74.59% and it is filtered by using the LC filter.

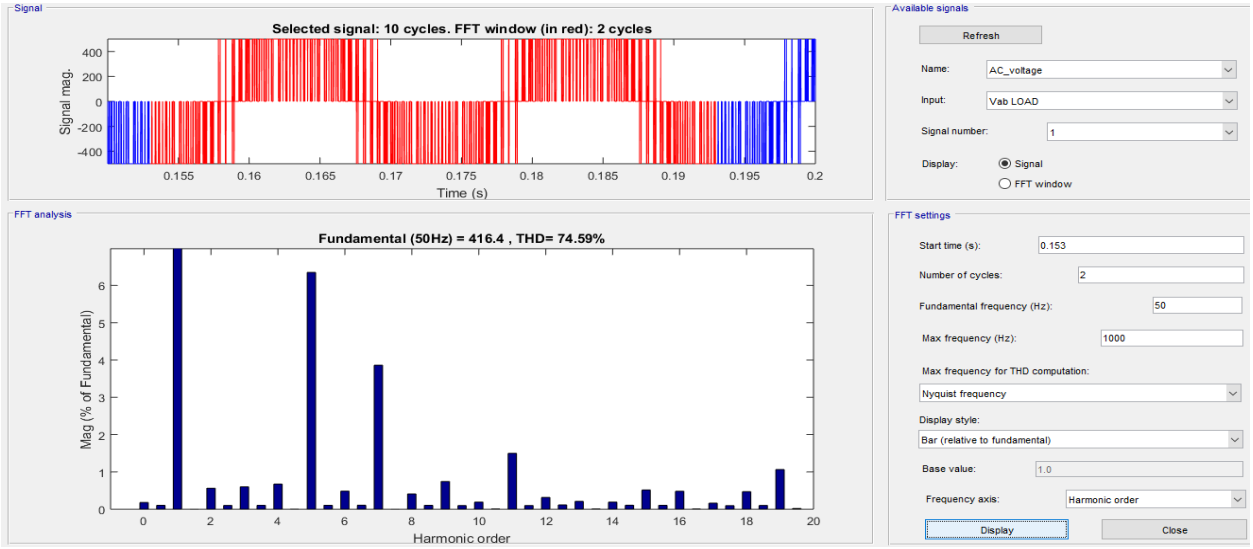

Figure 4. 7 Harmonic distortion before filtering

The harmonics generated by the inverter around multiples of 2 kHz carrier frequency are filtered by the LC filter. Notice harmonics around multiples of the 2 kHz carrier frequency. After filtering the harmonics is reduced to acceptable region. Accepted total harmonic distortion (THD) is below 3% and the reduced THD in this system is 2.21%.

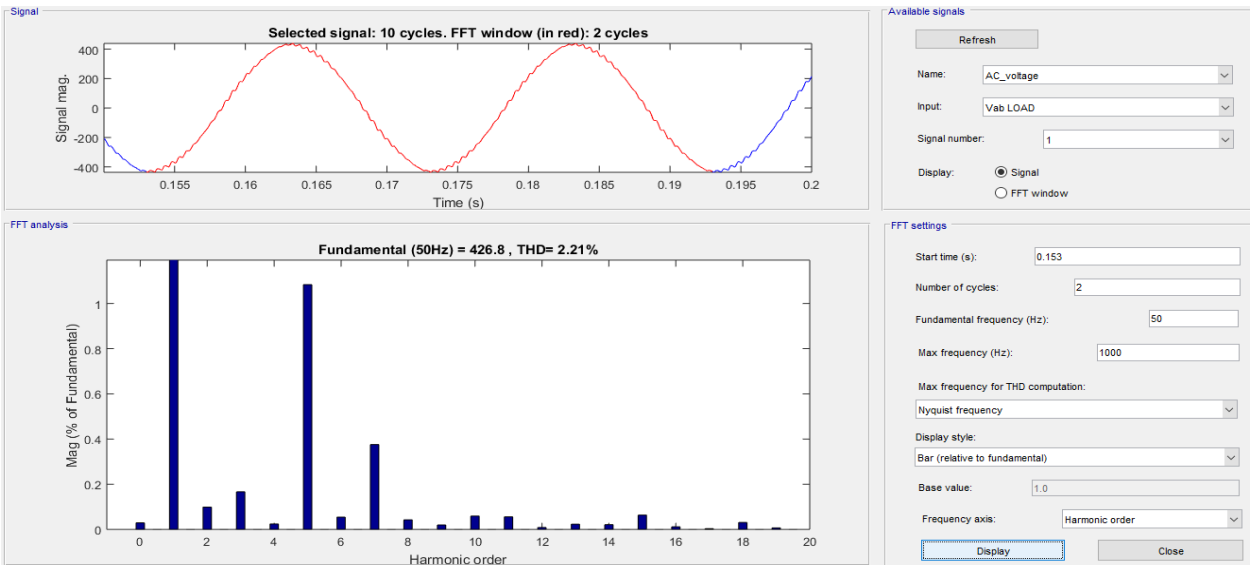

Figure 4. 8 Total harmonic distortion after filtering

4.4.4 Charging and discharging model of lithium-ion battery

A lithium-ion battery of 15.5 Ah and 3.7V nominal is selected for the EV storage application. The modified Shepherd model equation is used to develop the charge and discharge model of the lithium-ion battery. This model has no algebraic loop problem and may be modified with battery specifications for another battery model development. However, this battery model is considered to be operated at normal temperature.

$$V_{B\_ch}=E_0 - K\frac{Q}{it+0.1Q}xi^* - K\frac{Q}{Q-it}x\ it\ Ae^{-Bxit} - ixR, \quad 3.22$$

$$V_{B\_disch}=E_0 - K\frac{Q}{Q-it}xi^* - K\frac{Q}{Q-it}x\ it\ Ae^{-Bxit} - ixR, \quad 3.23$$

Where:

$V_{B_disch}$is the battery discharge voltage,

V_{B_ch} is the battery charge voltage,

E_0 is the constant voltage (V),

R is the internal resistance (Ω),

K is the polarization constant (Ah^{-1}) or resistance (Ω),

i is the battery current (A),

it is the extracted battery capacity (Ah)

Q is the maximum battery capacity (Ah)

(Ah), A is the exponential voltage (V),

B is the exponential capacity (Ah^{-1}), and

i* is the low frequency current (A).

The State-Of-Charge (SOC) of the battery (between 0 and 100%). The SOC for a fully charged battery is 100% and for an empty battery's 0%. The SOC is calculated as:

$$SOC = 100\left(1 - \frac{1}{Q}\int_0^t it(t)dt\right) \quad 3.24$$

4.4.5 Bidirectional DC-DC converter model for battery

The DC bus voltage is 500 Vdc therefore DC-DC bidirectional converter (i.e. buck boost converter) is needed to reduce 500 V bus voltage to 100 V for battery bank.

1) PI Controller and logic for the DC/DC converter

PI Tuning: Tuning the PI is not straight forward. However, the common way to do it is to put Ki to zero and Kp to fraction and according to the response on the scope start decreasing or increasing Kp. You will have a response near the desired value but not the exact desired

value because of the steady state error. Then you start put some values to Ki till you get the desired value. Sometimes you have to play with Kp and Ki put them to small numbers and start adjusting them according to the response you see on the scope.

The ideal way to do it, is to have the transfer function and tune the PI accordingly. However, such a system like the bidirectional is not linear, in other words, the circuits configuration changes with switching and the transfer function changes with it.

Current control: This is the current we control, it is being sent to the PI controller to be compared with the reference. For example, if you choose current reference to be -5, you will see here -5, if you choose 2, you will see here 2 and so on and so forth. For thesis work 3is chosen.

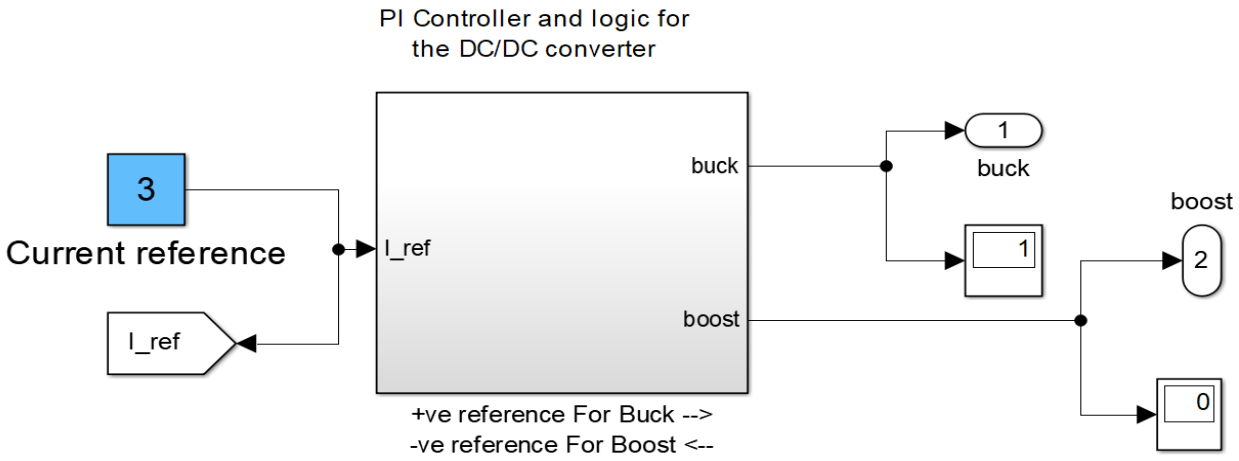

Figure 4. 9 PI Controller and logic for the DC/DC converter

Working principles: The measurement is compared with the reference, then we get the error the PI then translate the error to a duty cycle. For example, the measured current is 1A and the desired/ reference is 5A then the error is 4, however, the duty cycle only varies 0 to 1, therefore, we need a translator or converter to convert this error to something between 0 and 1, which is the PI. Since we know the range of the values of the input to the PI (i.e. error) and its output (i.e. duty cycle), this might be helpful also in tuning, to figure out Kp and Ki. Once we get the duty cycle, it is just a number and the IGBT switch only understand 1 or 0, then we compare the duty cycle number with a saw tooth signal (sawtooth vary from 0 to 1) to get pulses (i.e. zeros and ones) that go to the IGBT.

Lower -ve signs: is used because during boosting the current reverse direction and the measured current becomes negative, so to return to positive values we multiply by -1 and Upper -ve sign: So if the reference is -ve the logic understand it should boost, but in order not to miss up the controller we multiply it again with -1, so that it enter the summation positive as

it should be. The whole idea is to input the values to the controller positive numbers then we subtract.

The logic that decide whether the controller should boost or buck: For example: if the current reference is -ve (i.e. boosting), in the upper logic, -ve is not >= 0 then the switch will go down to get the signal from the PWM of the boost. For the lower logic, -ve is not > 0 then the switch will go down to zero pulses, therefore, the bidirectional will only boost.

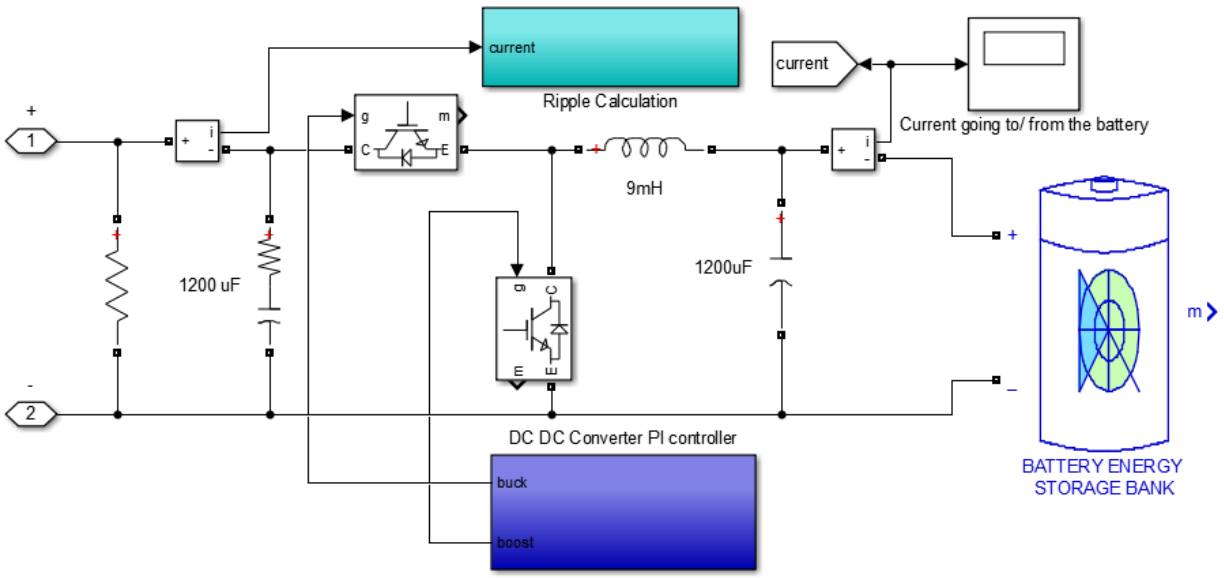

Figure 4. 10 Bidirectional DC-DC converter model for battery

4.5 Power flow management

4.5.1 Understanding power flow management

All the terminals connected to the DC bus can be classified into two types: power terminals and slack terminals. Power terminals indicate the sources, which either supply or consume power to/from the DC bus on their merits, and usually do not contribute to the control voltage of the bus. The DC loads, PV panels working in MPPT mode, are examples of power terminal sources. On the other hand, the function of slack terminal sources is to accommodate the power fluctuation caused by power terminals, and maintain power balance and stable voltage. BESS in voltage-controlled mode and VSCs are typical examples of slack terminals [52].

Each operation mode needs at least one slack terminal to balance overall power.On the contrary, when there are multiple slack terminals, cooperation should be done to avoid any possible conflict among them. The balance condition is guaranteed with the objectives of

maximum renewable energy extraction, optimizing usages of BESS, reducing energy imported from the AC grid, and maintaining bus voltage within the permitted range under the variation of the loads and sources.

Proper voltage:A power system is said to be well designed if it gives a good quality of reliable supply. Good quality basically means the voltage levels maintained constant or within the prescribed permissible limit. One important requirement of a distribution system is that voltage variations at consumer's terminals should be as low as possible. The changes in voltage are generally caused due to the variation of load on the distribution system. Too wide variations of voltage may cause erratic operation or even malfunctioning of consumers' appliances. To safeguard the interest of the consumers the government has enacted a law in this regard. The statutory limit of voltage variation is ±6% of declared voltage at consumers' terminals [53-54].

Considering this voltage variation limits operating range of DC bus voltage is divided into five regions

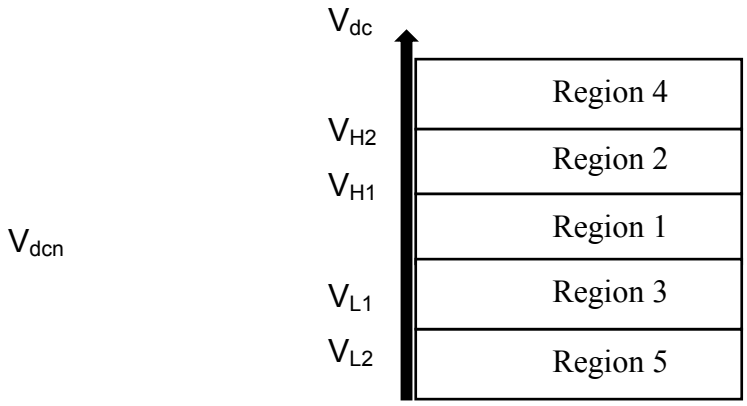

Figure 4. 11 Operation regions of DC bus voltage.

The figure description:

V_{dcn} = 500Vdc is the nominal voltage of the DC bus; V_{H2}=520Vdc is upper limit of the allowable Voltageof the DC microgridand V_{L2} = 480Vdc is lower limit of the allowable Voltage of the DC microgridand V_{H1} = 510Vdc is the point at which battery charging activated and V_{L1}=490Vdc is the point at which battery discharging activated.

4.5.2 Stand-alone Operation:

The BESS play an importance role in controlling the balance of power within the microgrid. **Region 1: $V_{L1} \leq V_{dcn} \leq V_{H1}$:**The BESS operate in idle mode to avoid frequent battery c harge/discharge. The powers from PV balanced with the load. Since there is no slack terminal , the bus voltage varies within region 1, corresponding to the change of load and PV power.

Region 2: $V_{H1} \leq V_{dcn} \leq V_{H2}$: When the power generated from the PV is larger than load power, the bus voltage increases and falls into region 2. The batteries start charging to store surplus energy and regulate the bus voltage. If BESS are charged to full state (SOC = SOCH), the batteries can no longer control the bus voltage, and the VSC is activated to switch the system into the grid-connected mode.

Region 3: $V_{L2} \leq V_{dcn} \leq V_{L1}$: The deficiency of power in the system leads to a decrease in the bus voltage. BESS are discharged to compensate the deficient power in the system. When batteries reach limited discharge rate (SOCL), the VSC is switched from idle mode to control voltage mode at V_{L2}, and the system consequently changes into grid-connected mode. When the DC micro-grid is working in regions 2 or 3, the surplus/deficient power can be stored/compensated by BESS through DC–DC converters.

4.5.3 Grid-Connected Mode:

In the case that there is a sudden loss of load or PV unit, over-voltage or under-voltage may occur, and the voltage will be out of permission range. This would lead to the instability of the system. To protect the DC microgrid under these abnormal conditions, it must be switched into the grid-connected mode.

In region 4 ($Vdc > V_{H2}$) or region 5 ($Vdc < V_{L2}$): when bus voltage reaches V_{H2} or V_{L2} values, the VSC is activated. Only the AC grid source works as a slack terminal to control the voltage of the DC bus.

Charge Controller of battery storage

In nearly all applications involving battery storage, a charge controller is necessary and at the same time must be able to discontinue power flow when the battery is fully charged or has reached a prescribed state. The controller should also be adjustable to ensure optimal battery system performance under various charging, discharging, and temperature conditions.

Charge controllers are used to regulate the flow of current to and from batteries in a micro-grid [48]. They are essential to protect the batteries and regulate the DC bus voltage. In this DC micro-grid a charge controller will control a bidirectional converter lowering the PV to zero the charge controller will activate the bidirectional converter to send the power from the batteries to the micro-grid.

The proposed fuzzy logic for a charge controller in a DC micro-grid check if the batteries are in the region of 20-90% and if they are depending on the power balance between the generation and load the batteries will either charge, discharge or will be in idle mode.

To ensure the secure and optimal operation of BESS a control strategy based on state of change (SOC) and bus voltage is proposed in Figure 4.10.

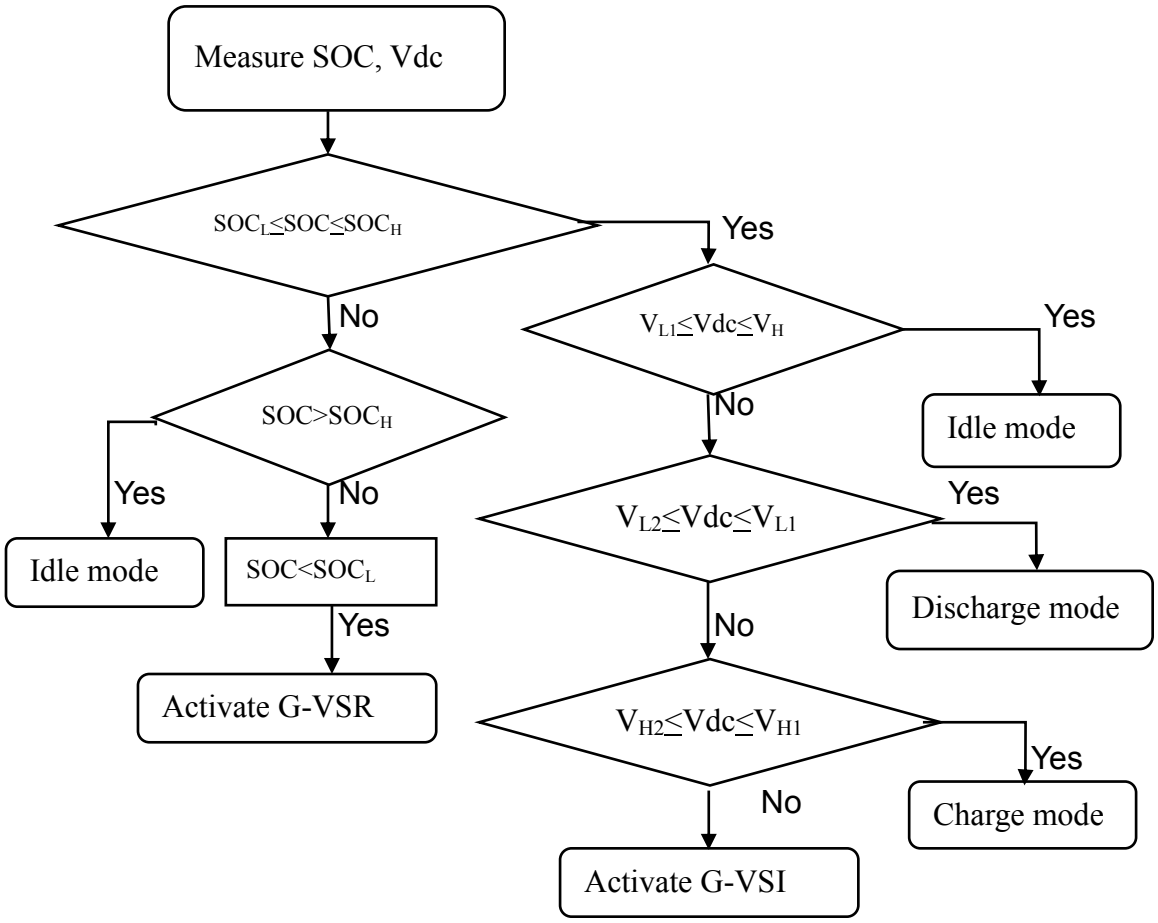

Figure 4. 12 Flow chart for Power management using fuzzy logic controller

Where

SOC = State of Charge of battery

SOCL = Lower state of charge =20%

SOCH = Higher state of charge = 90%

Vdc = Available DC bus voltage

VL1= Low bus voltage level 1 = 490 V

VL2 = Lower bus voltage level 2= 480 V

VH1 = High bus voltage level 1 = 510 V

VH2 = Higher bus voltage level 2 =520 V

Idle mode = means do nothing continue as it is

Charging mode = battery is activated to charge

Discharging mode = battery is activated to discharge

Activate G-VSR = means activate grid voltage source to rectifier mode

Activate G- VSI = means activate grid voltage source to inverter mode

System Description:

A simulation was implemented in Matlab/Simulink to verify the operation of the proposed DC m icrogrid and control strategy, in the following conditions:

The nominal voltage of DC bus Vdcn was set at 500 V; V_{H1} and V_{L1} were ±2% Vdcn, respectiv ely, while V_{H2} and V_{L2} was ±4% Vdcn, respectively. Thus, V_{H1} = 510 V; V_{H2} = 520 V; V_{L1} = 490 V; V_{L2} = 480 V.

4.5.4 Fuzzy Logic-Based Energy Management Rules

In this fuzzy logic energy management strategy, the bus voltage is taken as input variable. According to the design of the interconnected power system, the solar power is 400 kW and it is working as availability and send the available power to the DC Bus. The Battery State of Charge (SOC) is in between 0 and 100 %. To prevent the battery from being fully charged or discharged, the SOC of the battery is set between 0.2 and 0.9. The fuzzy collection of each variable is determined based on the fuzzy statistical principles, and the corresponding membership functions can be obtained. For the input variable, depending on DC Bus load conditions Bus voltage level is divided into five fuzzy sets: very low (VL), low (L),just right(J) high (H) and very high(VH). The output variables BatteryStatus is fuzzified into three fuzzy sets: charging (C), idle (I) and discharging (D) and GridStatus is also fuzzified into three fuzzy sets: rectifier mode (send) (R), OFF mode (O), and inverter mode(receive) (I)

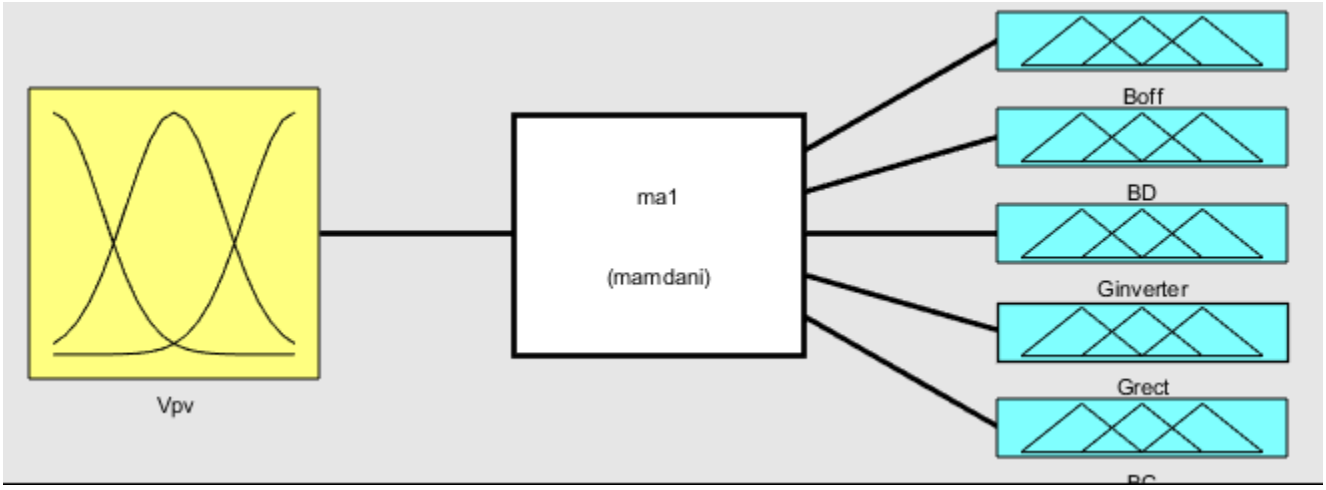

Figure 4. 13 Fuzzy logic function input and output

The input and output membership functions are shown in figure below (figure 5.12-5.14)

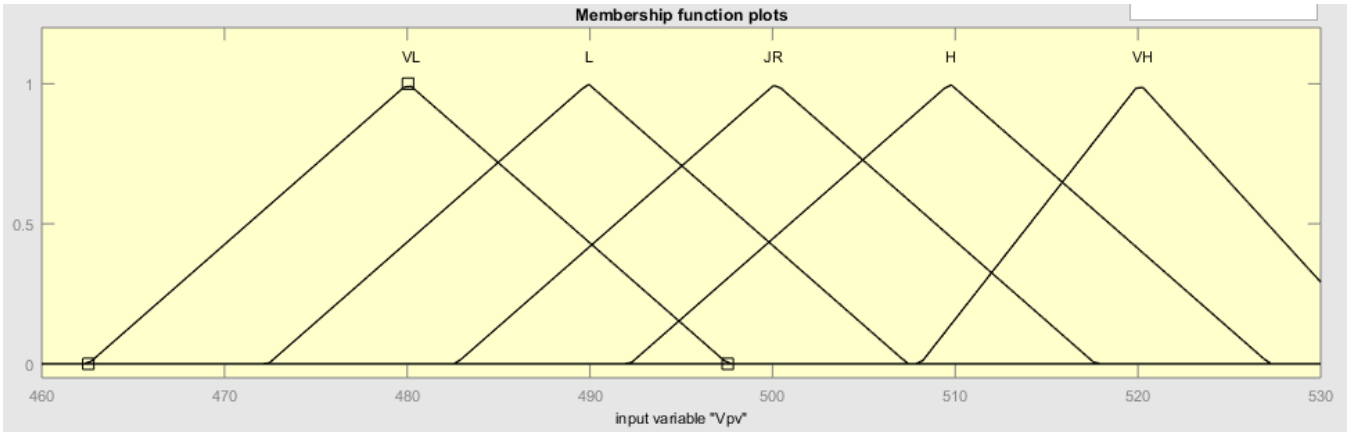

Figure 4. 14 Function of the bus voltage from PV system

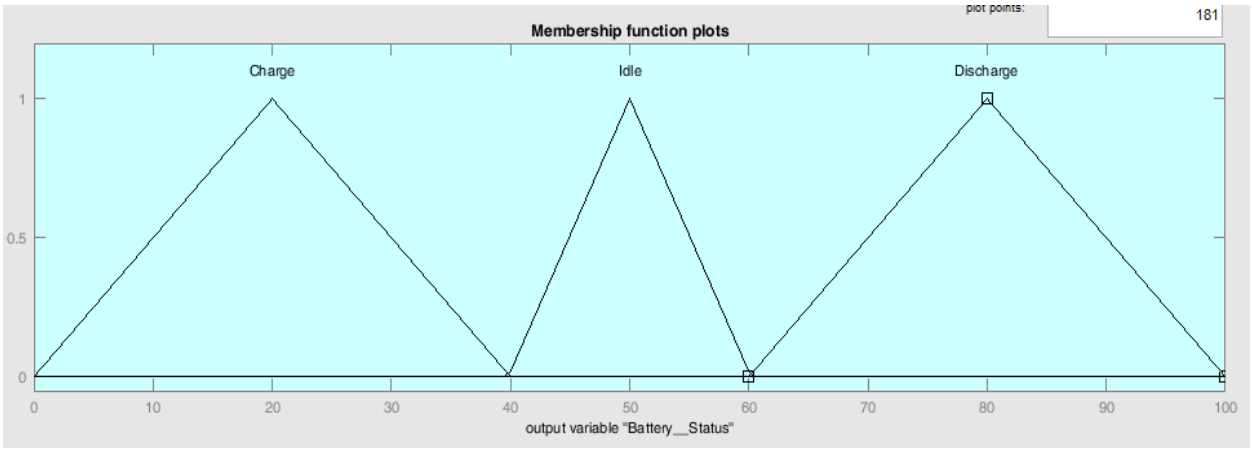

Figure 4. 15 Function of the battery status

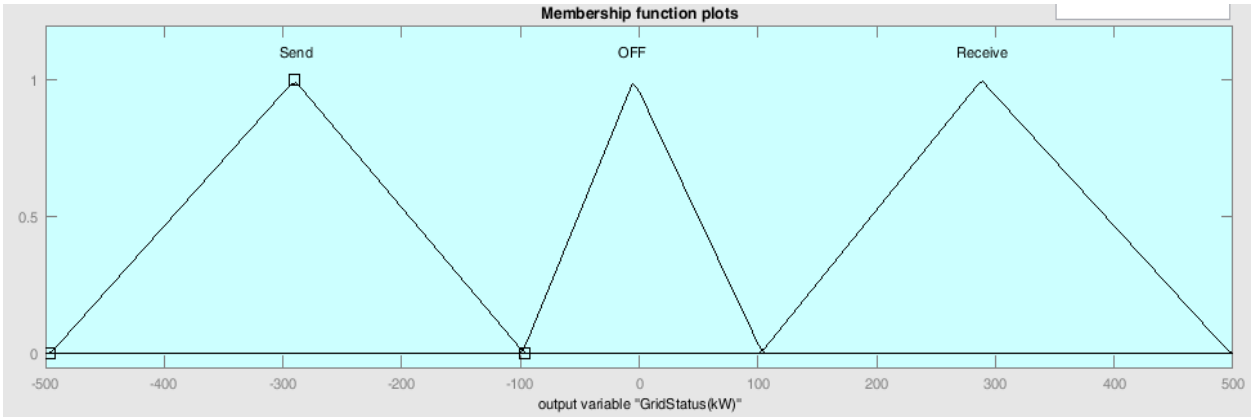

Figure 4. 16 Function of the Grid status

For different time load requirements, a reasonable fuzzy rule can be established for the power generation of the solar energy system and the current SOC of the battery, to improve the fuel economy of the vehicles as much as possible. For example, when the vehicle's load demand is high, the power that is generated by the renewable energy system is preferred and should be maximized to reduce the power supply of distribution grid; when the vehicle's load

demand is low, Under a light load, the power of renewable energy system should be injected to the power grid as far as possible. In this case, the output power of the renewable energy system needs to be controlled within a reasonable range. Based on the above principles, a total of 5 fuzzy rules are established and are described in fuzzy language (rules) as follows:

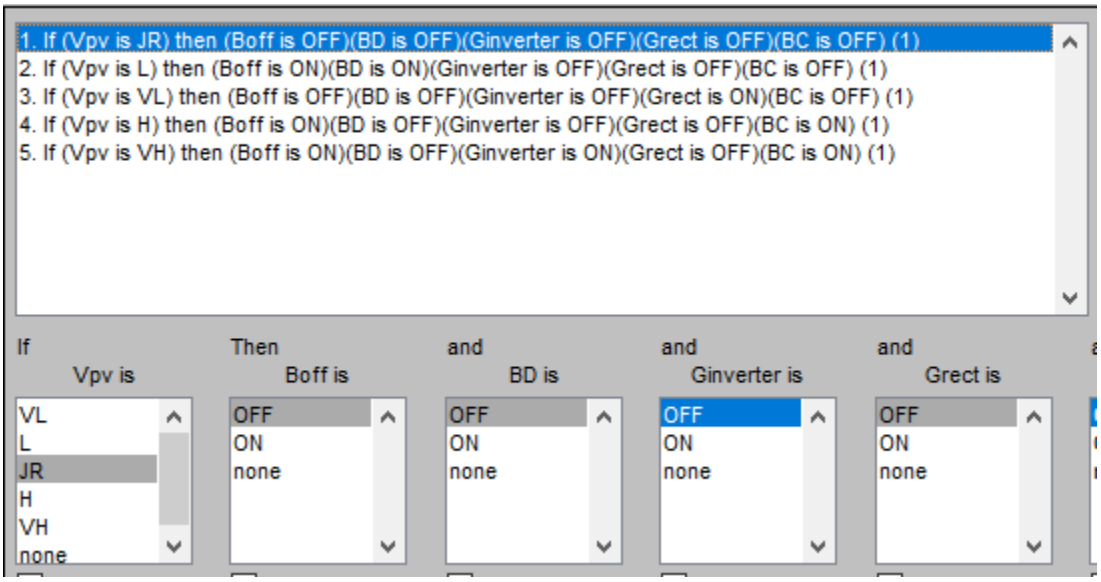

Figure 4. 17 Fuzzy logic controller output Rule

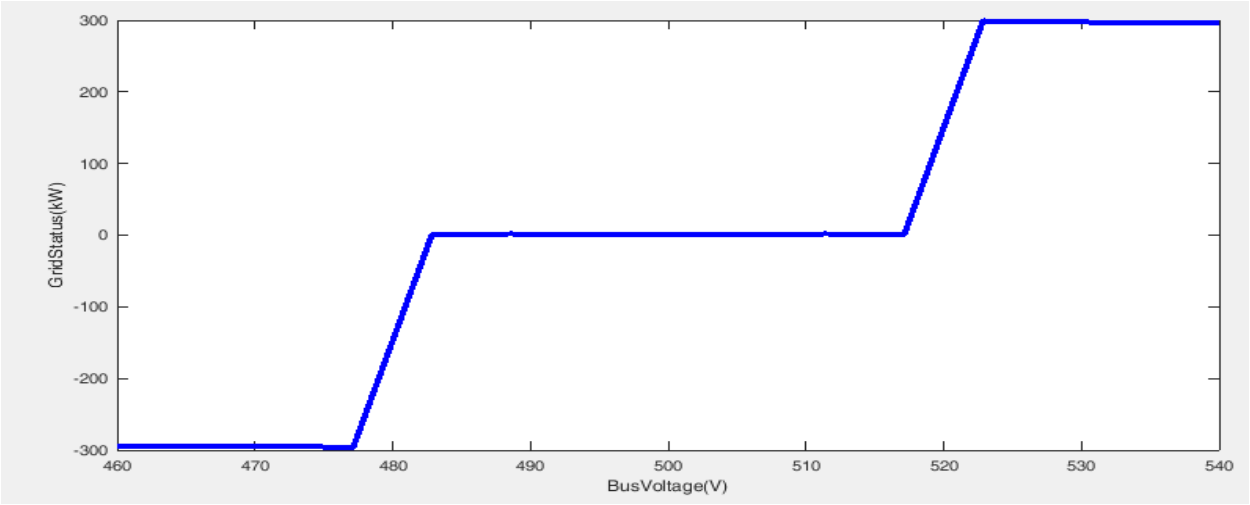

Figure 4. 18 Fuzzy logic controller surface view of Grid Status

This result shows that Grid status is in off mode when bus voltage is between 480 V and 520 V. In this region the load is served from solar PV system and BESS. When bus voltage is in between 490 V and 510 V PV only supplies demand. When bus voltage is in between 490 V and 480 V battery is changed to discharging mode. When bus voltage is in between 510 V and 520 V battery is changed to charging mode. Out of this region means when bus voltage is below 480 V grid is changed into rectifier mode and sending power to the DC bus through

rectifier to serve the loads. When dc bus voltage is above 520 V the grid is changed into the inverter mode and receive excess power from the dc bus.

This result shows that the grid status is positive means supplying around 300 kW power to EV and negative when receiving around 300 kW for this simulation case.

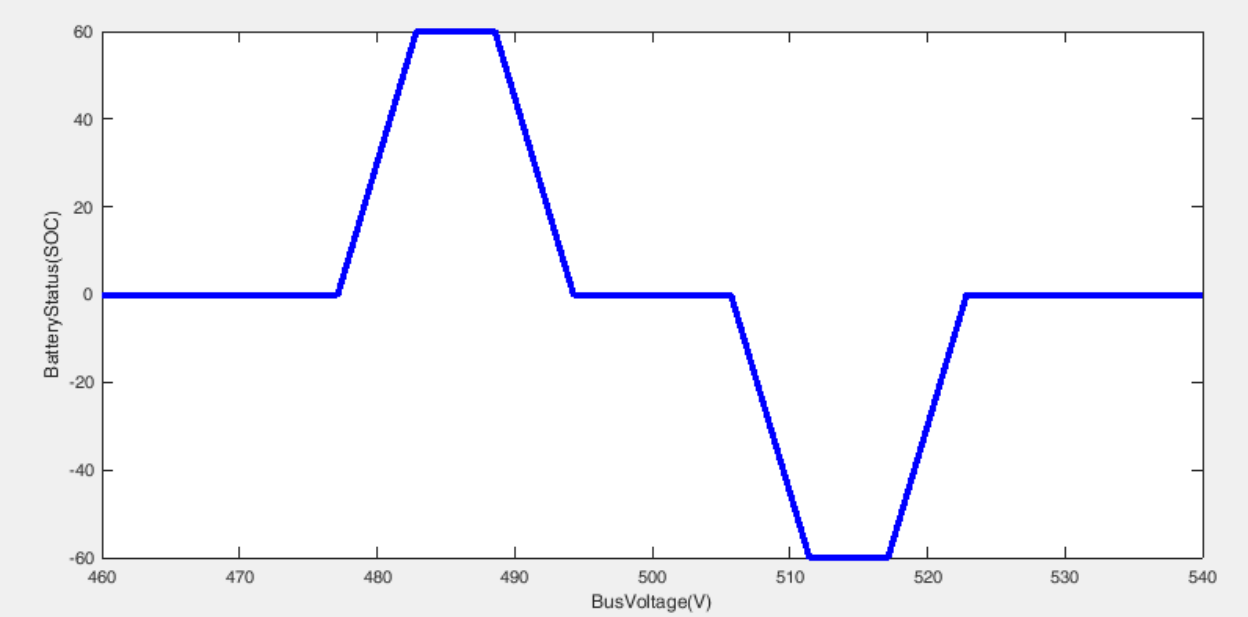

Figure 4. 19 Fuzzy logic controller surface view of Battery Status

This result shows that battery is in charging mode when SOC shows negative value and at 0(zero) it is in idle mode to control continuous charge and discharge of battery when load is fully served from PV system only. When SOC shows positive value battery is in discharging mode to serve additional energy with PV system needed by loads.

The system will charge vehicles continuously depending on bus voltage level followed by fuzzy logic controller from three sources: solar PV system, battery and grid. The system will send excess power to the grid when there is no electric vehicles to be charged. The amount of power from solar PV system is around 400 kW and the amount of energy from battery storage system is 250 kWh.

Table 4. 4 System rule of fuzzy logic controller

Bus Voltage (V) **Load availability**	**Battery status**			**Grid status**		**PV system Availability**
	C	**I**	**D**	**R**	**I**	
460 = high load	I	I	I	R	R	NO
470	I	I	I	R	R	NO
480	D	D	D	O	O	YES
485	D	D	D	O	O	YES
490	D	D	D	O	O	YES
495	I	I	I	O	O	YES
500	I	I	I	O	O	YES
505	I	I	I	O	O	YES
510	C	C	C	O	O	YES
520	C	C	C	O	O	YES
525	I	I	I	I	I	YES
530 = No load	I	I	I	I	I	YES

Where: C= Battery Charging, I= Battery idle, D= Battery discharging

R = Grid is in rectifier mode (send to Bus)

I = Grid is in inverter mode (receiving from Bus)

CHAPTER FIVE

5 RESULTS AND DISCUSSION

5.1 Introduction

This chapter gives simulation result and discussion of the research. The first part deals with automatic solar energy forecasting system while the second part deals with Modeling and simulation of DC Micro-grid for Electric Vehicle Charging Station with Power flow management using Fuzzy Logic controller.

5.2 PV Automatic Forecasting System Results and Discussions

5.2.1 Introduction

One of the most important challenges for the near future global energy supply will be the large integration of renewable energy sources into existing or future energy supply structure and obtain a precise balance between the electricity production and consumption at any moment. However, it has some difficulties to maintain this balance. Because the integration of renewable energy into an electrical network intensifies the complexity of the grid management (voltage fluctuations, local power quality and stability issues) and the continuity of the production/consumption balance due to their intermittent and unpredictable nature. The reliability of integration of renewable energy is then become dependent on the ability of the system to accommodate expected and unexpected changes (in production and consumption) and disturbances, while maintaining quality and continuity of service to the customers. Thus, it is very important to manage the system with various temporal horizons.

Thus to improve real-time control performance and reduce possible seasonal variation and negative impacts of renewable energy source systems, an accurate forecasting of the proposed renewable energy source output is required, which is an important function in the operation of an energy management system. It is also necessary for estimating the reserves, for scheduling the power system, for congestion management, for the optimal management of the storage.

In this section authordescribe the problem of daily solar radiation he tackle, including a brief description of the variables involved in the prediction problem and the objective data of radiation available for the study. Note that the total set of meteorological variables included as input predictive variables in this paper has not been, to our knowledge, considered in other studies about radiation prediction and it is a novel contribution of this research.

First of all, the objective variable (prediction target) for this problem is the irradiation that reaches the ground. Data from the Meteorological station of Hawassa were used. The data collected covers ranges from the 1st January 2017 to 31st December 2019, three years of daily measurements.

As the author is tried to introduce in chapter three big data driven technologies are becoming key to develop a model which can forecast solar energy. In this study the author developed a forecasting model which can forecast solar energy one day earlier. Machine learning is recognized as an efficient technique for forecasting as it offers a steady analysis based on the contributing features received from metrological stations. A forecasting system is a statistical model developed based on historical data of previous similar weather conditions and irradiance characteristics. Schematic illustration of the system is shown in Figure 5.1.

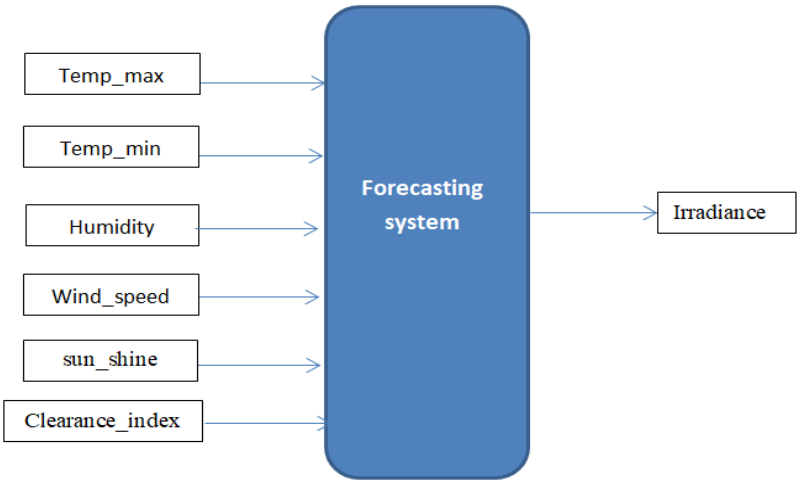

Figure 5. 1machine learning forecasting system

The machine learning models find relations between inputs and outputs; and this characteristic allow the use of machine learning models in this forecasting problems. In this study irradiance forecasting conducted based on time-series models which only consider the historically observed weather data and solar irradiance as input features and the systems can learn from data sets without being explicitly programmed. In the predictive learning problems, the system consists of a random “output” or “response” variable y (in this study next day irradiance) and a set of random “input” or “explanatory” variables x (historical weather data obtained from metrological stations). Using a “training” sample of known (y, x) values, the goal is to obtain an estimate or approximation, of the function mapping x to y, that minimizes the expected value of some specified loss function over the joint distribution of all (y, x)-values. The frequently measure parameters employed for loss functions include squared-error and

absolute error.

5.2.2 Evaluation of model accuracy

Evaluation, generally, measures how good something is. In machine learning evaluation is usually conducted at various steps of the model development such as during the training of a statistical model; for judging the improvement of the model after some modifications and for comparing various models. The evaluation here is conducted by comparing the forecasted outputs (or next day predicted irradiance) with observed data y (or observed or measured time series) which are also measured data themselves linked to an error (or precision) of a measure.

There are different tools for evaluation; the first is Graphic tools while the second common one is statistical tools. Graphic tools are available for estimating the adequacy of the model with the experimental measurements. In this study Scatter plots of predicted over measured irradiance is shown in Figure 5.2 which can reveal systematic bias and deviations depending on the irradiance conditions and show the range of deviations that are related to the forecasts. Figure 5. 2 shows the predicted irradiance when all the variables such as Date, Month, Temp_max, Temp_min, humidity, wind_speed, sun_shine and clearness_index are used. Clearly the scattered plot shows very few variations from the straight reference linear line shown in the plot. The approximate coefficients calculated by Jupiter notebook $6.23748390e^{-02}$, $5.75555951e^{-02}$, $-4.44331299e^{-03}$, $8.18021701e^{-04}$, $-1.15717916e^{-02}$ and $9.26412563e^{+00}$ for TEM_Min, TEM_max, wind_speed, humidity, sun_shine and clearness_index, respectively. These coefficients are used to show the model developed in the equation form as it is explained the model selected was linear regression. Thus, using these coefficients the proposed linear model is given in the following equation:

$$Irradiance = 0.0624T_{min} + 0.0576T_{max} - 0.0044W_S + 0.0008H_m - 0.0116S_S + 9.2641C_I \quad 5.1$$

Where T_{min} = minimum temperature

T_{max} = maximum temperature

W_s= wind speed

H_m = humidity

S_s= sun shine

C_I = clearness index

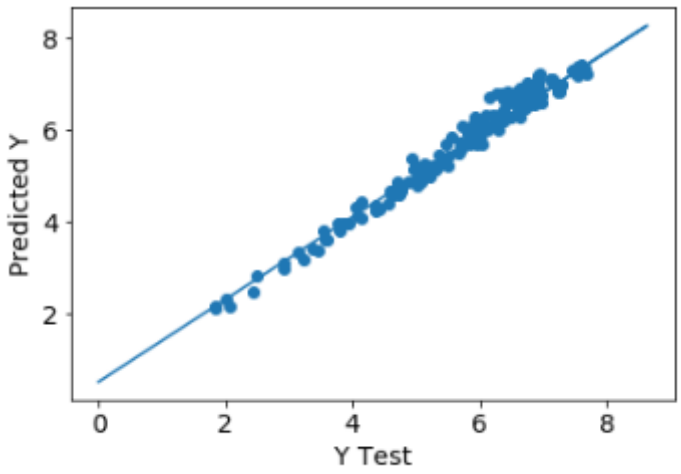

Figure 5. 2 Scatter plot of predicted vs. measured irradiance (test data)

The commonly used statistics include in machine learning and predictions are highlighted as follows:

1. Bias error (MBE): The mean bias error (MBE) represents the mean bias of the forecasting:

$$MBE = \frac{1}{N} x \sum_{i}^{N} (\hat{y}(i) - y(i)) \quad 5.2$$

With$\hat{y}$ being the forecasted outputs (or predicted time series), y the observed data (or observed or measured time series) and N the number of observations.

2. Mean absolute error (MAE): The mean absolute error (MAE) is appropriate for applications with linear functions, i.e., where the costs resulting from a poor forecast are proportional to the forecast error:

$$MAE = \frac{1}{N} x \sum_{i}^{N} |\hat{y}(i) - y(i)| \quad 5.3$$

3. Mean square error (MSE): it uses the squared of the difference between observedand predicted values. This index penalizes the highest gaps:

$$MSE = \frac{1}{N} x \sum_{i}^{N} (\hat{y}(i) - y(i))^2$$

5.4

MSE is generally the parameter which is minimized by the training algorithm.

4 .Root mean square error (RMSE): The RMSE is more sensitive to big forecast errors, and hence is suitable for applications where small errors are more tolerable and larger errors cause disproportionately high costs. It is probably the reliability factor that is most appreciated and used:

$$MSE = \sqrt{\frac{1}{N} x \sum_{i}^{N} (\hat{y}(i) - y(i))^2}$$

5.5

5. R-squared: R-squared is a statistical measure of how close the data are to the fitted regression line. It is also known as the coefficient of determination, or the coefficient of multiple determination for multiple regression. The definition of R-squared is fairly straight-forward; it is the percentage of the response variable variation that is explained by a linear model. Or:

$$\mathrm{R-squared} = \frac{\text{Explained variation}}{\text{Total variation}} \quad 5.6$$

R-squared is always between 0 and 100%: 0% indicates that the model explains none of the variability of the response data around its mean. 100% indicates that the model explains all the variability of the response data around its mean. In general, the higher the R-squared, the better the model fits your data.

Using these statistical methods the results obtained from our model developed using Jupiter notebook are summarized as follow

Table 5. 1 Forecasting accuracy statistical measurement

Statistical measuring tools	Results
MAE	0.162502869978
MSE	0.0402885226991
RMSE	0.20
R_squared	97.56%

Clearly from Table 5.1 the results shows as the model developed can forecast the next day irradiance with good prediction of 97.56%. Regression analysis is a set of statistical

methods used for the estimation of relationships between a dependent variable and one or more independent variables. It can be utilized to assess the strength of the relationship between variables and for modeling the future relationship between them.

Moreover the different errors calculated.The most common interpretation of r-squared is how well the regression model (prediction) fits the observed data (measured data). In this thesis an r-squared of 97.56% reveals that 97.56% of the data fit the regression model. Generally, a higher r-squared indicates a better fit for the model. In general the proposed model is strong enough to forecast irradiance of the next day with good quality.

5.3 Matlab Simulation Result and Discussion

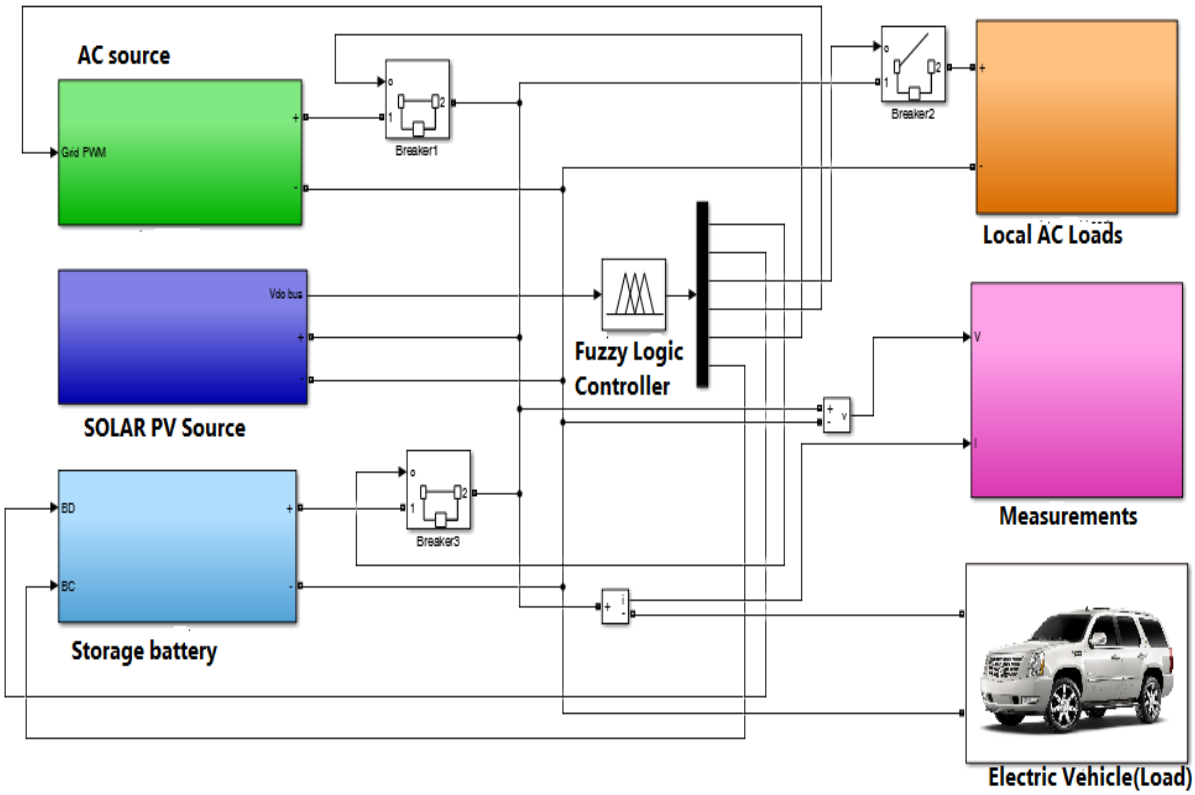

Figure 5. 3 MATLAB simulation of DC micro grid system with 500Vdc

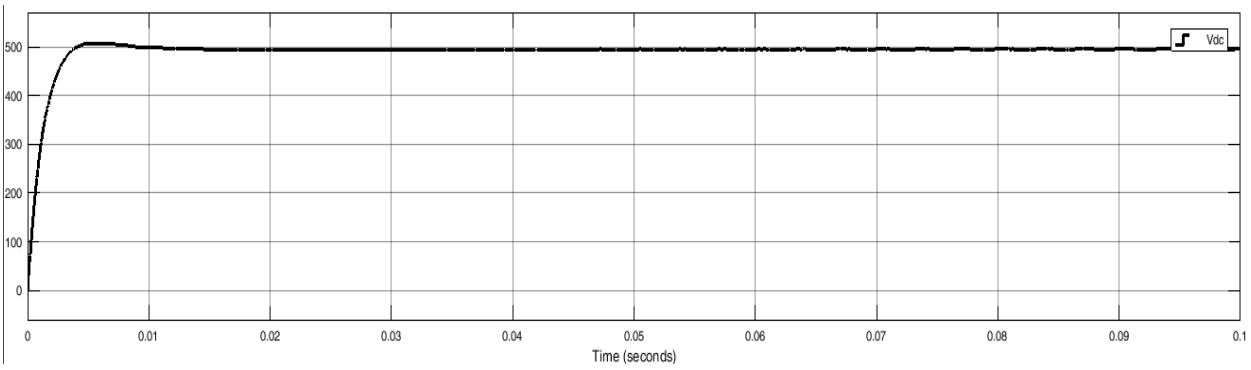

Figure 5. 4 DC output of micro-grid without load

The system output voltage for DC micro grid is 500 Vdc. To get this result the authordesigned the three inputs of the system to be 500 Vdc. The above result shows that the rectified output of grid, designed solar PV output and storage battery gives 500 Vdc.

5.4 Outputs of Fuzzy logic controller at different inputs

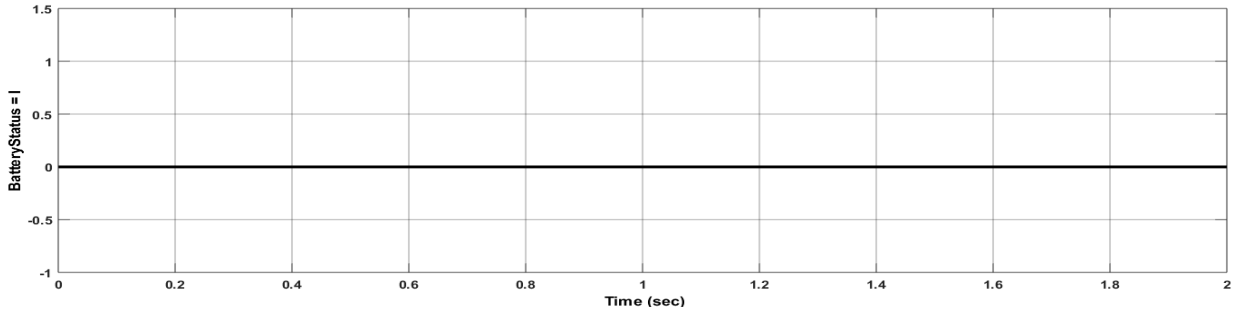

Fig. a: When bus voltage is below 480 Vdc

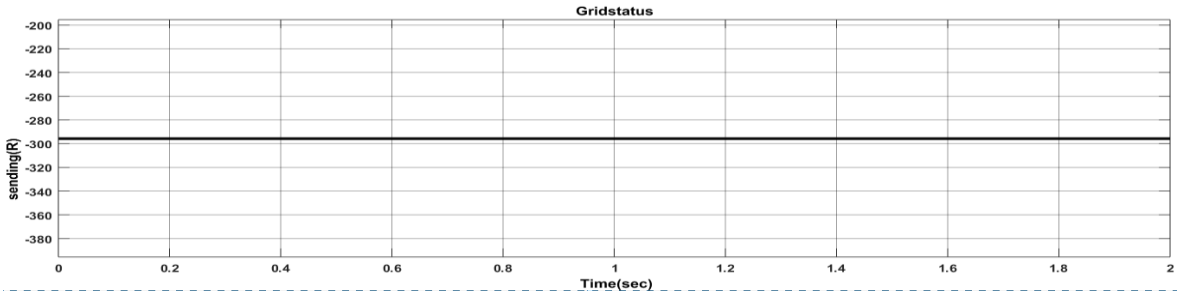

Fig. b: When bus voltage is below 480 Vdc

This result in fig. a and b: above shows the status of battery when the bus voltage from solar PV system is below 480 Vdc. At this time power supply from solar PV system is very low and battery has low SOC therefore storage battery turns to idle mode that is no energy is sent or received from battery and grid turns to rectifier mode and supply power to the load. From the result it shows that around 300 kW of power is taken from grid.

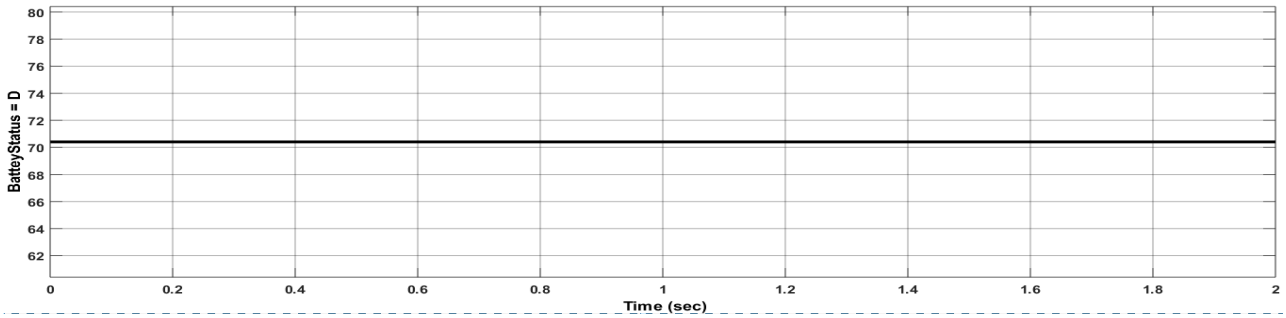

Fig. c: When bus voltage is in between 480 and 490 Vdc

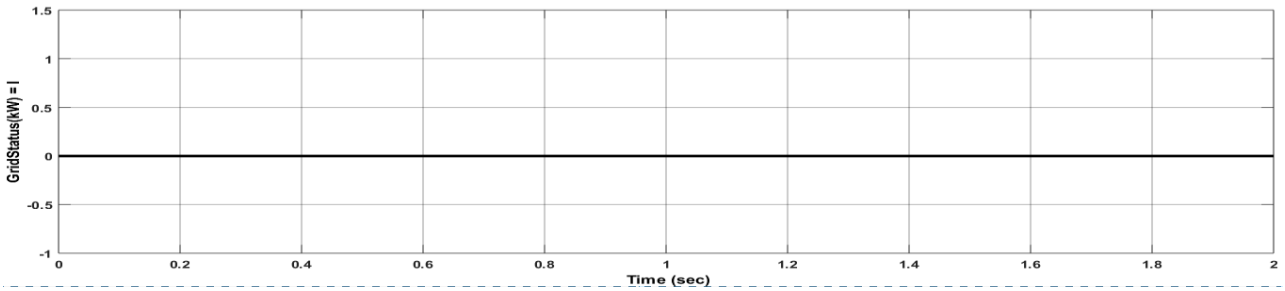

Fig. d: When bus voltage is in between 480 and 490 Vdc

This result in fig. c and d: above shows when the dc bus voltage from solar PV system is between 480 and 490 Vdc. At this time the load requirement is showing increment and solar PV system cannot serve the system alone. Therefore storage battery turns to discharging mode and starts to discharge to serve the load requirement with solar PV system. That it shows 60 kWh amount of energy is sent to the load from battery for this simulation. From the result figure it shows grid is in idle mode that means no contribution from grid.

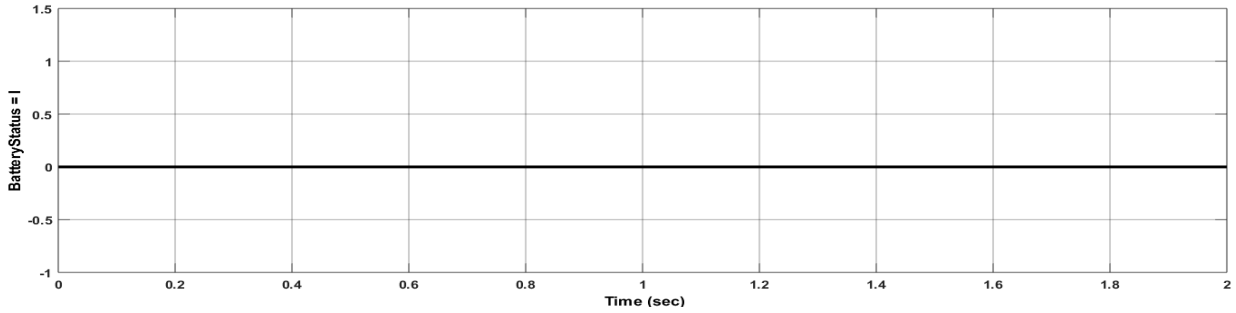

Fig. e: When bus voltage is 500 Vdc

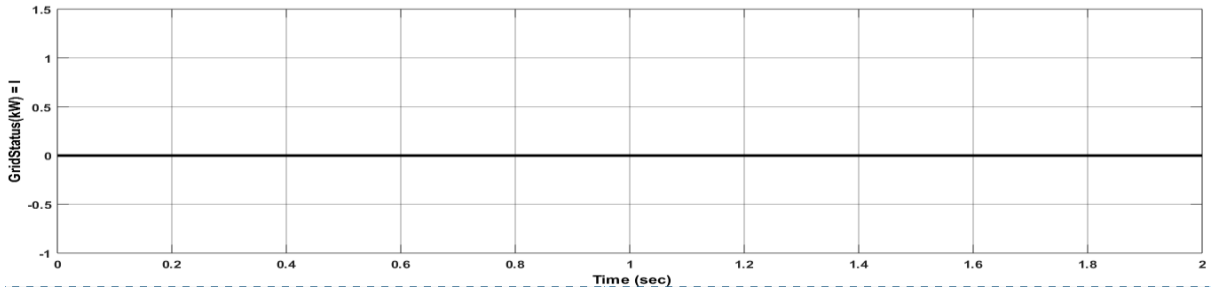

Fig. f: When bus voltage is 500 Vdc

This result in fig. e and f: above shows when the dc bus voltage from solar PV system is at 500 Vdc. At this time the load requirement and available power in solar PV system power is matched. The storage battery and grid turns to idle mode that mean there is no contribution from battery and grid that solar PV system serves alone.

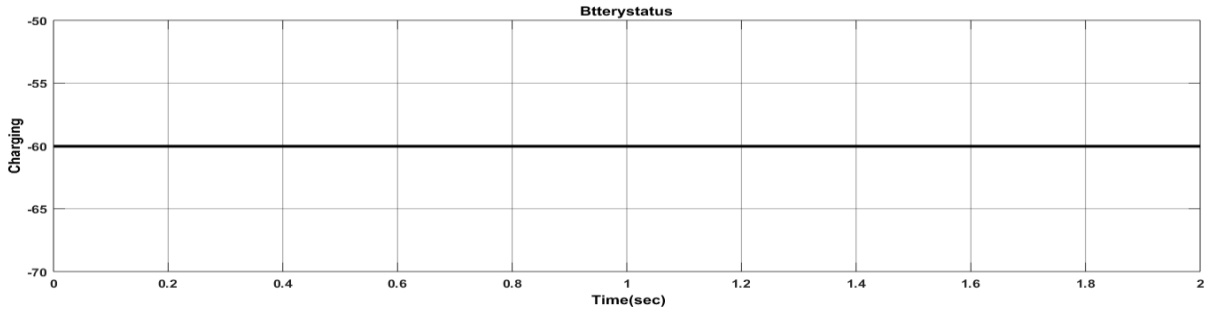

Fig. g: When bus voltage is in between 510 and 520 Vdc

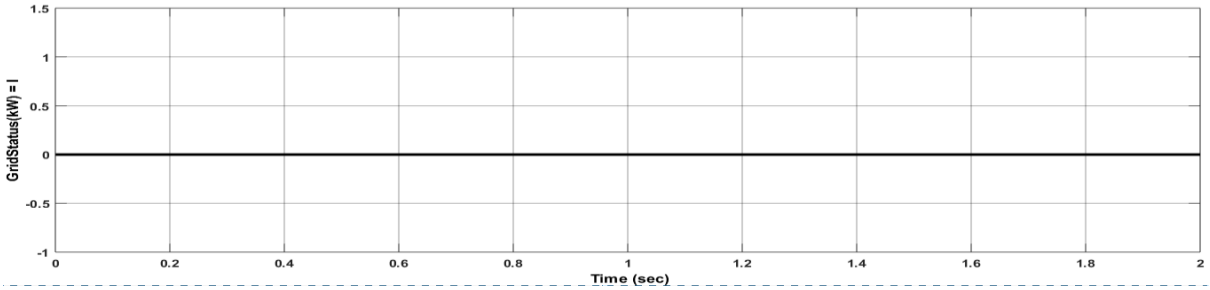

Fig. h: When bus voltage is in between 510 and 520 Vdc

This result in fig.g and h: above shows when the dc bus voltage from solar PV system is between 510 and 520 Vdc. At this time the available power in solar PV system is greater than the load power requirement. Therefore the storage battery turns to charging mode and starts to charge the battery from solar PV system. The result graph shows -60 kWh amount of energy is sent to the storage battery from the solar PV system and grid is in idle mode that means no contribution from grid or to grid.

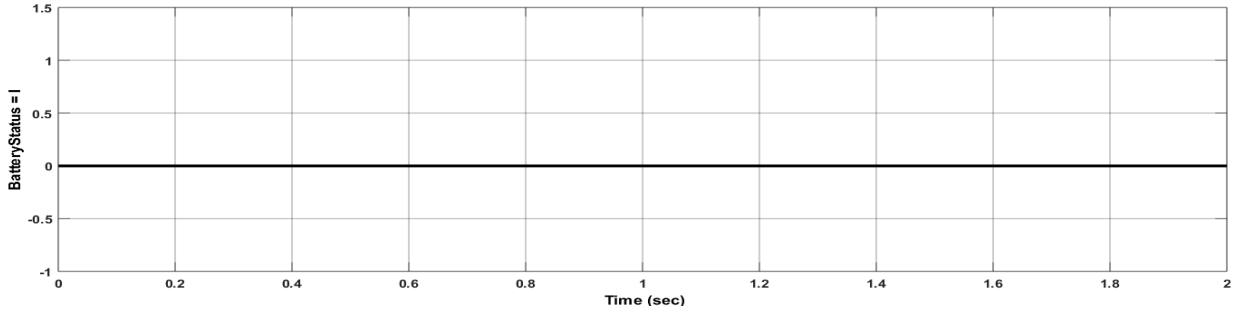

Fig. i: When bus voltage is above 520 Vdc

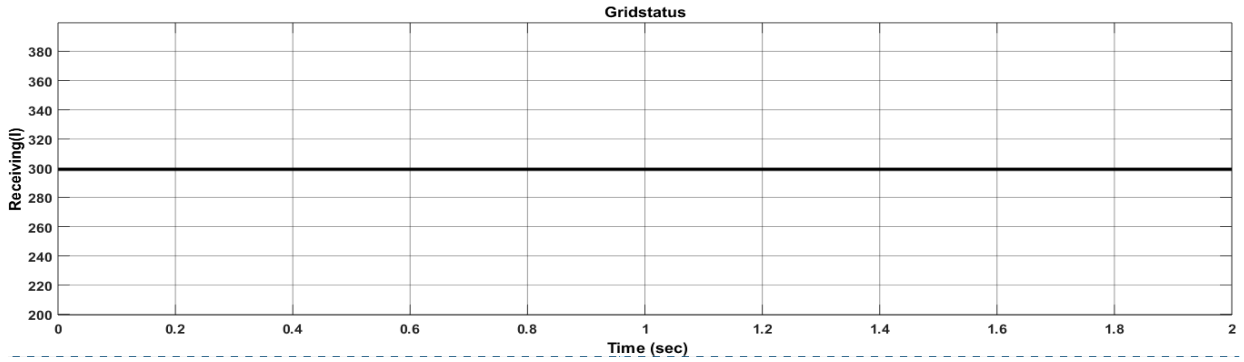

Fig. j: When bus voltage is above 520 Vdc

Figure 5. 5 The Fuzzy logic controller output at different load conditions (a-j)

This result in fig. i and j: above shows when the dc bus voltage from solar PV system is above 520 Vdc. At this time it shows that the power generation from solar PV system is very high and the load power requirement is very low. The storage battery is charged when the dc bus voltage is in between 510 and 520 Vdc and when SOC is at full. Therefore the battery turns to idle mode and the grid inverter is activated and the available power in solar PV system is sent to grid through inverter.

Load power responses without and with controller

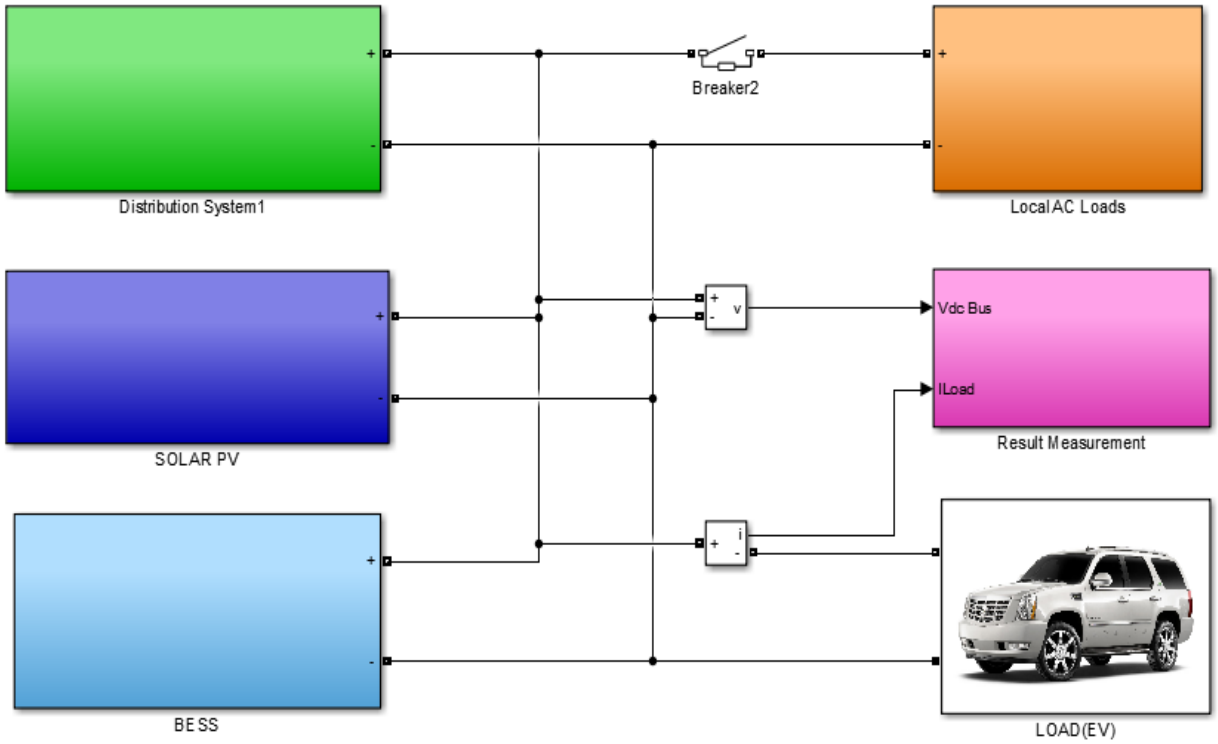

Figure 5. 6 Simulink block of the system without controller

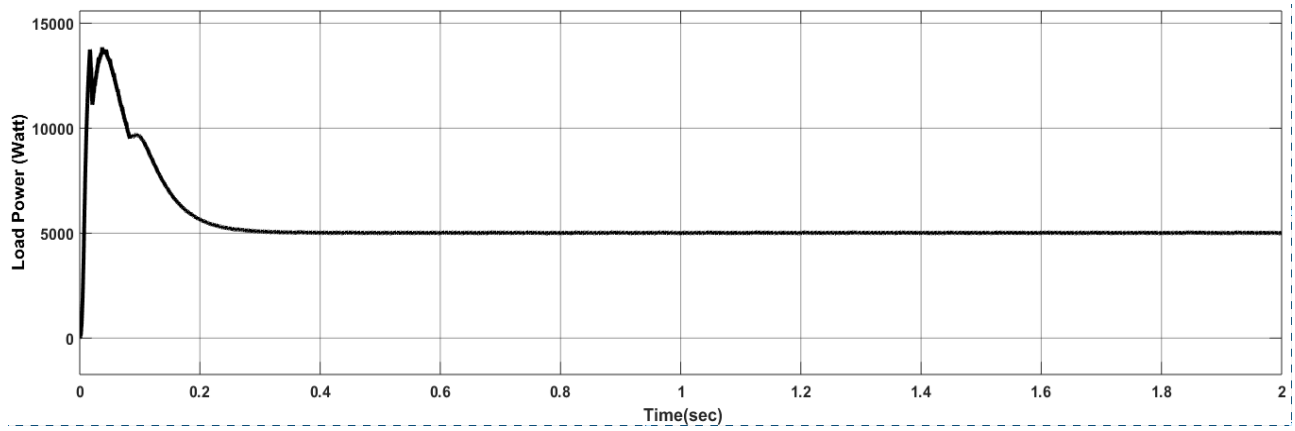

Figure 5. 7 Load power response with fuzzy logic controller

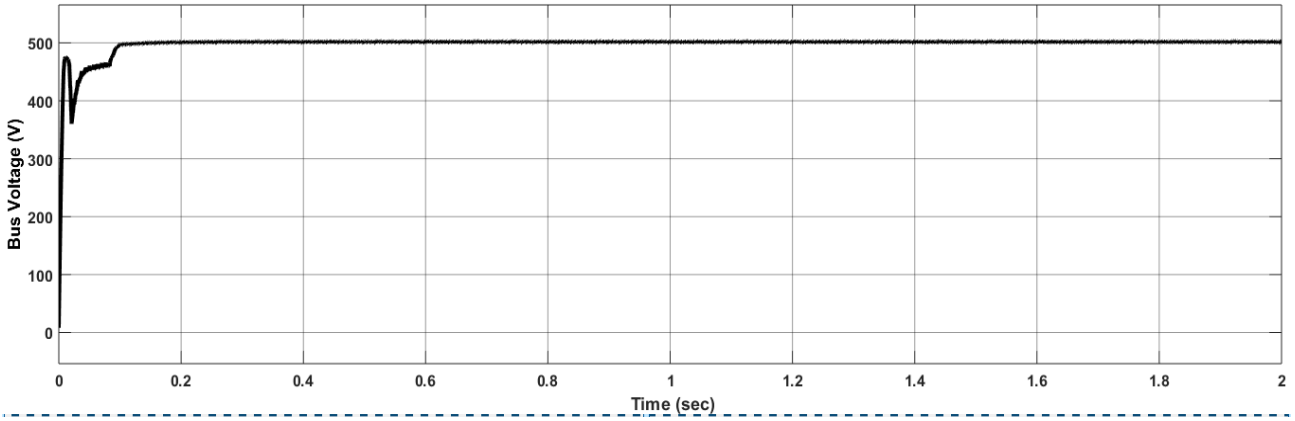

Figure 5. 8Dc bus Voltage response without fuzzy logic controller

This result shows the authorused 10 kW of PV for this simulation purpose only and DC motor as electric vehicle load which is 5 kW motor with 500 Vdc for simulation purpose. As you know electric motor starting current is three times of running current and this concept helps the author to conclude what will happen for the system bus voltage when load is increased with and without controller. As you see when the load increased in three times bus voltage comes to around 360 V without controller. Which brings disturbance in the system.

Load power responses with controller

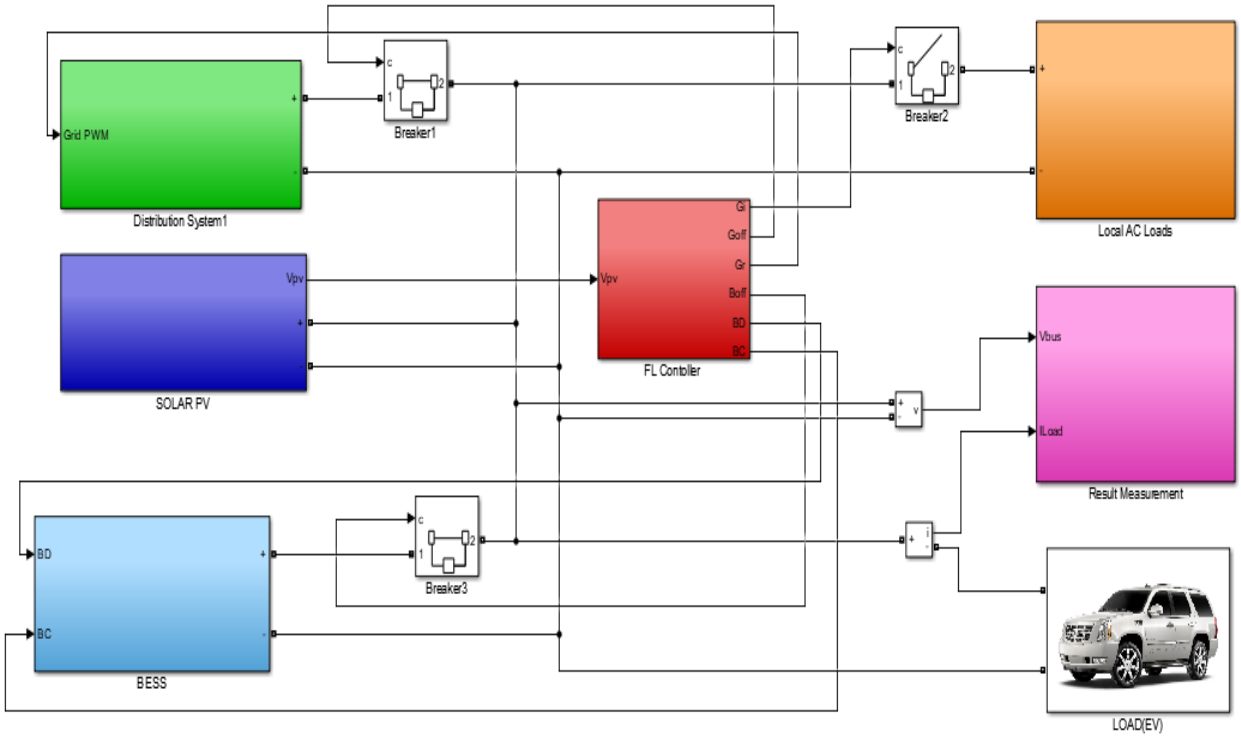

Figure 5. 9 Simulink block of the system with controller

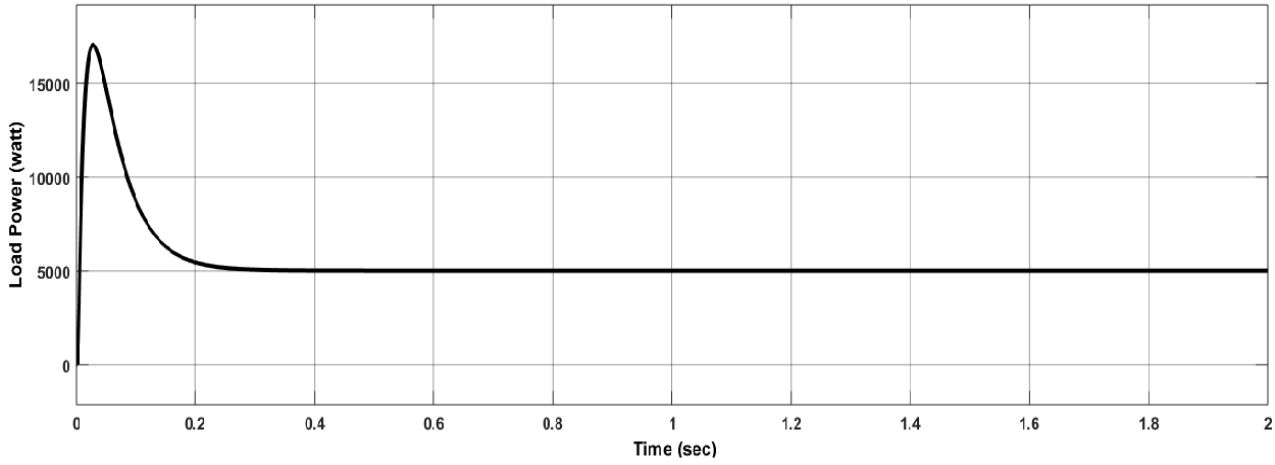

Figure 5. 10 Simulink block and Load power response with fuzzy logic controller

We have seen as described in above section what happened for bus voltage without controller. This problem is solved by using fuzzy logic controller. When controller is used in the system the bus voltage is within acceptable range and response is smooth and no disturbance happened.

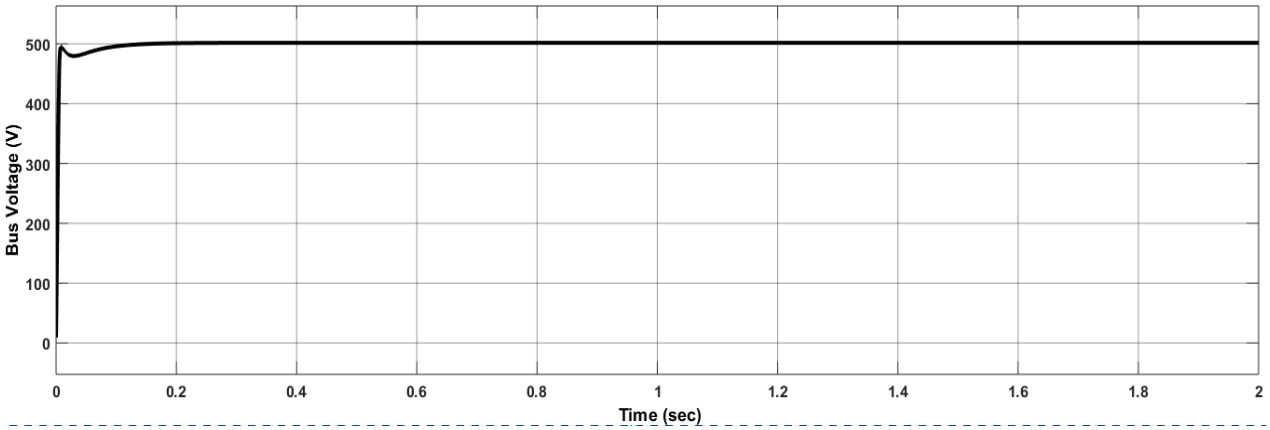

Figure 5. 11 Dc bus Voltage response with fuzzy logic controller

This result shows the DC bus voltage response with fuzzy logic controller. With fuzzy logic controller the bus voltage comes to 495 V from 500 V for microseconds. This shows controller improves power loss and controls bus voltage with in expected range.

Table 5. 2 Statistical analysis of voltage

Comparison	**Mean Voltage**	**Standard deviation of Voltage**
Without Controller	430	7.1
With Fuzzy logic controller	495	2.2

Table 5. 3 Responses

Responses	**Without Controller**	**With Fuzzy logic controller**
Response Time	4.516 ms	2.871 ms
overshoot	121.667%	0.704%

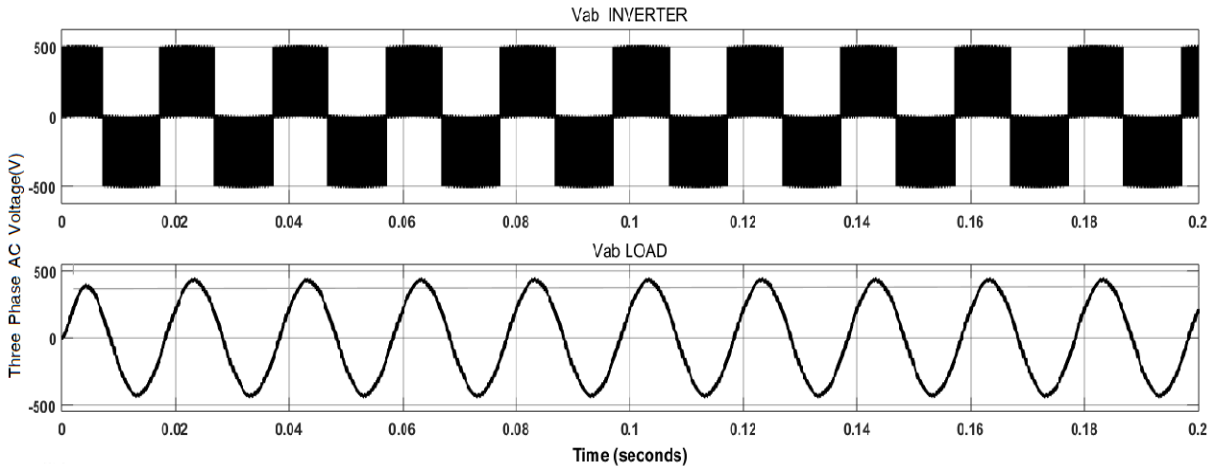

Figure 5. 12 System inverter output

The simulation output shown in figure 5.13 above is for sending excess power to nearest limited number of customers. When there is high amount of PV power output and the storage fully charged the system is ready to send excess power if there is no electric vehicle to be charged. For this reason the author designed the system by using inverter which changes the dc system to ac for the ac user customers. The IGBT inverter is controlled with PI regulator in order to maintain a 1pu voltage (380 Vrms 50 Hz) at the load terminal.

5.5 Cost Analysis of the system by homer pro software

The micro-grid under consideration is evaluated from a techno-economic point of view utilizingHOMER Pro software (version 3.14, Homer Energy LLC, Boulder, CO, USA), and specifically considering the Net Present Cost (NPC) as a metric to compare the various design options.

The primary objective of cost analysis was the minimization of the total NPC of the overall system, while no load shedding was allowed amongst a few other technical constraints. The optimization procedure evaluated thousands of design choices ranging from various capacities of the selected energy resources and converter as well as batteries combining different technical characteristics and capital costs. The analysis concluded that, for the given loads, the best system design is the one comprised of a PV array with a capacity of 400 kW, 680 kWh of lithium –ion batteries, and a converter with a power rating of 361 kW; the total NPC of this system equals $917,350.

Table 5. 4 Economics Comparison between grid only system and proposed system

Comparison parameters	Grid only system	Proposed System
Net Present Cost	$1.29 M	$917,350
CAPEX	$721,333	$835,333
OPEX	$43,651	$6,344
LCOE (per kWh)	$0.151	$0.152
CO2 Emitted (kg/yr)	0	0
Fuel Consumption (L/yr)	0	0

5.5.1 Grid Only System

The electric needs of Electric Vehicles are met with grid system only. The operating costs for energy is $43,651per year. If you use grid only for charging of EVs.

5.5.2 Solar, Battery and Grid Integrated System

Here the author proposed 400 kW of PV and 680 kWh of battery capacity reduce the operating costs to $6,344 per year. This implies as the hybrid system has investment payback of3.06 years and an IRR of 32.7%.

Table 5. 5 Investment cost of proposed system

Simple payback:	3.06yr		**Net Present Value:**	$368,276
Internal Rate of Return:	32.7 %		**Capital Investment:**	$114,000
Return on Investment:	28.7 %		**Annualized Savings:**	$37,306

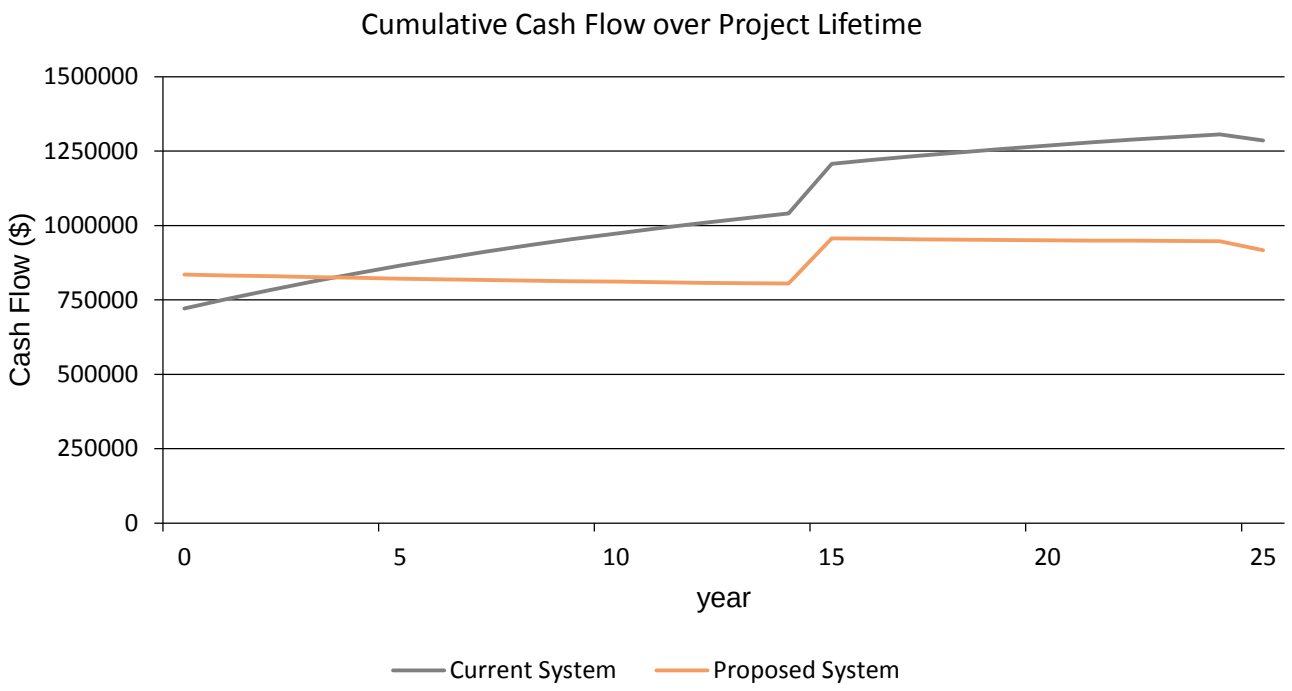

Figure 5. 13 Cumulative cash flow over project life time

Electric Consumption

This micro grid requires 2917 kWh/day and has a peak of 393 kW. In the proposed system, the following generation sources serve the electrical load.

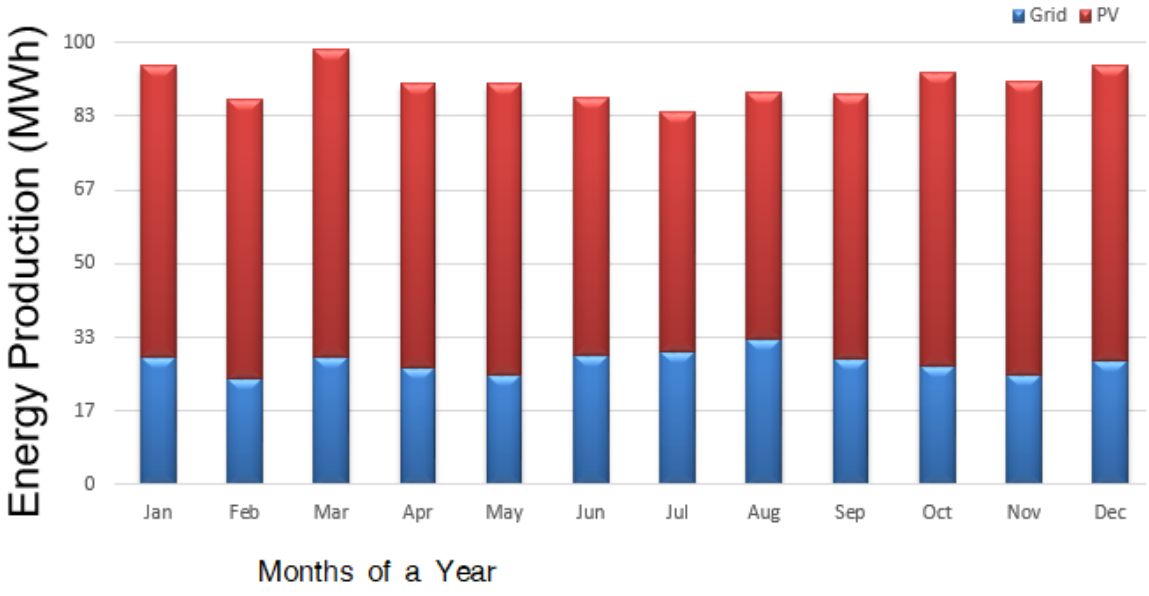

Figure 5. 14 Total energy production from two sources

PV: Solar PV

The Sola PV system has a nominal capacity of 400 kW. The annual production is 756,568 kWh/yr.

Table 5. 6 Solar PV system production and cost

Rated Capacity	400 kW		**Total Production**	756,568 kW
Capital Cost	$80,000		**Maintenance Cost**	10.0 $/yr
Specific Yield	1,891 kWh/kW		**LCOE**	0.00819 $/kWh
PV Penetration	115 %		**DC-AC Ratio**	1.00

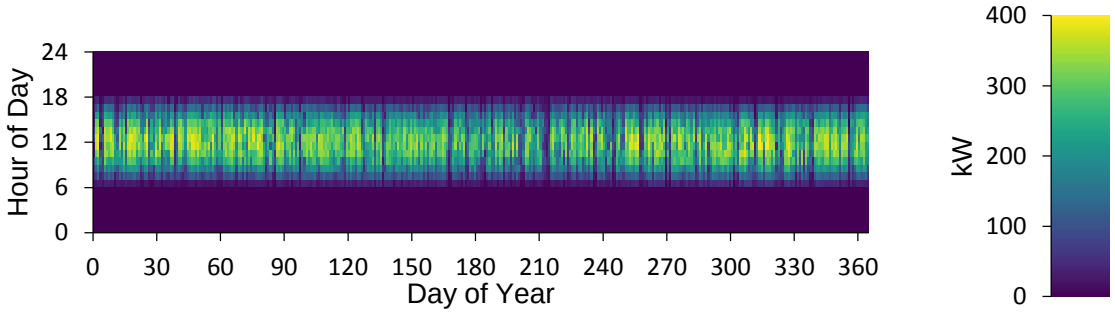

Figure 5. 15 Power production from solar PV system

Storage: Battery ESS

The battery energy storage system's nominal capacity is 680 kWh. The annual throughput is 596 kWh/yr.

Table 5. 7 Battery energy storage system capacity and cost

Rated Capacity	680 kWh		**Expected Life**	25yr
Annual Throughput	674 kWh/yr		**Capital Costs**	$30,000
Losses	8.55 kWh/yr		**Autonomy**	8hr

Grid

The annual energy purchased from the grid is 334,029 kWh and the annual energy sold to the grid is 407,677 kWh.

Table 5. 8 Grid energy flow and cost

Month	Energy Purchased (kWh)	Energy Sold (kWh)	Net Energy Purchased (kWh)	Peak Load (kW)	Energy Charge	Total
January	28,777	38,098	-9,321	303	-$427.94	-$427.94
February	24,039	36,972	-12,933	366	-$609.70	-$609.70
March	28,930	38,321	-9,391	350	-$431.22	-$431.22
April	26,488	34,445	-7,957	299	-$363.41	-$363.41
May	24,992	35,203	-10,211	294	-$475.36	-$475.36
June	29,111	29,781	-670	313	-$3.72	-$3.72
July	30,134	27,088	3,046	279	$179.38	$179.38
August	33,073	27,615	5,458	304	$300.50	$300.50
September	28,623	31,414	-2,790	280	-$108.11	-$108.11
October	26,796	35,267	-8,472	247	-$388.33	-$388.33
November	25,040	37,013	-11,972	277	-$561.60	-$561.60
December	28,026	36,460	-8,434	312	-$385.24	-$385.24
Annual	334,029	407,677	-73,648	366	-$3,275	-$3,275

Table 5. 9 Converter capacity and energy flow

Capacity	361 kW		**Hours of Operation**	5,504 hrs/yr
Mean Output	46.5 kW		**Energy Out**	407,677 kWh/yr
Minimum Output	0 kW		**Energy In**	422,463 kWh/yr
Maximum Output	361 kW		**Losses**	14,786 kWh/yr
Capacity Factor	12.9 %			

Time series charts:

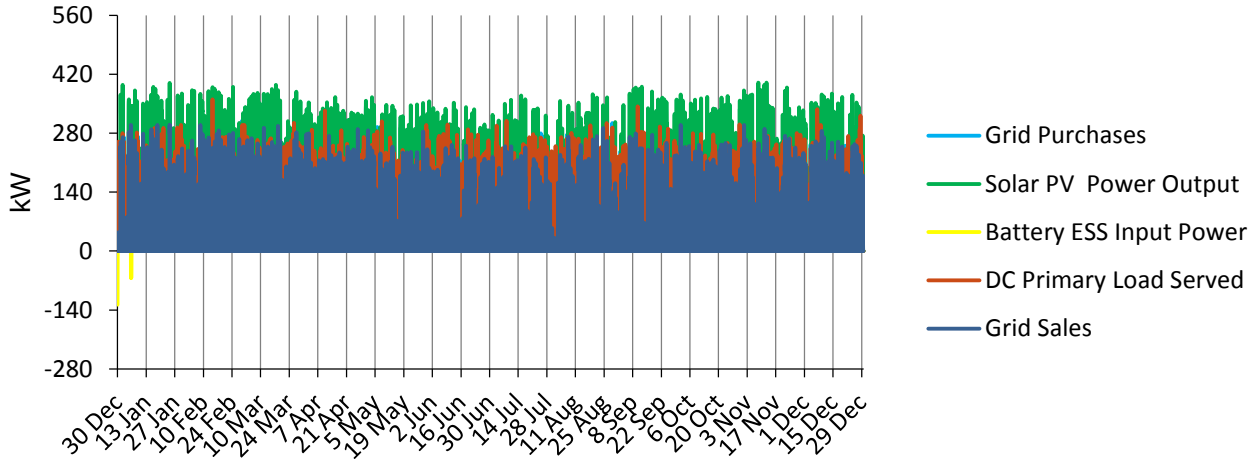

Figure 5. 16 Time series charts of the syste

CHAPTER SIX

6. CONCLUSION, RECOMMENDATION AND FUTURE WORK

6.1 Conclusion

In this study the author set three key goals in section one. The first goal was to design smart model which can automatically forecast solar energy generated for EV charging station based on Hawassa weather condition, Integration smart PV system, grid and energy storage using fuzzy logic algorithm for Ethiopia market as new experience, and Estimating of the operating costs for energy grid-renewable energy for Ethiopian market charging station.

The author used the historical data of Hawassa weather and developed a model which can predict the solar energy for the next day with accuracy of 97.56%. The result illustrates the developed automatic solar energy predicting system for Hawassa charging station which is helpful for energy management.

The system is designed using matlab/Simulink blocks and managed using fuzzy logic controller has been proposed for DC micro-grid to coordinate the power flow between solar PV, BESS and grid. The fuzzy logic controller keeps bus voltage within acceptable region regardless of variations in load and intermittent power of renewable energy sources. As it is shown from result without controller the bus voltage come to 360 V from 500 V when load of system increased three times of normal suddenly. This problem is solved with fuzzy logic controller the bus voltage comes to 495 V from 500 V which in acceptable region. This shows controller improves system disturbance and controls bus voltage with in expected region. According to the finding using fuzzy logic controller the response time is improved to 1.645 ms and bus voltage's standard voltage deviation 2.2.

The author also tried to investigate operational cost analysis and the findings shows that the operating costs for energy is $43,651per year if you use grid only for charging of EVs. The proposed by adding 400 kW of PV and 680 kWh of battery

capacity reduce your operating costs to $6,344 per yearwith annualized saving of $37,306

6.2 Recommendation

The DC microgrid system was designed by using historical data of weather conditions of the study site is collected from Hawassa metrological agency and solar irradiance data is collected from nasa by using longitude and latitudes of Hawassa city. The authorforecasted by using indirect method of forecasting that is solar irradiation of next day. To use direct forecasting method which is explained in section two historical data of solar power generated needed. Therefore my recommendation is for solar energy using companies of Hawassa city to record generated power hourly and daily.

Final recommendation is for Hawassa University institute of technology Electrical and computer department to give controlling algorithm as tutor for power students which is author faced as challenge due to power background.

6.3 Future Work

Any work should always leave one with new knowledge and a desire to take that new knowledge to the next level. The characteristics of this system presented an opportunity to explore many aspects within electrical engineering and allowed the designer to gain a diverse array of knowledge and experience. All in all, the research was a very challenging and complex work that turned out to be very rewarding and successful in the end. The research also led to many more questions and ideas as to how to improve the system functionality.

The most obvious future work pertaining to this research would be to:

- Implementing a communication system that can dynamically give the information about the status and operation mode.
- Adding pricing system when number of EV increased

REFERENCES

[1] Tie SF, Tan CW. A review of energy sources and energy management system in electric vehicles. Renew Sustain Energy Rev 2013; 20:82–102.

[2] International Energy Agency. Global EV Outlook, April 2013.

[3] Joachim Skov Johansen; Fast-Charging Electric Vehicles using AC September 2013

[4] Idaho national laboratory ;Advanced vehicle testing activity For more information, visit avt.inl.gov

[5] Volkswagen Group of America, Inc. Volkswagen Academy Printed in U.S.A. Basics of Electric Vehicles printed 2013

[6] Dhawad, Kushal (June 2017). "Charging connectors for Electric Vehicles at charging stations". International Journal of Recent Engineering Research and Development (IJRERD). 02 (6): 35–38 – via IJRERD

[7] D. Kumar, F. Zare, and A. Ghosh, \Dc microgrid technology: System architectures, ac grid interfaces, grounding schemes, power quality, communication networks, applications, and standardizations aspects," Ieee Access, vol. 5, pp. 12 230{12 256, 2017.

[8] KUPERMAN A, LEVY U, GOREN J, ZAFRANSKI A, SAVERNINA, PELED I. Modeling and control of a 50KW electric vehicle fast charger [C]// Electrical and Electronics Engineers in Israel (IEEEI), 2010: 188–192. (AGGELE

[9] D, CANALES F, ZELAYA-DE L PARRA H, COCCIA A, BUTCHER N, APELDOORN O. Ultra-fast DC-charge infrastructures for EV-mobility and future smart grids [C]// Innovative Smart Grid Technologies Conference Europe (ISGT Europe) IEEE PES, Gothenburg, Sweden, 2010: 1–8.

[10] BAUER P, ZHOU YI, DOPPLER J, STEMBRIDGE N. Charging of electric vehicles and impact on the grid [C]// MECHATRONIKA, 13th International Symposium, Teplice, 2010: 121–127.

[11] YILMAZ M, KREIN P T. Review of charging power levels and infrastructure for plug-in electric and hybrid vehicles [C]// Electric Vehicle Conference (IEVC), Greenville, 2012: 1–8.].

[12] N. Yang, B. Nahid-Mobarakeh, F. Gao, D. Paire, A. Miraoui, and W. Liu,\Modeling and stability analysis of multi-time scale dc microgrid," Electric Power Systems Research, vol. 140, pp. 906{916, 2016.

[13] SUL Seung-ki, LEE Sang-joon. An integral battery charger for four wheel drive [J]. Industry Applications, IEEE Transactions on Volume, 1995, 31(5): 1096–1099.

[14] BOJRUP M, KARLSSON P, ALAKULA M, SIMONSSON B. A Dual Purpose Battery Charger for Electric Vehicles [C]// Power Electronics Specialists Conference, PESC 98 Record, 29th Annual IEEE, Fukuoka, 1998: 565–570.].

[15] https://www.capitalethiopia.com/capital/marathon-to-assemble-hyund electriccars-in-ethiopia/ assessed on April 8, 2020

[16] Goldin, E.; Erickson, L.; Natarajan, B.; Brase, G.; Pahwa, A. Solar powered charge stations for electric vehicles. Environ. Prog. Sustain. 2014, 33, 1298–1308.

[17] Asif Faiz; Christopher S. Weaver; Michael P. Walsh (1996). Air Pollution from Motor Vehicles: Standards and Technologies for Controlling Emissions. World Bank Publications. p. 227. ISBN 978-0-8213-3444-7.

[18] Torch stone energy report on overview of electric vehicles (EVS). Date Accessed online sept. 2020

[19] Hendry, Maurice M. Studebaker: One can do a lot of remembering in South Bend. New Albany, Indiana: Automobile Quarterly. pp. 228–275. Vol X, 3rd Q, 1972. p231

[20] "Obama Administration Announces Federal and Private Sector Actions to Accelerate Electric Vehicle Adoption in the United States".

[21] "EU policy-makers seek to make electric transport a priority". Reuters. 3 February 2015.

[22] Katie Fehrenbacher. Tesla’s model 3 reservations rise to almost 400,000. [online] http://fortune.com/tesla-model-3-reservations-400000/, April 15 2016

[23] .SAE Electric vehicle and plug-in hybrid electric vehicle conductive charge coupler SAE standard J1772; 2012.

[24] Abdul Rauf Bhatti, Zainal Salam, MohdJunaidi Bin Abdul Aziz, Kong Pui Yee;A Comprehensive Overview of Electric Vehicle Charging using Renewable Energy:International Journal of Power Electronics and Drive System (IJPEDS) Vol. 7, No. 1, March 2016, pp. 114-123

[25] Ahamed, M.F.; Dissanayake, U.D.; De Silva, H.P.; Kumara, H.P.; Lidula, N.A. Designing and simulation of a DC microgrid in PSCAD. In Proceedings of the

2016 IEEE International Conference on Power System Technology (POWERCON),Wollongong, Australia, 28 September–1 October 2016; pp. 1–6.

[26] D. Kumar, F. Zare, and A. Ghosh, \Dc microgrid technology: System architectures, ac grid interfaces, grounding schemes, power quality, communication networks, applications, and standardizations aspects," Ieee Access, vol. 5, pp. 12 230{12 256, 2017.

[27] T. Dragicevi c, X. Lu, J. C. Vasquez, and J. M. Guerrero, \Dc microgrids part i: A review of control strategies and stabilization techniques," IEEE Transactions on power electronics, vol. 31, no. 7, pp. 4876{4891, 2016.

[28] N. Yang, B. Nahid-Mobarakeh, F. Gao, D. Paire, A. Miraoui, and W. Liu,\Modeling and stability analysis of multi-time scale dc microgrid," Electric Power Systems Research, vol. 140, pp. 906{916, 2016.

[29] Mukund R., “Wind and Solar Power Systems: Design, Analysis and Operation,” Second Edition, Taylor & Francis, 2006.

[30] Volker Quasching, “Understanding Renewable Energy System,” First Edition, Carl HanserVerlag GmbH & Co KG, 2005

[31] Aldo V. Da Rosa, 2005, “Fundamentals of Renewable Energy Processes,” Elsevier Inc., 2005

[32] M. Diagne, M. David, P. Lauret, J. Boland, N. Schmutz, Review of solar irradiance forecasting methods and a proposition for small-scale insular grids, Renew. Sustain. Energy Rev. 27 (2013) 65-76.

[33] Jiaming Li, John K. Ward , Jingnan Tong , Lyle Collins, Glenn Platt, Machine learning for solar irradiance forecasting of photovoltaic system: January 2016

[34] Hong-Tzer Yang, , Chao-Ming Huang, , Yann-Chang Huang, and Yi-ShiangPai, A Weather-Based Hybrid Method for 1-Day Ahead Hourly Forecasting of PV Power Output. IEEE TRANSACTIONS ON SUSTAINABLE ENERGY, VOL. 5, NO. 3, JULY 2014

[35] M. Saleh, Y. Esa, Y. Mhandi, W. Brandauer, and A. Mohamed, —Design and implementation of CCNY DC microgrid testbed‖, in Industry Applications Society Annual Meeting, 2016 IEEE, IEEE, 2016, pp. 1–7.

[36] Y. Ito, Y. Zhongqing, and H. Akagi, —DC microgrid based distribution power generation system‖, in Power Electronics and Motion Control Conference, 2004 IPEMC 2004. The 4th International, IEEE, vol. 3, 2004, pp. 1740–1745.

[37] M. Ahamed, U. Dissanayake, H. De Silva, H. Pradeep, and N. Lidula, ―Modelling and simulation of a solar PV and battery based DC microgrid system‖, in Electrical, Electronics, and Optimization Techniques (ICEEOT), International Conference on, IEEE, 2016, pp. 1706–1711.

[38] N. Moubayed, J. Kouta, A. El-Ali, H. Dernayka, and R. Outbib, ―Parameter identification of the lead-acid battery model‖, in Photovoltaic Specialists Conference, 2008. PVSC'08. 33rd IEEE, IEEE, 2008, pp. 1–6.

[39] X. Tan, Q. Li, and H. Wang, ―Advances and trends of energy storage technology in Microgrid‖, International Journal of Electrical Power & Energy Systems, vol. 44, no. 1, pp. 179–191, 2013.

[40] J. Xiao, L. Bai, F. Li, H. Liang, and C. Wang, ―Sizing of energy storage and diesel generators in an isolated microgrid using discrete Fourier transform (DFT)‖, IEEE Transactions on Sustainable Energy, vol. 5, no. 3, pp. 907–916, 2014.

[41] ThiThuongHuyen Ma, HamedYahoui , Hoang Giang Vu , Nicolas Siauve and Hervé Morel:A Control Strategy of DC Building Microgrid Connected to the Neighborhood and AC Power Network; May 2017

[42] SAE Electric vehicle and plug-in hybrid electric vehicle conductive charge coupler SAE standard J1772; 2012.

[43] H. -J. Zimmermann, Fuzzy Set Theory and Its Applications (2rd Ed.), Kluwer-Nijhoff ,Hinghum, 1991.

[44] L. A. Zadeh, Fuzzy sets, Information and Control, 1965, 8: 338–353.

[45] L. A. Zadeh, Fuzzy sets as a basis for a theory of possibility, Fuzzy Sets and Systems, 1978, 1: 3–28.

[46] Y. J. Lai and C. L. Hwang, Fuzzy Mathematical Programming Lecture Notes in Economics and Mathematical Systems 394, Springer-Verlag, Berlin, 1992.

[47] Hawassa city administration report

[48] Alajmi BN, Ahmed KH, Finney SJ, et al. (2011) Fuzzy-logic-control approach of a modified hill-climbing method for maximum power point in micro-grid stand-alone photovoltaic system. IEEE trans power Electron 26: 1022–1030

[49] SunartoKaleg, Abdul Hapid, M. RedhoKurnia: Electric vehicle conversion based on distance, speed and cost requirements; 2nd International Conference on Sustainable Energy Engineering and Application, ICSEEA 2014

[50] N. Mohan, T. M. Undeland, and W. P. Robbins, Power Electronics- Converters, Applications and Design, ser. 3rd ed. Media Enhanced Edition. John Wiley & Sons, 2003.

[51] Mukund R., “Wind and Solar Power Systems: Design, Analysis and Operation,” Second Edition, Taylor & Francis, 2006.

[52] ThiThuongHuyen Ma, HamedYahoui , Hoang Giang Vu , Nicolas Siauve and Hervé Morel:A Control Strategy of DC Building Microgrid Connected to the Neighborhood and AC Power Network; May 2017

[53] Roshan Chhetri, TshewangLhendup; VOLTAGE PROFILE IN DISTRIBUTION SYSTEM: Royal University of Bhutan; July 2015.

[54] ETHIOPIAN ENERGY AUTHORITY: QUALITY OF SERVICE STANDARDS for GRID supply ZERO DRAFT; January 2019 Addis Ababa

APPENDIX 1: Weather condition data of Hawassa city

Station Name	Element (Daily in %)	Year	Month	17	18	19	20	21	22	23	24	25	26	27	28	29	30	31
Hawassa	lative Humid	2018	Jul	90	66	60	69	74	69	na	79	67	64	69	62	63	63	72
Hawassa	lative Humid	2018	Aug	79	82	69	63	74	74	76	69	96	65	63	79	92	66	69
Hawassa	lative Humid	2018	Sep	59	59	63	63	69	59	63	78	78	57	66	52	60	51	
Hawassa	lative Humid	2018	Oct	54	55	63	59	51	51	61	68	56	61	59	57	45	57	48
Hawassa	lative Humid	2018	Nov	78	59	57	53	38	41	44	41	51	58	72	56	57	58	
Hawassa	lative Humid	2018	Dec	44	39	51	44	46	52	50	46	46	40	46	45	54	51	51
Hawassa	lative Humid	2019	Jan	35	48	37	58	39	40	35	40	42	37	45	42	45	40	37
Hawassa	lative Humid	2019	Feb	46	38	41	52	49	38	46	44	48	35	37	31			
Hawassa	lative Humid	2019	Mar	47	47	44	37	42	39	38	39	40	47	54	58	52	40	42
Hawassa	lative Humid	2019	Apr	55	56	63	61	56	63	57	76	63	55	53	63	59	47	
Hawassa	lative Humid	2019	May	61	62	66	83	68	61	70	65	63	63	66	69	69	69	66
Hawassa	lative Humid	2019	Jun	66	63	75	76	66	69	76	63	70	69	70	70	70	76	
Hawassa	lative Humid	2019	Jul	69	62	69	62	63	92	63	62	75	72	78	70	86	75	75
Hawassa	lative Humid	2019	Aug	72	82	69	58	82	71	69	69	69	63	62	72	82	69	69
Hawassa	lative Humid	2019	Sep	72	57	63	69	71	71	63	83	79	69	69	75	63	88	
Hawassa	lative Humid	2019	Oct	63	58	69	63	10	74	50	42	57	49	51	58	51	45	48
Hawassa	lative Humid	2019	Nov	51	51	58	58	58	63	66	83	69	82	60	62	56	57	
Hawassa	lative Humid	2019	Dec	50	57	56	56	54	60	52	54	57	51	57	63	61	66	46

Station Name	Year	Month	1	2	3	4	5	6	7	8	9	10	11	12	13	14	15	16	17
Hawassa	2018	Apr	0.47	0.48	0.48	0.54	0.50	0.62	0.54	0.38	0.38	0.56	0.38	0.47	0.43	0.54	0.27	0.62	0.21
Hawassa	2018	May	0.60	0.47	0.86	0.47	0.43	0.22	0.51	0.57	0.57	0.49	0.54	0.50	0.38	0.37	0.59	0.77	0.47
Hawassa	2018	Jun	0.53	0.25	0.57	0.75	0.63	0.75	0.89	1.07	0.86	0.59	0.66	0.91	0.79	0.64	0.41	0.56	0.86
Hawassa	2018	Jul	0.63	0.66	0.58	0.98	0.41	0.77	0.23	0.64	0.79	0.44	0.88	0.31	0.34	0.69	0.91	0.80	0.26
Hawassa	2018	Aug	0.58	0.44	0.81	0.59	0.58	0.60	0.64	0.62	0.51	0.42	0.44	0.62	0.72	0.85	0.84	0.62	0.55
Hawassa	2018	Sep	0.49	0.64	0.75	0.43	0.58	0.51	0.50	0.50	0.55	0.50	0.37	0.49	0.40	0.48	0.43	0.40	0.42
Hawassa	2018	Oct	0.31	0.44	0.21	0.15	0.18	0.32	0.21	0.32	0.22	0.35	0.14	0.26	0.32	0.31	0.51	0.34	0.22
Hawassa	2018	Nov	0.33	0.31	0.29	0.31	0.26	0.35	0.87	0.35	0.33	0.29	0.38	0.25	0.32	0.33	0.08	0.31	0.07
Hawassa	2018	Dec	0.57	0.42	0.40	0.34	0.32	0.45	0.79	0.56	0.25	0.27	0.37	0.75	0.66	0.55	0.53	0.30	0.37
Hawassa	2019	Jan	0.50	0.40	0.57	1.30	1.03	0.66	0.63	0.57	0.58	0.58	0.85	0.58	0.45	0.37	0.37	0.37	0.34
Hawassa	2019	Feb	0.75	0.49	0.64	0.64	0.72	0.57	0.52	0.63	0.39	0.52	0.59	0.64	0.77	0.48	0.56	0.53	0.55
Hawassa	2019	Mar	0.43	0.75	0.67	0.63	0.40	0.48	0.48	0.54	0.53	0.37	0.67	0.80	0.78	0.67	0.54	0.61	0.66
Hawassa	2019	Apr	0.56	0.50	0.36	0.46	0.52	0.40	0.44	0.62	0.40	0.29	1.50	0.27	0.43	0.64	0.45	0.41	0.43
Hawassa	2019	May	0.11	0.44	0.42	0.57	0.45	0.40	0.45	0.45	0.48	0.4	0.6	0.7	0.66	0.48	1.14	0.37	0.44
Hawassa	2019	Jun	0.53	0.31	0.42	0.50	0.50	0.31	0.57	0.78	0.68	0.63	0.76	0.57	0.46	0.46	0.54	0.65	0.74
Hawassa	2019	Jul	0.53	0.60	0.22	0.52	0.44	0.36	0.39	0.52	0.48	0.26	0.42	0.35	0.18	0.20	0.28	0.53	0.42
Hawassa	2019	Aug	0.42	0.56	0.73	0.37	0.16	0.35	0.73	0.37	0.32	0.01	0.23	0.47	0.09	0.21	0.76	0.12	0.10
Hawassa	2019	Sep	0.47	0.56	0.48	0.52	0.53	0.56	0.56	0.53	0.59	0.43	0.51	0.31	0.43	0.49	0.56	0.26	0.31
Hawassa	2019	Oct	0.25	0.21	0.26	0.15	0.29	0.21	0.29	0.31	0.21	0.28	0.13	0.36	0.22	0.31	0.46	0.39	0.70
Hawassa	2019	Nov	0.39	0.48	0.49	0.58	0.71	0.65	0.72	0.25	0.36	0.38	0.48	0.48	0.52	0.35	0.35	0.35	0.32
Hawassa	2019	Dec	0.17	0.18	0.23	0.25	0.27	0.36	0.42	0.32	0.23	0.23	0.33	0.43	0.37	0.39	0.51	0.30	0.38

Station Name	Year	Month	12	13	14	15	16	17	18	19	20	21	22	23	24	25	26	27	28
Hawassa	2018	Oct	8.0	9.4	9.0	9.5	3.5	6.2	6.0	4.0	10.2	8.0	8.0	6.4	6.3	6.0	6.8	4.6	6.0
Hawassa	2018	Nov	5.0	6.7	8.0	0.2	9.8	1.4	10.0	10.6	9.0	11.0	10.1	10.0	10.5	9.5	9.8	2.8	10.5
Hawassa	2018	Dec	9.3	10.2	10.6	10.2	10.5	10.2	10.0	9.4	10.5	10.2	10.6	10.0	9.1	10.2	9.1	9.0	8.5
Hawassa	2019	Jan	na	na	na	na	na	na	na	na	na	10.4	10.0	10.0	7.3	9.6	9.3	10.5	10.6
Hawassa	2019	Feb	8.6	8.5	7.8	7.3	7.9	9.0	10.5	8.0	7.0	4.0	8.7	10.7	8.0	8.8	10.2	11.2	8.3
Hawassa	2019	Mar	na	na	na	na	na	na	na	na	na	na	na	na	na	na	na	na	na
Hawassa	2019	Apr	na	na	na	na	na	na	na	7.8	9.5	8.3	8.6	9.7	na	8.3	10.0	8.3	7.0
Hawassa	2019	May	7.2	5.2	7.0	7.5	6.3	7.3	6.7	6.9	3.0	6.7	7.1	2.3	5.2	7.8	6.8	6.8	4.3
Hawassa	2019	Jun	5.7	3.0	na	3.1	7.0	5.5	7.2	3.6	7.5	8.1	4.2	4.5	3.7	6.0	9.0	4.1	6.2
Hawassa	2019	Jul	6.8	0.5	0.8	4.2	6.0	4.5	6.2	7.5	na	6.3	0.0	8.0	4.9	5.0	0.6	2.8	5.2
Hawassa	2019	Aug	5.0	0.0	3.2	7.0	4.3	1.5	4.0	9.0	7.3	4.0	6.5	5.3	3.5	7.0	5.9	6.5	5.0
Hawassa	2019	Sep	3.0	3.7	1.2	7.4	2.5	2.3	8.0	6.1	6.5	2.3	4.8	8.1	2.0	2.7	5.5	3.0	3.0
Hawassa	2019	Oct	NA	NA	NA	NA	NA	NA	NA	NA	NA	NA	NA	NA	NA	NA	NA	NA	NA
Hawassa	2019	Nov	NA	NA	NA	NA	NA	NA	NA	NA	NA	NA	NA	NA	NA	NA	NA	NA	NA
Hawassa	2019	Dec	NA	NA	NA	NA	NA	NA	NA	NA	NA	NA	NA	NA	NA	NA	NA	NA	NA

Station Name	Element (Daily)	Year	Month	14	15	16	17	18	19	20	21	22	23	24	25	26	27	28	29
Hawassa	Daily Max Te	2017	Apr	33.4	33.0	33.6	32.4	34.2	30.6	32.0	32.6	31.0	32.0	33.2	33.4	30.8	32.2	32.2	28.2
Hawassa	Daily Max Te	2017	May	27.0	26.6	28.0	28.0	26.2	27.8	27.8	28.2	28.0	27.6	27.5	28.4	29.4	29.2	27.8	25.0
Hawassa	Daily Max Te	2017	Jun	26.8	27.8	26.2	27.6	26.8	26.0	27.6	28.8	28.4	28.0	27.6	27.0	28.6	25.8	27.0	26.6
Hawassa	Daily Max Te	2017	Jul	27.6	26.2	26.6	28.5	27.0	24.8	21.2	26.6	25.4	26.2	27.6	24.8	25.2	24.8	27.2	27.4
Hawassa	Daily Max Te	2017	Aug	28.4	26.4	25.8	30.4	29.0	26.6	27.0	26.8	27.0	25.8	26.0	25.8	27.8	28.0	25.6	27.6
Hawassa	Daily Max Te	2017	Sep	26.0	28.4	26.4	26.8	27.2	26.6	27.4	27.4	25.8	27.0	26.2	26.2	27.6	27.2	27.0	24.6
Hawassa	Daily Max Te	2017	Oct	29.2	29.0	26.4	28.0	29.0	29.0	28.0	27.0	27.8	28.8	29.0	28.2	28.0	29.0	27.4	28.4
Hawassa	Daily Max Te	2017	Nov	29.6	28.0	28.2	28.0	28.6	28.0	27.8	29.2	28.8	30.8	30.6	27.6	27.8	28.4	27.4	28.0
Hawassa	Daily Max Te	2017	Dec	29.8	30.2	29.6	29.2	28.2	26.6	27.2	27.2	26.8	26.8	28.2	31.4	29.2	28.2	27.0	29.8
Hawassa	Daily Max Te	2018	Jan	27.8	29.0	28.8	29.8	30.0	30.6	29.6	29.0	29.8	30.2	30.8	30.0	31.2	30.0	29.4	30.4
Hawassa	Daily Max Te	2018	Feb	32.6	32.2	32.2	31.4	31.0	30.0	27.8	29.4	27.0	30.2	30.4	30.0	27.6	28.6	28.6	
Hawassa	Daily Max Te	2018	Mar	26.6	27.8	27.0	27.6	26.8	27.4	29.0	28.2	28.4	28.0	30.0	28.6	29.2	30.0	31.0	20.0
Hawassa	Daily Max Te	2018	Apr	27.0	26.0	26.4	25.4	27.8	26.8	28.0	27.0	27.0	27.2	28.4	29.4	29.2	23.4	27.4	27.4
Hawassa	Daily Max Te	2018	May	31.0	30.6	29.2	29.6	27.0	28.8	27.4	24.8	24.0	25.2	27.0	26.0	27.2	26.0	26.0	26.5
Hawassa	Daily Max Te	2018	Jun	25.0	25.4	26.0	26.4	26.6	25.0	24.4	25.0	26.0	23.5	21.8	25.0	22.4	25.2	25.6	24.0
Hawassa	Daily Max Te	2018	Jul	25.4	25.8	25.0	22.2	25.0	25.4	25.4	23.8	24.0	23.8	23.8	25.4	24.8	25.4	25.6	27.4
Hawassa	Daily Max Te	2018	Aug	26.2	26.2	25.2	25.2	25.2	26.0	26.0	24.0	24.6	24.2	25.4	22.0	24.0	27.0	26.8	21.0
Hawassa	Daily Max Te	2018	Sep	25.4	26.4	27.6	28.0	26.4	25.6	25.6	23.8	27.0	28.0	28.6	25.6	27.0	28.6	28.0	28.8
Hawassa	Daily Max Te	2018	Oct	29.8	27.6	27.4	28.0	27.2	26.0	28.4	29.6	29.0	29.6	26.8	28.0	26.4	26.8	27.2	28.8
Hawassa	Daily Max Te	2018	Nov	28.0	22.0	28.8	28.8	27.0	27.2	27.2	27.0	27.2	28.4	29.4	29.2	28.8	25.6	26.6	27.2
Hawassa	Daily Max Te	2018	Dec	28.0	28.0	28.0	28.8	28.0	28.0	27.4	27.8	28.4	27.8	27.6	27.0	28.0	29.0	29.8	29.0
Hawassa	Daily Max Te	2019	Jan	30.6	30.6	30.4	30.2	29.6	30.0	30.4	30.8	30.6	31.2	31.4	30.6	31.0	31.4	31.4	30.4
Hawassa	Daily Max Te	2019	Feb	32.0	30.4	31.8	31.6	31.8	31.8	32.0	27.6	29.8	30.4	30.2	31.2	31.8	32.0	32.4	NA
Hawassa	Daily Max Te	2019	Mar	32.0	32.4	31.6	32.4	31.6	31.8	32.0	32.4	32.4	33.2	32.4	32.8	32.4	30.0	30.6	31.8

APPENDIX 2: The whole system Simulink with controller